



Université du Québec
à Rimouski

**ÉTUDE DU PROFIL DE DURETÉ ET DE L'EFFET DE
BORD DES DISQUES ET ENGRÈNAGES DROITS TRAITÉS
THERMIQUEMENT PAR INDUCTION EN UTILISANT LES
CONCENTRATEURS DE FLUX**

PRÉDICTION ET OPTIMISATION NUMÉRIQUE ET EXPÉRIMENTALE

Mémoire présenté
dans le cadre du programme de maîtrise en ingénierie
en vue de l'obtention du grade « maître ès sciences appliquées »
(M. Sc. A.)

PAR

© Mohamed Khalifa

Mars 2019

Composition du jury :

Adrian Ilinca, président du jury, Université du Québec À Rimouski

Noureddine Barka, directeur de recherche, Université du Québec À Rimouski

Jean Brousseau, codirecteur de recherche, Université du Québec À Rimouski

**Hussein Ibrahim, examinateur externe, Institut technologique de maintenance
industrielle**

Dépôt initial le 15 Février 2019

Dépôt final le 25 Mars 2019

UNIVERSITÉ DU QUÉBEC À RIMOUSKI
Service de la bibliothèque

Avertissement

La diffusion de ce mémoire ou de cette thèse se fait dans le respect des droits de son auteur, qui a signé le formulaire « *Autorisation de reproduire et de diffuser un rapport, un mémoire ou une thèse* ». En signant ce formulaire, l'auteur concède à l'Université du Québec à Rimouski une licence non exclusive d'utilisation et de publication de la totalité ou d'une partie importante de son travail de recherche pour des fins pédagogiques et non commerciales. Plus précisément, l'auteur autorise l'Université du Québec à Rimouski à reproduire, diffuser, prêter, distribuer ou vendre des copies de son travail de recherche à des fins non commerciales sur quelque support que ce soit, y compris l'Internet. Cette licence et cette autorisation n'entraînent pas une renonciation de la part de l'auteur à ses droits moraux ni à ses droits de propriété intellectuelle. Sauf entente contraire, l'auteur conserve la liberté de diffuser et de commercialiser ou non ce travail dont il possède un exemplaire.

À ma famille

REMERCIEMENTS

Je tiens tout d'abord à remercier toutes les personnes chez le département de mathématiques, d'informatique et de génie à l'Université du Québec à Rimouski qui m'ont guidé tout au long de mon projet de maîtrise et avec lesquelles j'ai développé des liens particuliers.

Je remercie également mon directeur de recherche, Monsieur Noureddine Barka, qui a fait partie des acteurs bienveillants de ma formation, et pour la confiance qu'il a eue à mon égard lorsqu'il m'a confié ce projet de recherche. Malgré sa charge de travail, il a toujours été présent et à l'écoute. Je ne saurais le remercier suffisamment pour ses précieux conseils et ses méthodes de travail qui m'aident quotidiennement. Je tiens à remercier aussi mon codirecteur, Monsieur Jean Brousseau pour son encadrement, sa bienveillance et ses conseils.

Enfin, j'adresse mes remerciements à ma femme, ma famille et tous mes amis qui ont été toujours présents à mes côtés, ainsi que pour leur soutien, leur patience et leurs encouragements tout le long de mon projet.

AVANT-PROPOS

Ce projet de maîtrise en génie de type recherche a été réalisé dans les laboratoires de l'Université du Québec à Rimouski et en coopération avec le département de génie mécanique à l'École de Technologie supérieure à Montréal.

RÉSUMÉ

Le traitement thermique par induction est l'alternative économique et éprouvée aux procédés thermo chimiques visant à améliorer la résistance à l'usure et à la fatigue des pièces mécaniques. La rapidité du processus et sa capacité à traiter localement des composantes mécaniques ayant des formes géométriques complexes font de lui un puissant outil commercial pour les industriels. Le procédé de durcissement par induction est basé sur le couplage physique complexe des phénomènes électromagnétiques et de transfert de chaleur et fait intervenir un nombre important de paramètres de contrôles indépendants. Les caractéristiques mécaniques de la région traitée par induction dépendent principalement de la forme et de la profondeur du profil durcie, qui dépendent elles-mêmes des paramètres de contrôle du procédé. Ainsi, il est toujours nécessaire d'inspecter et de maîtriser l'effet de ces paramètres afin de construire le meilleur profil de dureté possible répondant aux exigences spécifiques d'exploitation. L'objectif de ce projet consiste alors à l'étude des paramètres électromagnétiques, mécaniques et géométriques intervenant en chauffage par induction, et destiné en particulier à l'étude de l'effet de bord, dans le cas exclusif des géométries tridimensionnelles axisymétriques et appliquées à l'acier 4340. L'approche proposée dans ce projet est structurée en trois grandes parties combinant la simulation, la planification d'expérience, l'analyse statistique, les réseaux de neurones, l'expérimentation et l'optimisation afin de créer un modèle prédictif de profil durci et optimiser l'effet de bord en fonction des paramètres de contrôle de procédé, et en utilisant entre autres les concentrateurs de flux électromagnétiques. À partir des équations de Maxwell et de transfert de chaleur, les phénomènes physiques ont été modélisés en simplifiant les lois de comportement des matériaux et en introduisant la densité de courant externe. Le problème a été abordé par la méthode des éléments finis avec des modèles en 2D et en 3D et mise en œuvre dans le logiciel COMSOL. Une campagne de simulation, d'essais expérimentaux et de mesures de profil durci a été réalisée à chaque partie de projet, et a permis de valider avec succès les hypothèses de la modélisation et de vérifier la qualité des résultats fournis par la simulation. Ce travail a permis de mettre à la disposition de l'industrie des recettes simples et fiables destinées à concevoir des profils durcis plus optimisés et de produire des composantes mécaniques industrielles de haute performance.

Mots clés : Traitement thermique par induction, Acier 4340, Profil de dureté, Effet de bord, Concentrateurs de flux, Engrenages, Réseaux de neurones, ANOVA, Optimisation.

ABSTRACT

Induction heat treatment is the economical and proven alternative to thermochemical processes used to improve the wear and fatigue resistance of mechanical parts. The speed of the process and its ability to treat locally mechanical components with complex shapes and geometries make it a powerful tool for industrial manufacturers. The induction hardening process is based on the complex physical coupling of both electromagnetism and heat transfer phenomena, which involve a large number of independent control parameters. The mechanical characteristics of the treated part after induction hardening depend mainly on the shape and depth of the hardness profile, which itself depends on the process control parameters. Thus, it is always necessary to inspect and control the effect of these parameters in order to build the best possible hardness profile meeting the specific operating requirements. The objective of this project is then to study the electromagnetic, mechanical and geometrical parameters involved in induction heating, including the study of the edge effect behavior, in the case of three-dimensional axisymmetric geometries, and applied to 4340 steel components. The approach proposed in this project is structured in three main parts combining simulation, experience planning, statistical analysis, neural networks, experimentation and optimization; to create a predictive model of hardened profile, and to optimize the edge effect according to the process control parameters, with the use of electromagnetic flux concentrators. From Maxwell's equations and heat transfer, physical phenomena were modelled by simplifying the behavior laws of materials and introducing the external current density. The problem was approached by the finite element method using 2D and 3D models and was implemented in the COMSOL software. A set of simulation, of experimental testing and hardness profile measurements were carried out at each step of the project, and successfully validated the modeling assumptions and verified the quality of the results provided by the simulation. This work has thus made it possible for the industry engineers and manufacturers to use simple and reliable recipes for designing more optimized hardness profiles and to produce mechanical components with high performance.

Keywords : Induction heat treatment, 4340 Steel, Hardness profile, Edge effect, Flux concentrators, Gears, Neural networks, ANOVA, Optimization

TABLE DES MATIÈRES

REMERCIEMENTS.....	ix
AVANT-PROPOS	x
RÉSUMÉ	xi
ABSTRACT.....	xii
TABLE DES MATIÈRES	xiii
LISTE DES TABLEAUX	xvii
LISTE DES FIGURES	xviii
INTRODUCTION GÉNÉRALE	1
0.1 MISE EN CONTEXTE.....	1
0.2 PROBLEMATIQUE	5
0.3 OBJECTIFS	10
0.4 METHODOLOGIE.....	12
0.5 ORGANISATION DU MEMOIRE	14
CHAPITRE 1 ÉTUDE DE SENSIBILITÉ DE PROFIL DE DURETÉ D'UN DISQUE EN ACIER 4340 TRAITÉ PAR INDUCTION EN FONCTION DES PARAMÈTRES MACHINES ET FACTEURS GÉOMÉTRIQUES AVEC VALIDATION EXPÉRIMENTALE	15
1.1 RÉSUMÉ EN FRANÇAIS DU PREMIER ARTICLE.....	15
1.2 SENSITIVITY STUDY OF HARDNESS PROFILE OF 4340 STEEL DISK HARDENED BY INDUCTION BY THE VARIATION OF MACHINE PARAMETERS AND GEOMETRICAL FACTORS	17
1.2.1 Abstract	17
1.2.2 Introduction.....	17
1.2.3 Formulation.....	19
1.2.4 Simulation model.....	22

1.2.4.1	Determination of power under typical configuration	23
1.2.4.2	Mesh convergence study	25
1.2.4.3	Temperature and induced current distribution	26
1.2.4.4	Case Depth Deduction From Temperature Curves	28
1.2.4.5	Experimental Validation.....	29
1.2.4	Sensitive study - temperature	32
1.2.4.1	Simulation Data.....	33
1.2.4.2	Contributions on final temperature distribution	34
1.2.4.3	Simulated versus predicted temperatures	35
1.2.4.4	Parameters effects.....	36
1.2.5	Sensitivity study of case depth	39
1.2.5.1	Parameters effects.....	40
1.2.5.2	Simulated versus predicted case depths	42
1.2.6	Experimental validation	43
1.2.7	Conclusion.....	45
CHAPITRE 2 OPTIMISATION DE L'EFFET DE BORD D'UN DISQUE EN ACIER 4340 CHAUFFÉE PAR INDUCTION AVEC DES CONCENTRATEURS DE FLUX UTILISANT UN MODÈLE DE SIMULATION PAR ÉLÉMENTS FINIS AXISYMMÉTRIQUE ET AVEC VALIDATION EXPÉRIMENTALE		47
2.1	RÉSUMÉ EN FRANÇAIS DU DEUXIÈME ARTICLE	47
2.2	OPTIMIZATION OF THE EDGE EFFECT OF 4340 STEEL SPECIMEN HEATED BY INDUCTION PROCESS WITH FLUX CONCENTRATORS USING FINITE ELEMENT AXIS-SYMMETRIC SIMULATION AND EXPERIMENTAL VALIDATION.....	49
2.2.1	Abstract	49
2.2.2	Introduction	49
2.2.3	Methodology	51
2.2.4	Parametric study	52
2.2.4.1	Material characterization.....	52
2.2.5	Geometry	53

2.2.6 Optimization study.....	54
2.2.6.1 Numerical Simulation	57
2.2.7 Experimental validation	61
2.2.7.1 Experimental setup.....	62
2.2.7.2 Metallographic Analysis	63
2.2.8 Discussion	64
2.2.9 Conclusion	67
 CHAPITRE 3 RÉDUCTION DE L'EFFET DE BORD À L'AIDE DE LA MÉTHODOLOGIE DE SURFACE DE RÉPONSE ET DE LA MODÉLISATION D'UN RÉSEAU NEURAL ARTIFICIEL D'UN ENGRENAGE DROIT TRAITE PAR INDUCTION AVEC DES CONCENTRATEURS DE FLUX	69
3.1 RÉSUMÉ EN FRANÇAIS DU DEUXIÈME ARTICLE	69
3.2 REDUCTION OF EDGE EFFECT USING RESPONSE SURFACE METHODOLOGY AND ARTIFICIAL NEURAL NETWORK MODELING OF A SPUR GEAR TREATED BY INDUCTION WITH FLUX CONCENTRATORS.....	71
3.2.1 Abstract	71
3.2.2 Introduction.....	71
3.2.3 Theoretical Background.....	73
3.2.3.1 Induction heating process	73
3.2.3.2 Predictive modeling using RSM	75
3.2.3.3 Predictive modeling using ANN	76
3.2.4 Simulation Model.....	77
3.2.4.1 Process Parameters Selection.....	77
3.2.4.2 Experimental design.....	80
3.2.5 Results and discussion	82
3.2.5.1 Temperature Analysis	82
3.2.5.2 ANOVA Analysis on Temperature difference	83
3.2.5.3 Contributions on temperature difference	86
3.2.5.4 RSM of temperature difference using ANOVA	90

3.2.5.5 ANN modeling of Case Depth Gap.....	92
3.2.5.6 Case Depth Prediction	93
3.2.5.7 Case Depth Difference Prediction	94
3.2.5.8 Experimental Validation of the ANN Model	96
3.2.6 Conclusion.....	101
CONCLUSION GÉNÉRALE	103
RÉFÉRENCES BIBLIOGRAPHIQUES	109

LISTE DES TABLEAUX

TABLE 1.1 : SIMULATION PARAMETERS WITH FIXED MACHINE POWER	25
TABLE 1.2: VALIDATION TEST PARAMETERS	30
TABLE 1.3 : SIMULATION PLANNING	32
TABLE 1.4 : TEMPERATURE AT THE MIDDLE OBTAINED BY SIMULATION (°C).....	33
TABLE 1.5 : TEMPERATURE AT THE EDGE OBTAINED BY SIMULATION (°C).....	34
TABLE 1.6 : CONTRIBUTION FACTOR PERCENTAGE FOR EACH PARAMETER ON EDGE AND MIDDLE TEMPERATURE	35
TABLE 1.7 : CONTRIBUTIONS IN THE EDGE	39
TABLE 1.8 : CONTRIBUTIONS AT THE MIDDLE	40
TABLE 1.9 : EXPERIMENTAL PLANNING.....	44
TABLE 2.1 : CHEMICAL COMPOSITION OF 4340 STEEL [71].....	52
TABLE 2.2. INITIAL PARAMETERS USED IN OPTIMIZATION PROCESS.	57
TABLE 2.3. CASE DEPTH MEASURED FOR EACH INDUCTION HEATING METHOD.....	65
TABLE 3.1 : PARAMETER CONFIGURATION.....	79
TABLE 3.2 : SIMULATION PARAMETERS	80
TABLE 3.3 : SCRATCHING PARAMETERS AND THEIR LEVEL.....	81
TABLE 3.4 : PERCENT CONTRIBUTIONS OF PROCESS PARAMETERS	84
TABLE 3.5 : ANALYSIS OF VARIANCE RESULTS ON TEMPERATURE DIFFERENCE AT THE TIP	87
TABLE 3.6 : ANALYSIS OF VARIANCE RESULTS ON TEMPERATURE DIFFERENCE AT THE ROOT	87
TABLE 3.7 : COEFFICIENT OF DETERMINATION FOR THE PREDICTION MODEL	89
TABLE 3.8 : PARAMETERS USED IN VALIDATION OF THE NEURAL NETWORK	97
TABLE 3.9 : COMPARISON OF MEASURED AND ANN PREDICTED CASE DEPTH ON THE GEAR TIP.....	100
TABLE 3.10 : COMPARISON OF MEASURED AND ANN PREDICTED CASE DEPTH ON THE GEAR ROOT	100

LISTE DES FIGURES

FIGURE 0.1 : UNE DETERIORATION EXCESSIVE DES DENTS D'ENGRENAGES (GARDEN STREET METALS. CINCINNATI, OHIO).....	2
FIGURE 0.2 : BOBINES D'INDUCTION AVEC DES CHAMPS ELECTROMAGNETIQUES GENERES PAR CHAQUE TYPE [20]	3
FIGURE 0.3 : DURCISSEMENT D'UN ENGRENAGE PAR INDUCTION [22]	4
FIGURE 0.4 : EFFET DE BORD REMARQUABLE POUR UNE SECTION DE DISQUE EN ACIER 4340 TRAITEE PAR INDUCTION SANS CONCENTRATEURS DE FLUX [50].	8
FIGURE 0.5 : DISTRIBUTION DE CHAMPS ELECTROMAGNETIQUE DANS UNE BOBINE A DEUX TOURS (A) SANS CONCENTRATEURS DE FLUX (B) AVEC CONCENTRATEURS DE FLUX [20].	9
FIGURE 1.1 :SCHEMATIC REPRESENTATION OF MODEL COMPONENTS	23
FIGURE 1.2 : TEMPERATURE EVOLUTION ACCORDING THE MACHINE POWER	24
FIGURE 1.3 : FINAL TEMPERATURE ACCORDING THE MESH SIZE	25
FIGURE 1.4 : FINAL MESH OPTIMIZED BY CONVERGENCE STUDY	26
FIGURE 1.5 : DISTRIBUTIONS OF INDUCTION CURRENT (A/M ²) AND TEMPERATURE (°C)	27
FIGURE 1.6 : TEMPERATURE DISTRIBUTION AT THE EDGE AND MIDDLE PROFILE	28
FIGURE 1.7 : TYPICAL HARDNESS PROFILE BY INDUCTION HEATING	29
FIGURE 1.8 : INDUCTION MACHINE AND OPERATION SYSTEM.....	30
FIGURE 1.9 : HARDNESS PROFILE OBTAINED BY EXPERIMENTS.....	31
FIGURE 1.10 : HARDNESS CURVE ON EDGE AND MIDDLE OBTAINED AFTER THE EXPERIMENTAL TEST	32
FIGURE 1.11 : SIMULATED TEMPERATURES VERSUS PREDICTED TEMPERATURE AT MIDDLE AND EDGES	36
FIGURE 1.12 : EFFECT OF GEOMETRY FACTORS AND MACHINE PARAMETERS ON TEMPERATURE (A) MIDDLE AND (B) EDGE	37
FIGURE 1.13 : RESPONSE SURFACE METHODOLOGY OF SURFACE TEMPERATURE (A) MIDDLE (B) EDGE	38
FIGURE 1.14 : EFFECT OF GEOMETRY FACTORS AND MACHINE PARAMETERS ON CASE DEPTH (A) MIDDLE AND (B) EDGE	41
FIGURE 1.15 : RESPONSE SURFACE METHODOLOGY OF CASE DEPTH IN (A) MIDDLE AND AT (B) EDGE	42

FIGURE 1.16 : SIMULATED DEPTHS VERSUS PREDICTED DEPTHS IN (A) MIDDLE AND (B) EDGES	43
FIGURE 1.17 : CROSS-SECTION OF HARDNESS PROFILE OBTAINED BY TEST 2 (A) AND TEST 3 (B)	44
FIGURE 1.18 : PREDICTED AND MEASURED HARDNESS CURVES FOR TEST 2, (A) EDGE AND (B) MIDDLE	45
FIGURE 2.1 : EVOLUTION OF ELECTRICAL, MAGNETIC AND THERMAL PROPERTIES VS TEMPERATURE OF THE 4340 STEEL [72].....	53
FIGURE 2.2 : SCHEMATIC PRESENTATION OF THE MODEL GEOMETRY	54
FIGURE 2.3 : FLOWCHART OF THE OPTIMIZATION PROCEDURE	55
FIGURE 2.4 : 2D MODEL SHOWING NODES TO EVALUATE AT THE MEDIUM AND THE EDGE..	56
FIGURE 2.5 : EVALUATION OF OBJECTIVE FUNCTION IN EACH GLOBAL ITERATION DURING OPTIMIZATION PROCESS	58
FIGURE 2.6 : TEMPERATURE DISTRIBUTION SURFACE AFTER THE HEATING PROCESS (A) WITH INITIAL PARAMETERS (B) WITH OPTIMAL PARAMETERS	59
FIGURE 2.7 : TEMPERATURE PROFILE IN THE MIDDLE AND THE EDGES WITH INITIAL GAP PARAMETERS	60
FIGURE 2.8 : TEMPERATURE PROFILE IN THE MIDDLE AND THE EDGES WITH OPTIMIZED GAP PARAMETERS	61
FIGURE 2.9 : INDUCTION MACHINE AND OPERATION SYSTEM	61
FIGURE 2.10 : EXPERIMENTAL SETUP SCHEME	62
FIGURE 2.11 : HARDENED PROFILES REVEALED AFTER NITAL ETCHING: (A) WITH NO FLUX CONCENTRATOR (B) WITH FLUX CONCENTRATORS USING OPTIMIZED PARAMETERS.	63
FIGURE 2.12 : HARDNESS PROFILE (A) WITHOUT FLUX CONCENTRATORS (B) WITH FLUX CONCENTRATORS AND OPTIMIZED PARAMETERS	64
FIGURE 2.13 : BAR GRAPH OF AVERAGE AND STANDARD DEVIATION OF CASE DEPTH FOR EACH INDUCTION HEATING METHOD	66
FIGURE 3.1 : MODEL WITH FLUX CONCENTRATORS.....	78
FIGURE 3.2 : TEMPERATURE VS IMPOSED CURRENT DENSITY.....	80
FIGURE 3.3 : TEMPERATURE (°C) AND CURRENT DENSITY (A/MM ²) DISTRIBUTION AT THE END OF HEATING (A) EDGE AND (B) MIDDLE.....	83
FIGURE 3.4 : MAIN EFFECT PLOT OF TEMPERATURE VERSUS SIMULATION PARAMETERS	85
FIGURE 3.5 : SIMULATED VS ANOVA PREDICTED TEMPERATURE (A) MEDIUM (B) EDGE PLAN	86

FIGURE 3.6 : MAIN EFFECT PLOT OF TEMPERATURE DIFFERENCE VERSUS SIMULATION PARAMETERS.....	88
FIGURE 3.7 : SIMULATED TEMPERATURE DIFFERENCE VS PREDICTED BY ANOVA	89
FIGURE 3.8 : RSM OF TEMPERATURE DIFFERENCE BASED ON ANOVA ANALYSIS (A) TIP (B) ROOT.....	91
FIGURE 3.9 : ARCHITECTURE OF THE ANN MODEL USED FOR PREDICTION OF THE FINAL CASE DEPTHS.....	92
FIGURE 3.10 : TRAINING, VALIDATION AND TEST MEAN SQUARED ERRORS (PERFORMANCE IS 8.48×10^{-4}).....	93
FIGURE 3.11 : SIMULATION VS ANN PREDICTED CASE DEPTH	94
FIGURE 3.12 : SIMULATED VS PREDICTED CASE DEPTH GAP ON THE TIP AND THE ROOT USING ANN	94
FIGURE 3.13 : CASE DEPTH GAP ON TIP AND ROOT BASED AS PREDICTED BY ANN ANALYSIS	96
FIGURE 3.14 : MACHINE POWER VS IMPOSED CURRENT DENSITY.....	98
FIGURE 3.15 : SHAPE OF THE CASE-HARDENED PROFILE ON THE TIP AND THE ROOT OF TEST 03 (A) EDGE (B) MEDIUM	98
FIGURE 3.16 : HARDNESS MEASUREMENT ON THE TIP AND THE ROOT OF TEST 03 (A) EDGE (B) MEDIUM	99
FIGURE 3.17 : MEASURED VS PREDICTED CASE DEPTH DIFFERENCE ON THE TIP AND THE ROOT	101

INTRODUCTION GÉNÉRALE

0.1 MISE EN CONTEXTE

Presque tout ce dont l'humanité a besoin pour la civilisation actuelle dépend des métaux. Des énormes quantités de fer et d'aciers sont utilisées dans les automobiles, les avions, les navires, les ponts, les bâtiments, les machines et dans nombreux autres produits et applications industrielles et domestiques chaque jour. Les exigences actuelles demandent une grande variété d'outils en aciers de haute qualité, y compris les outils ayant subi des durcissements fins ou profonds en surface pour la fabrication de produits fonctionnant à des conditions extrêmes et capables de bien résister à l'usure, aux chocs et à la chaleur.

Autrefois, le durcissement des outils en aciers ayant de faibles teneurs en carbone se faisait par traitement thermique classique dans lequel la pièce était chauffée en entier dans un four jusqu'à l'austénitisation complète, et trempé dans l'eau ou l'eau salée. De nos jours, le traitement thermique n'est plus un processus simple. Il comprend un ensemble d'étapes et procédures complexes qui doivent être suivis attentivement afin procurer aux pièces traitées toutes les propriétés leur permettant de fonctionner sans défaillances prématuées. Un bon métallurgiste devrait non seulement savoir et comprendre le comportement des métaux mis en question, mais aussi être capable de prédire et tester les propriétés métallographiques à la fin de traitement thermique comme la dureté, la ductilité et l'endurance des pièces traitées. Comme illustré à la **Figure 0.1**, une détérioration excessive des dents d'engrenage peut se produire si les processus métallurgiques appropriés de durcissement ne sont pas bien employés. Prédire le comportement interne de l'acier pendant les processus de chauffage, de trempe, de recuit, de revenu et autres processus de traitements est un défi passionnant. L'acier subit des changements fondamentaux et le métallurgiste doit prédire les changements qui se produisent en fonction de la composition de l'acier et des traitements thermiques auxquels il est soumis.

Plusieurs techniques de traitement thermique sont employées actuellement pour traiter superficiellement les composants d'acier. Ils sont classés principalement en deux groupes : les traitements thermiques sans modification de la microstructure et les traitements thermochimiques. Les premiers visent à durcir la surface de composants à des profondeurs relativement minces par rapport à leur taille (0.8 à 3.5mm environ) [1], c'est par exemple le cas de durcissement au laser [2-4], durcissement par flamme [5, 6], durcissement par induction [7-10], durcissement par torche à plasma et durcissement par faisceau d'électrons [11, 12]. Dans le deuxième groupe, celui des traitements thermochimiques, on retrouve par exemple la cémentation, la nitruration et la carbonitruration. Dans ce cas, le traitement se fait avec diffusion d'éléments non métalliques en surface de la pièce afin d'augmenter sa dureté. Ces procédés se font dans des fours avec des hautes concentrations de gaz d'hydrocarbures ou azoté, comme le propane ou gaz naturel ou l'ammoniac.



Figure 0.1 : Une détérioration excessive des dents d'engrenages (Garden Street Metals. Cincinnati, Ohio)

Parmi les techniques de durcissement cité ci-dessus, le traitement thermique par induction a démontré son succès dans l'industrie métallurgique grâce à sa productivité remarquable, son efficacité énergétique et sa capacité à manipuler et traiter des pièces métalliques ayant des formes géométriques complexes par exemple pour les engrenages [10].

Ce procédé de chauffage par induction est devenu populaire dans de nombreuses applications industrielles telles que le brasage [13, 14], le moulage [15, 16] et aussi pour le

durcissement en surface appliquée sur les pièces mécaniques utilisées dans les applications automobiles et aérospatiales [17-19]. Le traitement thermique par induction est un procédé de chauffage sans contact direct entre l'inducteur et la pièce à traiter et s'applique généralement sur des matériaux ayant une perméabilité magnétique relativement élevée. Comme présenté dans la **Figure 0.2**, le chauffage se produit à l'intérieur et près de la surface de la pièce, ceci est le résultat de la circulation en circuit fermé des courants électriques dites courants induits ou courants de Foucault. Ces courants sont le résultat de l'exposition de la pièce en métal à un champ électromagnétique générée par un courant alternatif externe circulant dans une bobine en cuivre et caractérisé par sa fréquence f et la densité du courant induit (J_0). La résistance électrique à l'intérieur de la pièce génère de la chaleur [20, 21]. Grâce à un phénomène connu sous le nom de « l'effet de peau », le courant et la chaleur ne se concentrent en surface ou dans la peau de la pièce.

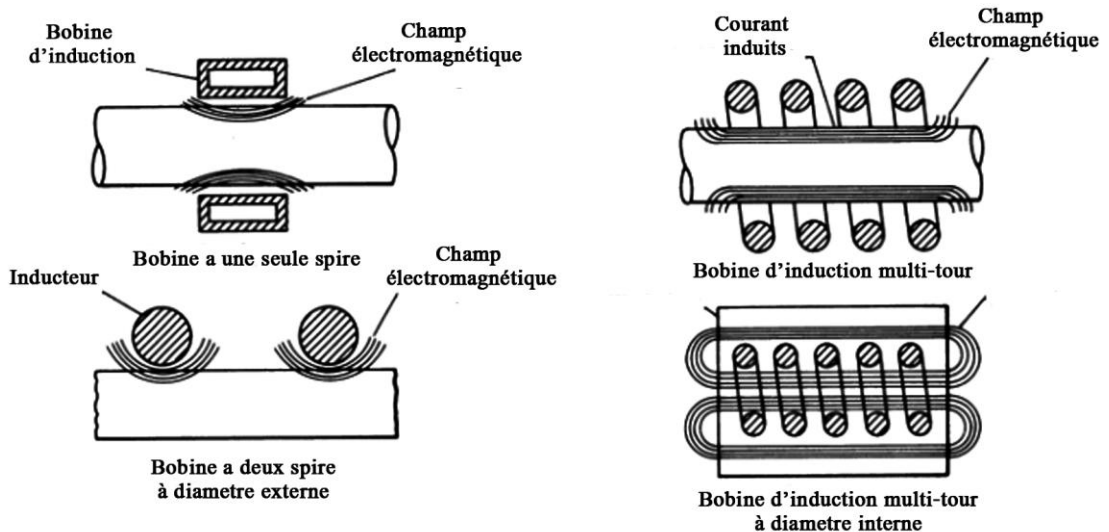


Figure 0.2 : Bobines d'induction avec des champs électromagnétiques générés par chaque type [20]

Pour augmenter la dureté de la pièce, cette dernière doit être chauffée à des hautes températures pour transformer la structure métallographique en austénite. Lorsque la surface reçoit suffisamment de chaleur- dont la température est supérieure à la température minimale pour la transformation en austénite, et inférieure à la température de fusion de l'acier-, la pièce

est refroidie rapidement dans un milieu de trempe. Cette trempe a pour but de transformer la totalité de structure austénitique en structure martensitique très dure après refroidissement et exploitable dans des applications nécessitant des performances élevées en matière de dureté. La profondeur durcie peut être contrôlée avec plus de précision lors du durcissement par induction que dans tout autre procédé. La profondeur et le profil durci peuvent être contrôlés en variant la fréquence, le courant et le temps de chauffe. Plus la fréquence est élevée (haute fréquence), plus le courant a tendance à circuler près de la surface extérieure de la pièce.

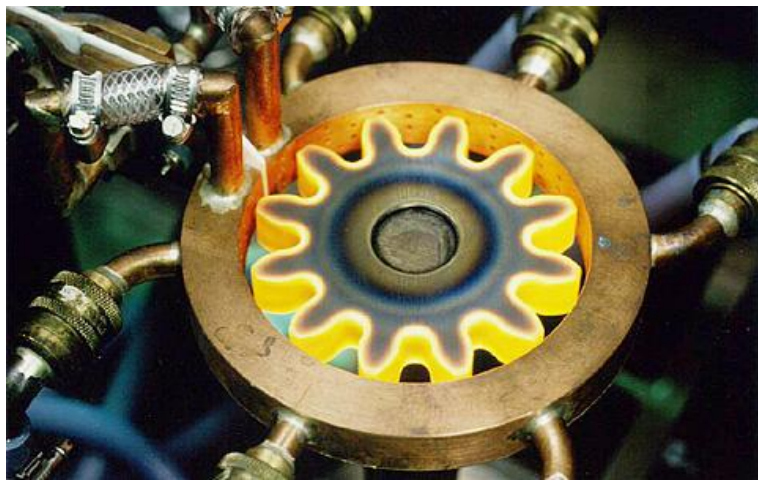


Figure 0.3 : Durcissement d'un engrenage par induction [22]

Le traitement par induction est utilisé pour une grande variété d'applications. Il est largement utilisé pour durcir les engrenages (**Figure 0.3**), les dents de pignons, les arbres de pompes et moteurs, les cames, les vilebrequins, etc. Il présente de nombreux avantages par rapport à d'autres procédés de durcissement. De tous les procédés permettant le durcissement en surface, c'est le plus efficace énergétiquement. Aucun temps de chauffage n'est requis avant l'induction et les pièces peuvent être chauffées en moins d'une seconde. Lorsque les pièces sont durcies en grande quantité, le coût unitaire de traitement est ainsi très faible. Le principal inconvénient de traitement par induction est le coût élevé des machines et des matériaux nécessaires au processus, de plus, l'inducteur en cuivre nécessite généralement une conception sur mesure dépendamment de l'application et la géométrie visé du composant à traiter. Les pièces couramment utilisées pour le traitement par induction sont généralement

en acier à teneur moyenne en carbone (0,35% à 0,60%). La dureté finale est aussi fonction de la teneur en carbone de l'acier qui est traité. Par conséquent, une dureté élevée ne peut être atteinte que si l'acier utilisé est fortement allié.

0.2 PROBLEMATIQUE

Le traitement thermique par induction est une combinaison complexe entre plusieurs phénomènes physiques comme l'électromagnétisme, le transfert de chaleur et la métallurgie des métaux. Les paramètres liés à la conception et au fonctionnement du procédé de traitement thermique par induction dépendent toujours des besoins et des résultats désirés. Le fait que le procédé de traitement thermique par induction est un procédé sans contact direct entre l'inducteur et la pièce avec donne à l'induction l'avantage de traiter une grande variété de pièces mécaniques avec géométries simples ou complexes. En contrepartie, le procédé est difficile à maîtriser parce qu'il fait intervenir deux phénomènes physiques principaux, le physique d'électromagnétisme et le transfert de chaleur produite à l'intérieur de la pièce. Gérer en même temps ces deux phénomènes physiques présente des difficultés au niveau de la simulation et de l'expérimentation. De plus, les données sur les propriétés des matériaux ne sont pas toujours précises et varient de façon différente avec la température. La mesure adéquate de la température et du courant de la machine pendant le processus de chauffage est une tâche expérimentale toujours difficile à réaliser avec précision en raison du taux de chauffage très rapide.

Pour prédire le résultat d'un traitement thermique par induction, il est important de connaître le profil de distribution de température au cours et à la fin de procédé de chauffage qui est directement lié au comportement des champs électromagnétiques à l'intérieur de la pièce. Le chauffage à l'intérieur de la pièce est généré par l'effet Joule qui est causé par la circulation des courants induits. Ceux-ci ont la même fréquence que le courant alternatif AC externe circulant dans l'inducteur. Ces courants se localisent de façon non uniforme à travers la pièce et particulièrement près de la surface (effet de peau) et des bords de la pièce. Ce phénomène est connu sous le nom d'effet de bord et n'apparaît que si le courant est alternatif,

comme illustré dans la **Figure 0.4**. La distribution des courants induits ainsi la puissance interne générée par effet Joule est plus profonde au niveau des bords et diminue au milieu de la pièce. Cette couche de densité maximale est caractérisée par l'épaisseur δ à partir de la surface et qui est définie par l'épaisseur pour laquelle on retrouve 86% des courants induits. à cette épaisseur dépend de plusieurs paramètres comme la fréquence et les propriétés magnétiques de la pièce [23], la forme, la position relative de la pièce avec l'inducteur et la géométrie de l'inducteur qui influent aussi la distribution finale de la température. Bien que le durcissement par induction soit bien établi parmi les industriels, les besoins d'optimisation de ce processus sont toujours nécessaires. Pour garantir une distribution uniforme de température à la fin de la chauffe, il est toujours nécessaire de prédire avec précision la distribution des champs électromagnétiques produite par l'inducteur sous différentes conditions d'opérations. La distorsion de ces champs électromagnétiques au bord des pièces traitées particulièrement les pièces de formes cylindriques comme les disques et les engrenages- est la raison principale de la non-uniformité de profil de température à la fin de traitement. Des études profondes sur cet effet ont été conduites depuis les années 1970 jusqu'au nos jours [23, 24]. Les travaux de recherches réalisés précédemment dans le domaine du traitement thermique par induction présentent plusieurs approches numériques et expérimentales qui englobent pratiquement toutes les applications possibles de ce procédé, en commençant par le soudage, le moulage ainsi que le durcissement des métaux, etc. auparavant, des efforts ont été déployés pour modéliser le traitement thermique par induction [25-28] et les processus de carburation [29, 30].

L'étude du procédé de traitement thermique par induction présente plusieurs difficultés au niveau de la simulation et de l'expérimentation. Il y a une difficulté à modéliser la physique d'induction électromagnétique et le transfert thermique et qui comprend plusieurs paramètres et phénomènes physiques couplés ensemble. De plus, les données sur les propriétés matérielles ne sont pas précises et varient de façon différente avec la température. La mesure adéquate de la température à la surface de la pièce pendant le processus de chauffage est une tâche expérimentale difficile en raison du taux de chauffage rapide. Les chercheurs ont

proposé des méthodes expérimentales et statistiques qui pourraient être utiles pour résoudre ces problèmes.

Pour faire une bonne étude statistique, il faut choisir les paramètres appropriés, bien conduire les essais expérimentaux et analyser correctement les résultats obtenus. Des chercheurs ont proposé cette approche par simulation [31-33], par simulation avec validation [34, 35], et expérimentation avec stratégie de planification [36-39]. Hömberg et al. [40] ont étudié le durcissement par induction multifréquence incluant les transitions de phase et les effets mécaniques par simulation. Urquiza et al. [41] ont étudié l'effet de trempe impliquée dans le durcissement par induction, y compris les effets mécaniques sur l'acier 42CrMo4. Jakubovičová et al. [42] ont étudié l'optimisation du processus de chauffage par induction afin d'obtenir une température de surface uniforme. Barglik et al. [43], Cajner et al. [44] et Sadeghipour et al. [45] ont étudié le traitement thermique par induction en modélisant le modèle numériquement sur différents types de pièces mécaniques. Kristoffersen et al. [38] ont étudié l'influence des paramètres du processus de durcissement par induction sur les contraintes résiduelles. Barka et al. [32] ont réalisé une étude sensibilité du profil de dureté de l'échantillon 4340 chauffé par induction à l'aide de la modélisation axisymétrique. Ces études ont permis de mieux comprendre le comportement du procédé de chauffage et de trempe par induction électromagnétique afin de prédire la dureté, les contraintes résiduelles, la déformation et la distribution finale de la température.

Toutefois, en ce qui concerne les engrenages par exemple, il est difficile d'atteindre cet objectif en ajustant uniquement les paramètres de la machine et/ou le changement de la géométrie de l'inducteur. La revue de littérature a démontré que des modèles de simulation ont été développés et permettent l'analyse du profil de dureté en fonction des propriétés du matériau ou en fonction des paramètres de la machine [20-21]. Plusieurs études menées ont conclu que pour converger vers une prédiction fiable et précise du processus de durcissement, il est important de trouver une autre méthode pour contrôler le chauffage à la surface (effet de bord) [46-48].

Plus précisément, dans les travaux précédents, les auteurs ont décrit les effets bénéfiques des concentrateurs de flux pour les géométries du type disque en utilisant un modèle axisymétrique [46]. D'autres études ont appliqué cette technique pour valider son applicabilité dans un modèle numérique 3D [49].

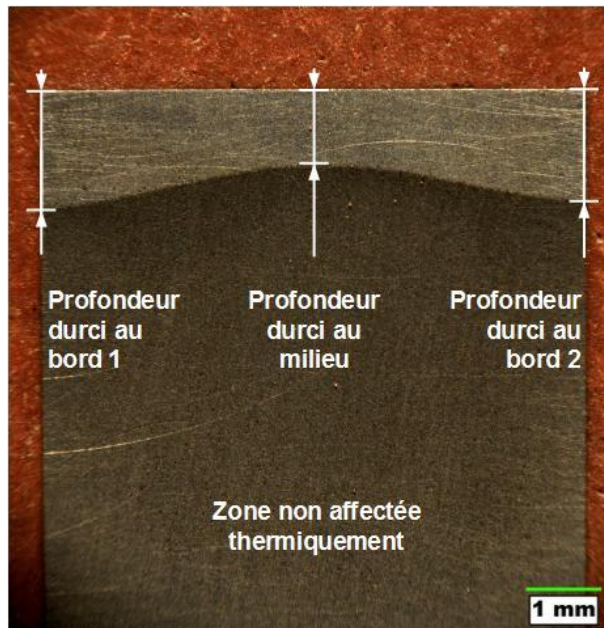


Figure 0.4 : Effet de bord remarquable pour une section de disque en acier 4340 traitée par induction sans concentrateurs de flux [50].

La technique la plus utilisée de nos jours pour contrôler la dispersion des champs électromagnétiques consiste à utiliser des concentrateurs de flux sur l'inducteur. L'emploi de ces concentrateurs permet de concentrer les champs électromagnétiques sur des régions spécifiques de la pièce, et d'éviter que le flux électromagnétique diverge et se développe dans des zones non désirées. Comme illustré dans la **Figure 0.5** Cette technique permet d'augmenter l'efficacité du procédé de traitement et d'obtenir des profils plus uniformes de température entre le bord et le milieu de la pièce. Le matériel utilisé pour la fabrication des concentrateurs de flux est généralement constitué de laminages découpés dans des alliages magnétiques à grains orientés, dont la quantité dépend de la gamme de puissance et fréquence

utilisée. La forme de ces concentrateurs est aussi dépendante de la forme et la géométrie de pièce traité [51].

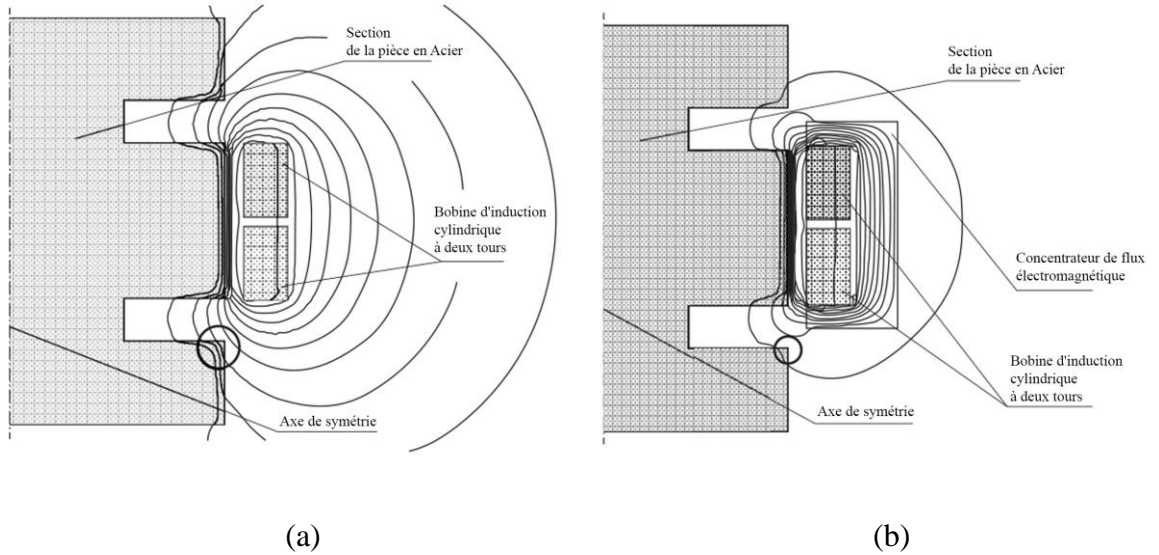


Figure 0.5 : Distribution de champs électromagnétique dans une bobine à deux tours
(a) sans concentrateurs de flux (b) avec concentrateurs de flux [20].

L'emploi de ce type de concentrateurs inclut plusieurs inconvénients. En effet, leur coût d'exploitation élevé étant donné qu'ils doivent être conçus et fabriqués sur mesure pour chaque application présente l'inconvénient majeur. D'autre part, lors de l'exploitation et durant le processus de traitement et chauffage, les concentrateurs de flux peuvent avoir un refroidissement insuffisant, entraînant une surchauffe et une défaillance prématuée. Aussi, les éléments de serrage entre l'inducteur en cuivre et les laminages subissent de grandes intensités de courant, et ceci peut conduire à la surchauffe et même à la fusion de ces éléments. Toutefois, tous les concentrateurs de flux se dégradent naturellement en fonction du temps en service en raison de l'intensité du champ électromagnétique et de la chaleur reçue par rayonnement durant le traitement, ce qui nécessite toujours des entretiens en continu [20].

La distribution des champs électromagnétiques à la surface des pièces traitées peut être contrôlée avec d'autres configurations possibles [49, 52]. Barka et al. [53] ont introduit une

nouvelle approche pour optimiser le processus de chauffage par induction à l'aide d'un type différent de concentrateurs de flux et l'ont appliqué à des engrenages cylindriques en acier 4340. Selon cette approche, il s'agit de mettre en sandwich la pièce à traiter (pièce maîtresse) ayant une forme cylindrique au milieu de deux autres pièces ayant la même forme et géométrie (pièces esclaves). Les deux dernières permettent la redistribution et la linéarisation des champs électromagnétiques à la surface de la pièce maîtresse, ce qui diminue l'effet de bord. Cette approche est très prometteuse notamment sur les plans techniques et économiques.

0.3 OBJECTIFS

Dans les études précédentes, les chercheurs se sont concentrés plus à l'étude d'effets de changement des paramètres liés à la machine à induction et la géométrie de l'inducteur lui-même qu'à la distribution finale de température et le profil de dureté à la surface des pièces traitées. Ils ont aussi travaillé au développement de techniques permettant de contrôler et optimiser le procédé lui-même (efficacité énergétique et augmentation du temps de production, etc.).

Quant à lui, le présent projet vise à étudier et optimiser le profil durci à partir de la distribution finale de température des pièces en acier 4340 traitée thermiquement par induction avec l'emploi des concentrateurs de flux de type maître esclave. En se basant sur des modèles de simulation par éléments finis avec validation expérimentale, le premier objectif spécifique de ce projet propose d'étudier les différentes corrélations et l'influence des paramètres machines et géométriques sur la répartition de température à la fin d'une période de chauffe appliquée sur des pièces en acier 4340 ayant une géométrie simple. La sélection des paramètres les plus importants du procédé sera basée sur des travaux de recherches antérieures. Pour atteindre ce premier objectif, la détermination des interactions entre ces paramètres, suite à des analyses statistiques de variation de température dans les régions d'intérêt, est essentielle afin de fournir les informations nécessaires pour établir des modèles de prédiction robustes et fiables. Le deuxième objectif consiste à développer des

méthodes et outils numériques d'optimisation couplées avec un modèle numérique de simulation 2D par éléments finis appliqués sur des géométries simples comme les disques, et dont le but est de minimiser le gap de température entre le milieu et le bord de la pièce et d'uniformiser le profil durci en utilisant des concentrateurs de flux type maître esclave. Les paramètres à optimiser dans cette partie seront les facteurs géométriques caractérisant le procédé. Des tests expérimentaux seront effectués pour valider cette approche. Le troisième objectif vise à étudier l'effet de bord avec des concentrateurs de flux en l'appliquant sur des engrenages. De même, dans cette partie, des approches statistiques seront adoptées pour étudier l'effet de bord et en se basant sur les résultats d'un ensemble de simulations par éléments finis conduit sur un modèle 3D. Ces résultats serviront aussi à créer des modèles prédictifs par réseaux de neurones artificiels. Ceux-ci présentent une variante précise et bien structurée capable d'estimer le profil final de température au bord et au milieu d'une dent d'engrenage et de fournir assez d'information sur le comportement de profil durci en fonction des paramètres clés du procédé de traitement thermique avec des concentrateurs de flux. La robustesse et la fiabilité de ces modèles de prédiction seront toujours évaluées à l'aide des tests de validations expérimentales.

- Plus spécifiquement, le projet permet de: Mener une étude de sensibilité de profil de dureté d'un disque en acier 4340 traité par induction en fonction des paramètres machines et facteurs géométriques avec validation expérimentale.
- Minimiser l'effet de bord d'un disque en acier 4340 traité par induction avec des concentrateurs de flux utilisant un modèle de simulation d'éléments finis axisymétrique avec validation expérimentale.
- Réduire l'effet de bord à l'aide de la méthode des surfaces de réponses et de la modélisation avec des réseaux de neurones artificiels d'un engrenage droit traité par induction avec l'emploi des concentrateurs de flux.

0.4 METHODOLOGIE

Afin de répondre aux objectifs soulignés du mémoire, une stratégie de recherche basée sur la simulation numérique est adoptée en trois phases ; en effet, le procédé de traitement thermique par induction fait intervenir un couplage de deux physiques complexes, l'électromagnétisme et le transfert de chaleur. Ainsi, la modélisation par éléments finis offre l'avantage de bien comprendre et maîtriser le procédé avec des outils de simulation puissante. Dans ce sens et dans une première phase, il s'agit de bien formuler les équations mises en jeu (équations de Maxwell pour l'électromagnétisme avec les équations de transfert de chaleur), de manière à bien identifier les paramètres de contrôle de procédé et afin de caractériser mathématiquement le physique de chauffage par induction, appliqué sur un composant de géométrie simple. La résolution de ces équations sera conduite avec le logiciel de simulation COMSOL Multiphysics sur des modèles en 2D et 3D. Toutes les simulations seront accomplies avec des études de convergence qui permettent d'avoir un bon compromis entre le temps de calcul et une précision satisfaisante des résultats. Des plans d'expériences et une analyse statistique des interactions entre les paramètres d'entrées et les paramètres de sortie caractérisant l'effet de bord et la distribution de température à la fin de la période de chauffe permettront le développement de modèles de prédictions simplifiés. Ceux-ci seront ensuite validés expérimentalement. Une deuxième phase de ce projet consiste à développer des outils d'optimisation numériques de température couplés avec le logiciel de simulation, appliqués sur la même géométrie étudiée dans la première phase, mais avec l'ajout des concentrateurs de flux de type maître esclave. Les résultats permettent d'apprécier qualitativement et de mesurer quantitativement l'effet de la technique des concentrateurs de flux. Dans cette phase, l'influence des paramètres géométriques distinctifs du procédé sur la variation d'effet de bord à la fin du traitement est étudiée. Des tests expérimentaux de validation permettront de valider à la fois les travaux d'optimisations numériques et l'approche adoptée pour la réduction d'effet de bord avec l'utilisation des concentrateurs de flux.

Une troisième phase consiste à construire des modèles prédictifs par réseaux de neurones en se basant sur les variables les plus influentes déterminées dans les étapes

précédentes. L'ensemble des données d'apprentissage sont obtenues d'une campagne de simulation effectuée sur le logiciel de simulation COMSOL et dont les niveaux des paramètres d'entrées sont identifiés en utilisant la méthode Taguchi, l'objectif étant d'obtenir le maximum de résultats avec le minimum d'essais. Les simulations et la validation expérimentale de cette phase sont effectuées sur des engrenages, pièces mécaniques de géométries plus complexes, afin de valider l'approche des concentrateurs de flux et les modèles de prédictions précédents.

Tous les travaux de simulation numériques sont effectués avec le logiciel de simulation COMSOL. Ce logiciel permet de simuler de nombreux phénomènes physiques et applications en ingénierie, et tout particulièrement les phénomènes couplés comme dans le cas des traitements thermiques par induction. Les travaux d'optimisation sont effectués avec l'interface « LiveLink » avec programmation de script dans l'environnement MATLAB. Les essais expérimentaux sont réalisés avec une machine à induction située à l'école de technologie supérieure à Montréal. Cette machine est équipée d'un générateur de fréquence radio à thyristors (200 kHz) et qui peut atteindre une puissance maximale de 450kW. L'inducteur utilisé est usiné en cuivre de type un tir, et ayant une section utile de 7 x 7 mm. L'analyse des phases et l'évaluation de la dureté à la surface des pièces traitées sont accomplies grâce à un microscope « Clemex MMT Type A » associé avec un microduromètre automatisé ayant un pénétrateur de type Vickers et en utilisant une charge de 300g. Les disques et engrenages étudiés sont fabriqués en acier 4340. Cet acier allié au nickel-chrome-molybdène est reconnu pour sa ténacité et sa capacité à atteindre des résistances élevées si traité thermiquement. Dû à sa très bonne résistance à la fatigue, cet acier est largement employé dans l'industrie automobile et aérospatiale.

Chaque étude s'achève par l'élaboration d'un rapport sous forme d'article. Le présent mémoire regroupe les trois articles écrits pendant les études de maîtrise.

0.5 ORGANISATION DU MEMOIRE

Outre cette introduction générale, ce mémoire est composé de trois chapitres rédigés sous forme d'articles, et il renferme une conclusion générale. L'introduction générale fait la lumière sur le procédé de traitement thermique en général, et expose également la problématique, les objectifs et la méthodologie de ce projet de recherche. Le premier chapitre présente une analyse des effets et des interactions des facteurs caractérisant le procédé de traitement thermique par induction sur la distribution de la température et la profondeur durcie d'un disque en acier 4340 chauffé par induction. Le deuxième chapitre présente une étude d'optimisation du profil durci d'un disque en acier 4340 soumis entre deux concentrateurs de flux et en se basant sur des méthodes numériques itératives. Le problème d'optimisation est résolu avec la méthode quasi-Newton et les résultats de simulation sont validés expérimentalement. Le troisième chapitre présente une étude de l'effet des paramètres caractérisant le processus de chauffage par induction sur la distribution finale de la température et la dispersion de la profondeur durcie sur des engrenages droits placés entre deux concentrateurs de flux. Dans le cadre de cette étude, des modèles prédictifs sont développés par la méthode d'analyse de la variance et avec des réseaux de neurones artificiels. Finalement, la conclusion générale complète la mémoire en soulignant les liens entre les objectifs énoncés et les résultats obtenus dans le cadre de ce projet, et en ouvrant ainsi des pistes pour d'autres travaux de recherches.

CHAPITRE 1

ÉTUDE DE SENSIBILITÉ DE PROFIL DE DURETÉ D'UN DISQUE EN ACIER 4340 TRAITÉ PAR INDUCTION EN FONCTION DES PARAMÈTRES MACHINES ET FACTEURS GÉOMÉTRIQUES AVEC VALIDATION EXPÉRIMENTALE

1.1 RÉSUMÉ EN FRANÇAIS DU PREMIER ARTICLE

Un processus de traitement thermique par induction adéquat doit toujours identifier, au préalable, la distribution finale de la température et le comportement du profil de dureté dans des régions spécifiques du composant traité, en fonction des paramètres intervenants dans le processus de traitement thermique. Dans ce sens, cet article présente une analyse des effets de certains facteurs géométriques liés aux paramètres du composant à traiter, de l'inducteur et de la machine à induction sur la distribution finale de la température et de la profondeur durcie d'un disque en acier 4340 chauffé par induction. Un modèle de chauffage par induction a été créé sous le logiciel de simulation COMSOL, définissant un groupe de paramètres de ce processus suivi d'une étude de maillage. Un algorithme développé sous Matlab et couplé au modèle de simulation a été conçu pour générer un grand nombre de simulations et d'extraire les profils de température pour chaque combinaison de paramètres. La profondeur durcie est ensuite interpolée à partir des données de température collectées et une analyse statistique a été développée pour créer un modèle de prédiction du profil de dureté. Les tests expérimentaux réalisés sur le même processus supportent les résultats du modèle numérique et approuvent la simulation, le modèle de prédiction et l'étude statistique.

Mots clés – Chauffage par induction, Simulation, Validation expérimentale, Étude de sensibilité, Disque en acier 4340

Ce premier article, intitulé « *Sensitivity Study of Hardness Profile of 4340 Steel Disc Hardened by Induction According to Machine Parameters and Geometrical Factors* », fut

co-rédigé par moi-même ainsi que par le professeur Noureddine Barka, le professeur Jean Brousseau et le professeur Philippe Bocher. Il fut accepté pour publication dans sa version finale en **12 octobre 2018** par les éditeurs de la revue « **The International Journal of Advanced Manufacturing Technology** ». En tant que premier auteur, ma contribution à ce travail fut la recherche sur l'état de l'art, le développement de la méthode, la création des modèles de simulation et de prédition, la gestion des données et résultats et la rédaction d'article. Les professeurs Noureddine Barka et Jean Brousseau ont fourni l'idée originale. Ils ont aidé à la recherche sur l'état de l'art, au développement de la méthode ainsi qu'à la révision de l'article. Le professeur Philippe Bocher, quatrième auteur, a contribué à l'exécution des tests expérimentaux. Une version électronique de cet article a été présentée avec l'identifiant numérique suivant : <https://doi.org/10.1007/s00170-018-2892-y>.

1.2 SENSITIVITY STUDY OF HARDNESS PROFILE OF 4340 STEEL DISK HARDENED BY INDUCTION BY THE VARIATION OF MACHINE PARAMETERS AND GEOMETRICAL FACTORS

1.2.1 Abstract

An adequate induction heat treatment operation should always identify, previously, the probable temperature distribution and hardness profile behavior in specific regions of the treated component according to heating process parameters. This paper presents an analysis of the effects of some geometrical factor related to the component and the coil and machine parameters on temperature distribution and case depth of an AISI 4340 steel disk heated by induction. A COMSOL model defines a group of process parameters followed by a mesh study. A MATLAB algorithm coupled to the simulation model was designed to handle a large number of simulations and export temperature profile data. The case depth is then interpolated from collected temperature data and a statistical analysis was developed to create the hardness prediction model. The experimental tests conducted under the same process parameters support the numerical model results and approve the simulation, the prediction modeling and the statistical study.

Index Terms— Induction heating, Simulation, Experimental validation, Sensitive study, 4340 steel disk

1.2.2 Introduction

For many years, induction heating has shown its success in the metallurgical industry, his remarkable productivity, energy efficiency and capacity to manipulate complex parts and various metal shapes has made it a popular tool in many industrial heat treatment applications like melting, injection molding, brazing and surface hardening [15, 54, 55]. Steel hardening by induction is a widespread application of induction heating that uses heat generated by electromagnetic fields and induced currents with rapid cooling (quenching) to increase the surface hardness of the steel [8, 40, 56]. The process consists of creating high heat intensity

at concentrated region on the surface of the metallic part. An alternative current characterized by its intensity and frequency is supplied to a coil. A magnetic field, which generated immediately inside the coil, induces a current at the metal part. This current creates heat due to Joule effect. As a result, the temperature rises at heated location up to austenitization point. Induction heating could be applied to a wide variety of shapes and sizes and requires no physical contact between the treated component and induction coil [10, 43, 57]. The AC induced current flowing decreases its density from the surface toward the internal part of the part. As a result, the produced heat distribution will be concentrated from the surface into a specific internal distance known as the penetration depth. After quenching, a very hard martensite structure will be created in the heated region defined from the surface up to the penetration depth.

The penetration depth is related essentially to current frequency, but other process parameters could also affect the depth of this concentrated region such as the machine and geometrical parameters. Machine parameters include current frequency (Fr), power density (P_M) and duration of the heating process (T_H) while geometrical parameters concerns the shape, the size, dimensions and relative positions of the treated component with an induction coil [32, 54]. The most important geometrical and machine parameters to consider in any induction heat application are the size of the treated object and its position beside the induction coil, where the most important machine parameters are current frequency, current density and heating time [32, 33].

The study of induction heat treatment process has several difficulties at the simulation and experimental level. There is a difficulty in managing the complex electromagnetic and heating physics that includes several parameters and coupled physical phenomena. Moreover, material property data are not accurate and vary dissimilarly with the temperature. Measuring adequately the temperature and the machine current during the heating process is a hard and challenging experimental task due to the quick heating rate. Researchers have proposed experimental and statistical methods that may be relevant to solve such problems. To make a good statistical study, it is necessary to choose the right parameters, to conduct

the experimental tests well and to analyze the obtained results adequately. There is researchers that proposed this approach by simulation [25, 31, 32], by simulation with validation [35, 53, 58], and experimentation with planning strategy [36-39]. These studies are carried out to analyze various mechanical and thermal effect on a wide and different part shape, using electromagnetic induction process, in order to qualify or improve hardness, residual stress, deformation and final temperature distribution. Researchers made possible by simulation and/or experiment tests and mathematical models are analyzed generally with L_9 to L_{34} orthogonal array of combination parameters chosen by several methods including Taguchi method and synthesized with statistical model including regression and ANOVA techniques with verification by confirmation tests. The chosen combination parameters include either machine parameters, like power, heating time and speed [31, 33, 39, 58], either machine and quenching parameters [36, 37], either machine parameters and metallurgical factors [38] or only geometrical part versus induction coil parameters [35]. This literature review demoted that there are no previous works that have combined both simulation and experimentation in statistical analyzes that include studying both of the machine parameters with the main geometric factors of the process. Therefore, the aim of this study is to develop a model that describes the hardness profile as a function of both geometrical and machine parameters based on a L_{81} orthogonal array. First, a 2D asymmetric model was developed, mesh studied and then validated by experimental data. Second, a Matlab algorithm was developed and coupled with Comsol to carry out the simulations with different set of parameters' configurations. Finally, Prediction equations of temperature profile and hardness depth were obtained by statistical analysis and partial experimental validation of extracted data.

1.2.3 Formulation

The formulation of induction heating process is described by an electromagnetic field (Maxwell's equations) in time-varying form neglecting displacement field. Which could be written as [54, 59] :

$$\text{Gauss's law} \quad \nabla \cdot D = \rho^{\text{charge}} \quad (1)$$

$$\text{Faraday's law} \quad \nabla \times E = -\frac{\partial B}{\partial t} \quad (2)$$

$$\text{Gauss's law for magnetism} \quad \nabla \cdot B = 0 \quad (3)$$

$$\text{Ampere's law} \quad \nabla \times H = J \quad (4)$$

With E , D , H and B describe respectively the electric field intensity (V/m), electric flux density (C/m^2), magnetic field intensity (A/m) and magnetic flux density (T). ρ^{charge} is the electric charge density (C/m^3) and J is the conduction current density (A/m^2) and could be expressed by Ohm's law:

$$J = \sigma E \quad (5)$$

E and D , H and B are related using equations 6 and 7.

$$D = \epsilon E \quad (6)$$

$$B = \mu H \quad (7)$$

With σ , ϵ and μ represents, respectively, the electrical conductivity (S/m), permittivity (F/m) and magnetic permeability (H/m) of the material. These parameters are temperature dependent and the material is considered to be homogenous. Since B satisfies a zero divergence condition, equation becomes

$$B = \nabla \times A \quad (8)$$

Where A is the magnetic vector potential. Since the field is time-harmonic, assumption of harmonically oscillating currents with single frequency make possible to write Eq. 2 in complex form such that

$$\nabla \times E = j\omega B \quad (9)$$

$$\nabla \times E = j\omega \nabla \times A \quad (10)$$

$$\nabla \times (E - j\omega A) = 0 \quad (11)$$

The curl is zero, the term $E - j\omega A$ will be equal to the gradient of a scalar function φ such that

$$\nabla \varphi = E - j\omega A \quad (12)$$

After multiplying with σ and inserting Eq. 5, Eq. 10 could be written as:

$$J = -\sigma \nabla \varphi - j\sigma \omega A \quad (13)$$

The current density could be written as the sum of an induced current J_i and an imposed external source current in the induction coil, J_0 such that:

$$J_i = -j\sigma \omega A \quad (14)$$

$$J_e = -\sigma \nabla \varphi \quad (15)$$

Inserting Eq. 7, eq. 8 and eq. 11 in eq. (4) gives

$$\frac{1}{\mu} (\nabla \times \nabla \times A) = J \quad (16)$$

$$\frac{1}{\mu} (\nabla \times \nabla \times A) = J_e - j\sigma \omega A \quad (17)$$

The resolution of Eq. 14 made it possible to determine the current density as a function of magnetic vector potential A which in turn could be deduced by resolving Eq. 17. The amount of heat generated inside the metal part due to joule heating is evaluated using the following equation.

$$Q_{ind} (W) = \int_v \frac{|J^2|}{\sigma} dV \quad (18)$$

The heat generated by induction is introduced into the heat equation in order to calculate the temperature distribution in the part. In induction heating, the heat transfer is described by Fourier's equation and it's given by [54]:

$$\rho C \frac{\partial T}{\partial t} = \nabla \cdot (k \nabla T) + Q_{ind} \quad (19)$$

Where T is the temperature (K). ρ , C and k are non-linear temperature dependent properties and represent respectively the mass density (kg/m^3), the specific heat ($\text{J}/\text{kg.K}$) and the thermal conductivity ($\text{W}/(\text{m.K})$) of material. A part of energy is lost by convection and radiation due temperature differences between part and surrounding air. Convection and radiation heat flux losses q_c and q_r between the workpiece and open air are defined respectively as

$$q_c = h_c(T_s - T_a) \quad (20)$$

$$q_r = \varepsilon \sigma_s (T_s^4 - T_a^4) \quad (21)$$

Where h_c is the convection coefficient, ε is the emissivity and σ_s is the Stefan-Boltzmann constant.

1.2.4 Simulation model

A disk made from low-alloy Steel (AISI 4340) is placed inside 8 x 8 mm square coil. The geometrical parameters to be considered are the width of the disk (mm) and its relative distance with the coil (gap (mm)). The model is represented in **Figure 1.1**. Due to geometry symmetrical properties, the model could be reduced from a 3D model into a 2D axisymmetric model, this geometry reduction increase the numerical computation time and gives approximately the same results. Temperature distribution in the part is evaluated by defining three points, T_M is the point on the middle of the surface, and T_{E1} and T_{E2} are the point on

the edge of outside surface. Due to symmetrical properties of the disk, the two edges will have the same temperature distribution so T_{E1} will be equal to T_{E2} .

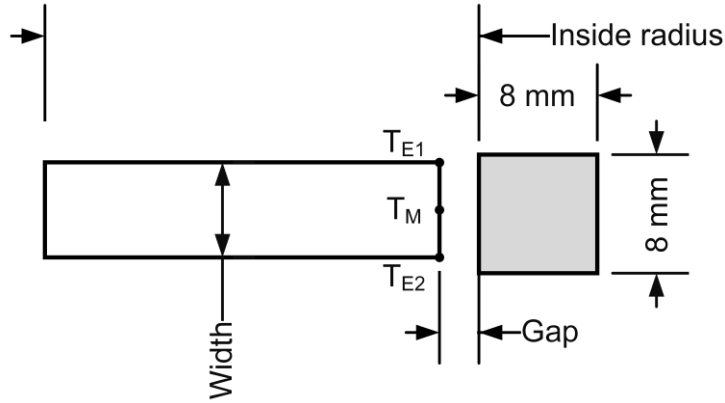


Figure 1.1 :Schematic representation of model components

1.2.4.1 Determination of power under typical configuration

Using induction-heating systems to harden the part requires changing its surface layer microstructure by heating it to temperatures that are above or inside the austenitization range. The temperature distribution after heating will not be uniform between the surface layer and the inner portion of the disk, and it will decrease rapidly while getting closer to the middle surface and the disk center [7]. The mesh size is very refined and it is fixed at 0.2 mm that generates 33677 elements and 135072 degrees of freedom. The heating time (T_H) is fixed at 0.5 s and the width (W_P) is fixed at 6.5 mm. Finally, the gap (G_s) is fixed at 2.5 mm. The outer surface exactly into the austenite transformation temperature will not ensure that the heat will propagate sufficiently along the internal part of the part and that will have no effect in changing the surface microstructure inside the disk. Since the high frequency heating is only studied, the frequency is fixed at 200 kHz. The last parameter to tune is the imposed current density (J_0). This parameter is replaced by the real machine power using the approximated ratio developed by Barka et al. [9]. The **Figure 1.2** shows the evolution of final temperature according the machine power. It is interesting to remark that the temperatures are identical at low power and the offset continues to increase to reach maximal value at 80

kW. The temperatures have a parabolic evolution and some variation caused by the material properties are occurred between 55 kW and 65 kW. To ensure that a transformation will occur inside the part, and that 100 percent austenite will be formed within treated area, the temperature used for austenitization must be above Ac₃, surface middle temperature of 900°C will be considered sufficient to meet these conditions. Considering all geometrical and machine parameters, the most flexible input parameter is power delivered by the machine into the induction coil because it can be changed softly and precisely from the simulation software by the machine operator with no risk of error. All the machines and geometrical parameters, except the input power, will be fixed into reference level as shown in **Table 1.1**. The input power values vary from 10 kW to 100 kW in the simulation with a step of 10 kW and very smooth mesh size of 0.1mm to see in which point the surface middle temperature T_M will exceed 900 °C.

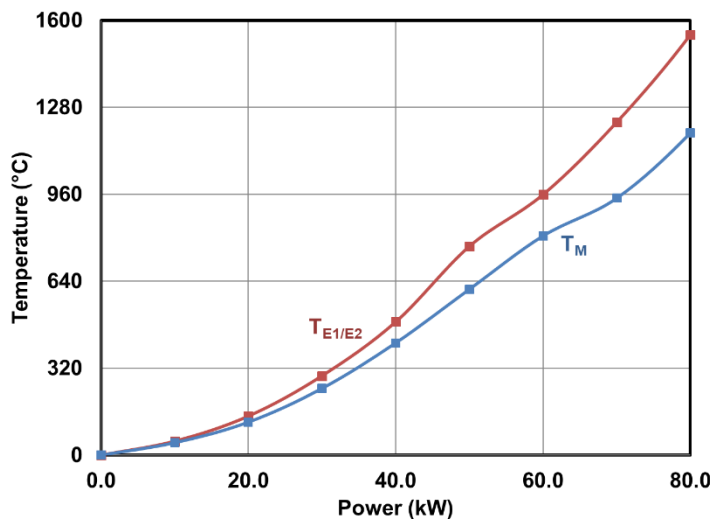


Figure 1.2 : Temperature evolution according the machine power

The edge and middle temperatures increase with power and could attempt very high levels that exceed the melting point from 80 kW. The edge temperature increases faster than the middle temperature due to the edge effect phenomena. Edge temperature exceeds 900 °C starting from 57 kW power machine value while middle temperature exceeds it with 66.5 kW input power value. A reference values are given in the **Table 1.1**.

Table 1.1 : Simulation parameters with fixed machine power

Parameters	P_M	T_H	W_P	G_s	F_R
Level	66.5	0.5	6.5	2.5	200
Unit	kW	s	mm	mm	kHz

1.2.4.2 Mesh convergence study

To determine the appropriate mesh size value, a mesh convergence study was carried out by Comsol. The default parameters of frequency, process duration, part width, the gap, and machine power were chosen to reach the austenitization point at the part surface ($T_M = 900 \text{ } ^\circ\text{C}$). **Figure 1.3** illustrates the evolution of temperature using the same machine parameters and geometrical factors according to meshing size. The truncation errors affect the evolution at the top of the value 0.45 mm, while the numerical errors affect this temperature down 0.15 mm.

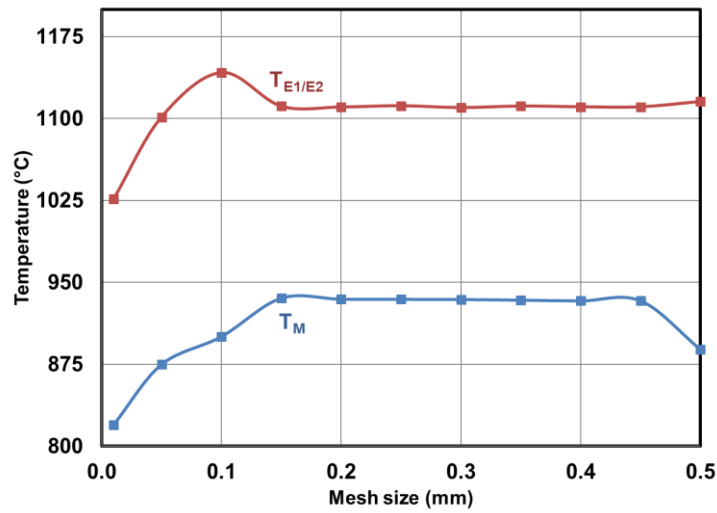


Figure 1.3 : Final temperature according the mesh size

Figure 1.4 shows the final configuration of optimal mesh obtained using the convergence study. Indeed, a simple section does not represent a good approximation of the problem since the induced currents are distributed at external surface.

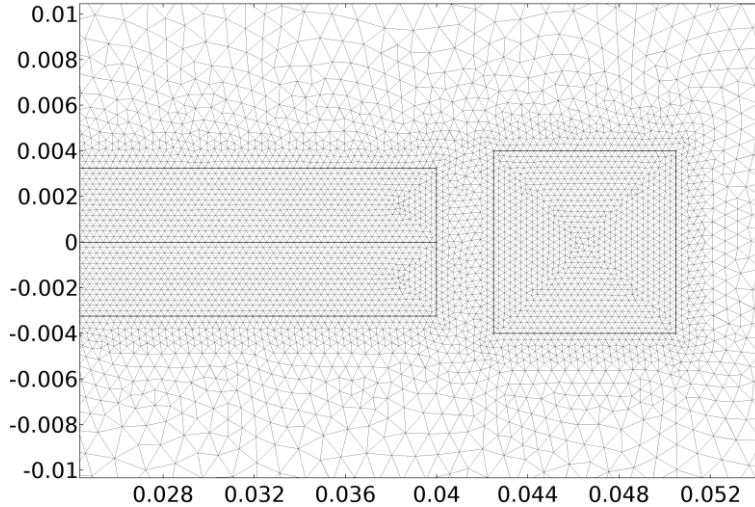


Figure 1.4 : Final mesh optimized by convergence study

1.2.4.3 Temperature and induced current distribution

Figure 1.5 shows the distributions of the total current density and the temperature after a heating time of 0.5 s in the case of high-frequency heating. The initial density of the current in the coil (J_0) is adjusted to also have a maximal temperature of 1100 °C. The currents are concentrated, in this case, on a thin layer in the edges of the coil and in the part because of the skin depth. The temperature profile is profounder at the edges than the middle plane since the currents are more concentrated at the corners of the coil. The preliminary results clearly show the presence of two electromagnetic effects, the skin effect and the edge effect. These results also show that the temperature distributions are a direct consequence of the currents induced in the part and this profile has a considerable effect on the final hardness profile.

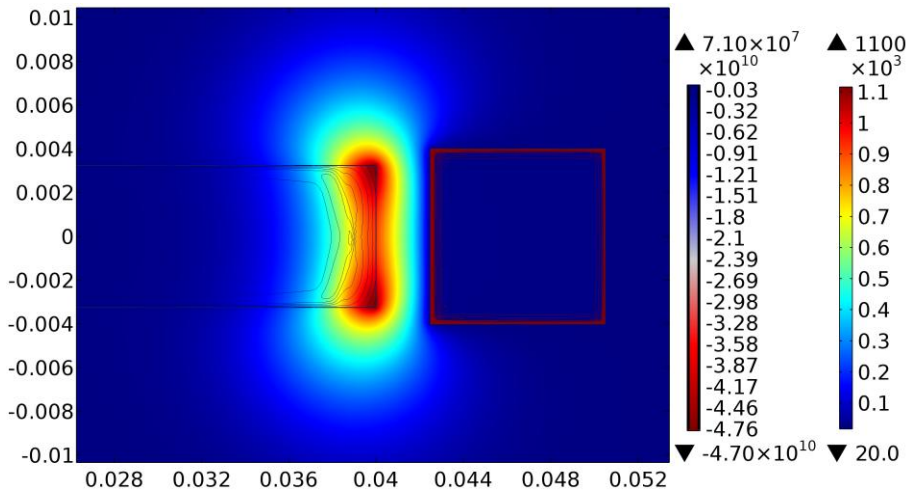


Figure 1.5 : Distributions of induction current (A/m^2) and temperature ($^\circ\text{C}$)

The temperature is at its maximum on the surface and decrease rapidly toward the disk center. Edge temperature is slightly higher than the middle, but still both have the same temperature profile for every heating step time. In the HF case, the temperatures are distributed over a larger area on the edge compared to the middle plane. In addition, the maximum temperature values record a clear offset of 280 °C between the edge and the middle (see **Figure 1.6**). The heated zone on the edge reaches 260 °C at a depth of 4 mm and 230 °C at the middle plane at the same depth. The temperature curve following the depth at the end of heating makes it possible to predict the hardened region and suggests that the region near the edges is transformed into hard martensite while that at the middle plane of the part does not reach the temperature necessary to martensite transformation. Similarly, if the temperature of 600 °C is assumed a legitimate assumption, the depths affected are 2.1 mm at the edge and 1.6 mm at the middle plane.

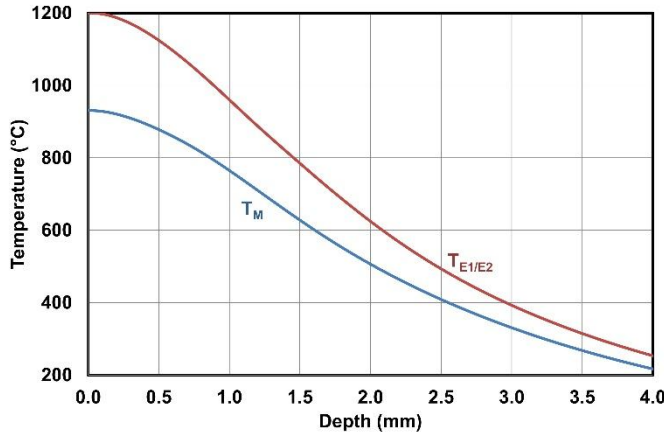


Figure 1.6 : Temperature distribution at the edge and middle profile

In order to interpret a temperature profile into a hardness profile, the critical austenitization temperatures Ac_1 and Ac_3 that characterize the heated region after 0.5 s must be considered. Thus, the temperature Ac_1 characterizes the onset of the formation of the austenite while the temperature Ac_3 characterizes the end of the martensite returned (initial microstructure) and all the regions heated above this temperature are austenitized to 100%. The region between the Ac_1 and Ac_3 temperatures is a mixture of austenite and unconverted returned martensite. The final temperature distribution has a direct impact on the hardness profile in the part and its evolution as a function of depth (surface hardness and hardened depth). If the assumption that all regions heated above Ac_3 (100% austenite) become martensite lasts after cooling and that this temperature for a heating time of 0.50 s is approximated to 850 °C, it is possible to appreciate the hardened depth for both the MF and HF cases on the edge and the middle plane.

1.2.4.4 Case Depth Deduction From Temperature Curves

The simulated case depth is deduced from critical transformation temperatures distribution across the disk assuming that a rapid cooling (quenching) is done perfectly after the heating process to form a new and hard martensite microstructure. The transformation temperatures are identified to be the critical temperature Ac_1 (825 °C) corresponds to the

apparition of first austenite germs. Ac_3 ($850\text{ }^{\circ}\text{C}$) corresponds to the temperature at which the last germs of austenite appear. Finally, the critical temperature (Tr) fixed at $640\text{ }^{\circ}\text{C}$ is assumed to be the lowest temperature that affects the part microstructure [48]. In fact, this temperature characterizes the depth where the hardness recovers the initial value in the part core. To retrieve the corresponding critical depth d_i for each critical temperature Ac_1 , Ac_3 and Tr , a linear interpolation function was used between the closest higher temperature and closest smaller temperature values with their corresponding depth values from the simulation results (see **Figure 1.7**). High surface hardness is related to martensite formation, which in turn is dependent upon heating to austenite range and cooling rate. Therefore, the simulation results and temperature distribution could reveal the shape and size of the hardened region and case depth.

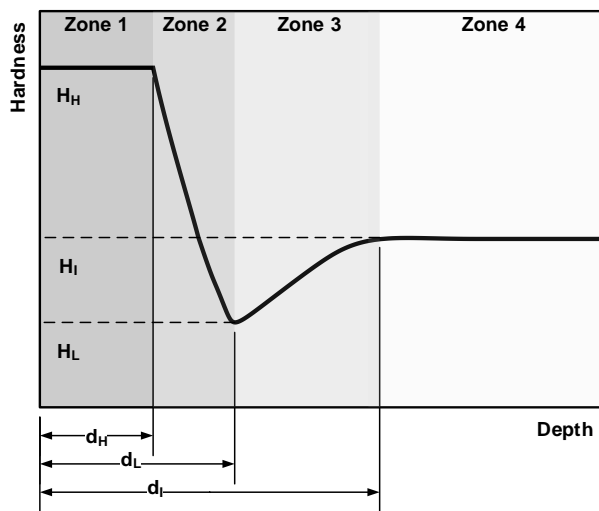


Figure 1.7 : Typical hardness profile by induction heating

1.2.4.5 Experimental Validation

Experimental validation tests are performed using the induction machine located at the École de Technologie Supérieure (Montréal, Canada). This machine contains solid-state converters (10 kHz) and thyristor radio frequency generator (200 kHz). The first one provides a maximum power of 550 kW and the second generator delivers a maximum power of

450 kW. This machine is capable of controlling both frequencies using the sequential double frequency heating concept and it is a numerically commanded using two numerical axes (see **Figure 1.8**).

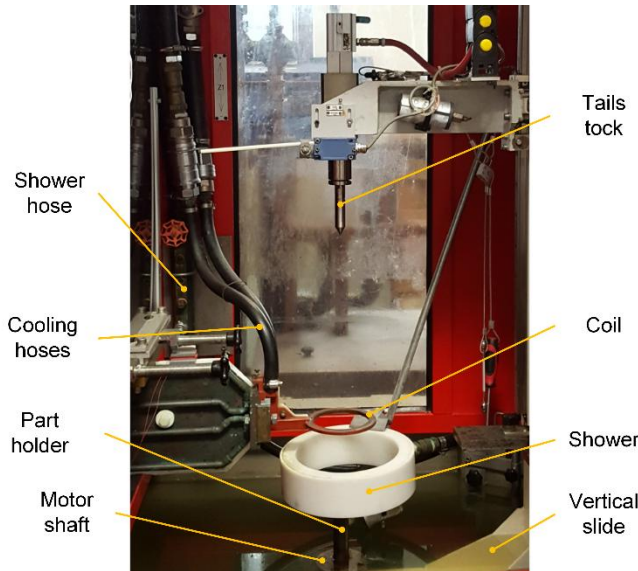


Figure 1.8 : Induction machine and operation system

The first test was done under the following machine parameters and geometry configuration. This tuning data illustrated in **Table 1.2** is used to validate the first model developed by simulation.

Table 1.2: Validation test parameters

Parameters	P_M	T_H	W_P	G_s	F_r
Level	72.6	0.5	6.5	2.5	200
Unit	kW	s	mm	mm	kHz

The hardness profile at the edge and middle of the disk obtained by the previous configuration is shown in **Figure 1.9**.

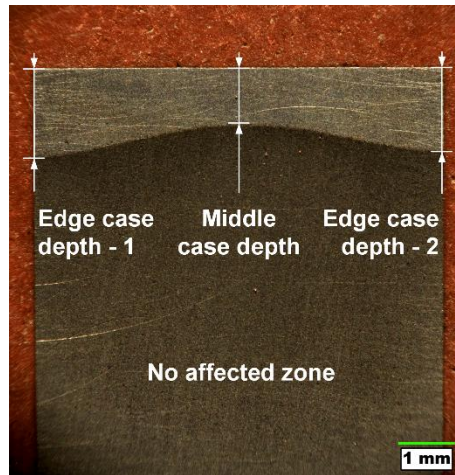


Figure 1.9 : Hardness profile obtained by experiments

It is important to note that the hardness profile is not uniform across the part section. Due to the edge effect, the magnetic field is concentrated more at the edges than in the middle. This fact generates a deep layer with important concentrated currents that heat more the edges than the middle. After being transformed to austenite, the regions are transformed to thin martensite. Due to lack temperature diffusion and skin effect, the non-affected zone towards the center of the disk remains with its initial hardness value and no structural and phase change occurs in this region.

As illustrated in **Figure 1.10**, the hardness curve measured at the edge and the middle has a typical hardness profile as expected with significant difference on critical depth for both positions, due to edge effect. It can be shown that a conformity in the shape exists between simulation and experimental tests for both edge and middle profile. One can remark that the hardness at the surface are slightly the same at the middle and the edges. It is also interesting to observe that the low hardness is about 370 HV and the over-tempered zones have the same width in both cases.

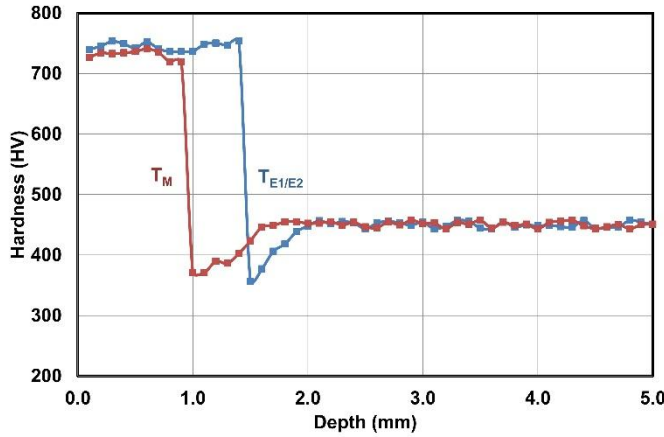


Figure 1.10 : Hardness curve on edge and middle obtained after the experimental test

1.2.4 Sensitive study - temperature

A sensitivity study was performed to determine the effects of geometrical (G_s and W_p) and machine parameters (P_m and T_h) with a fixed HF frequency (200 kHz). In order to avoid reaching melting point temperature during the heating process especially at the edge; which refers to the maximum configuration parameters and considering that temperature at the middle surface must reach at least austenitization points at the end of the process, which refers to the minimum configuration parameters, a range of parameters between maximum and minimum group values are chosen based on Taguchi method and verified by simulation (**Table 1.3**). Each of the four independent variable will be calculated in three levels, giving 81 possible configurations and corresponding to the 81 simulations.

Table 1.3 : Simulation planning

Parameters	P_m	T_h	W_p	G_s
Level 1	70	0.4	6.3	2.4
Level 2	72.5	0.45	6.5	2.5
Level 3	75	0.5	6.7	2.6
Unit	kW	s	mm	mm

The classical technique for handling simulation is exploited manually, but since the number of configuration is great and the mesh is very condensed, this kind of manual work of input and result extraction will take a very long time [32]. To optimize this time and effort problem, all 81 simulations were automatized by writing a MATLAB code coupled with a COMSOL built-in functions. This automated method solution reduced the calculation and results extraction into just six hours even with a very condensed mesh size. Results were the temperature distribution alongside the edge and the middle plan of the heated disk. Statistical analysis was performed to analyze the effect of these independent geometrical and machine parameters on temperature distribution and hardness profile.

1.2.4.1 Simulation Data

The following data presented in **Tables 1.4** and **1.5** are extracted from results simulations and summarize the temperature values at middle and edge of the part. It can be shown that final process temperatures are above the austenitization temperature Ac_3 as desired and respects the non-melting condition for the middle region but it can be reached at the following condition at the edge (75 kW, 0.5 s, $G_s = 2.4$ mm and $W_p = 6.3$ mm), and the following configuration is the extreme case and temperature is at its highest values.

Table 1.4 : Temperature at the middle obtained by simulation (°C)

P_M (kW)	70	70	70	72.5	72.5	72.5	75	75	75	
T_H (s)	0.4	0.45	0.5	0.4	0.45	0.5	0.4	0.45	0.5	
G_s (mm)	W_p (mm)	Middle Temperature (°C)								
2.4	6.3	898.69	932.71	990.54	929.15	991.98	1059.52	985.20	1055.49	1149.86
2.4	6.5	875.11	921.33	963.82	918.52	965.41	1051.26	951.35	1029.52	1077.01
2.4	6.7	863.52	901.28	966.58	919.76	966.56	1015.29	956.30	1014.84	1115.50
2.5	6.3	886.47	910.39	953.67	903.01	956.44	1007.69	941.00	1008.05	1092.41
2.5	6.5	878.42	891.80	931.04	889.07	932.74	982.96	928.18	979.81	1068.63

2.5	6.7	868.44	911.22	920.28	881.94	921.71	964.80	911.76	972.26	1033.97
2.6	6.3	843.64	868.30	934.02	866.08	907.10	965.83	897.91	960.29	1028.68
2.6	6.5	829.53	886.57	920.58	886.71	891.26	957.98	903.40	959.04	1006.20
2.6	6.7	842.04	881.34	883.10	879.11	898.37	941.02	890.88	937.82	986.56

Table 1.5 : Temperature at the edge obtained by simulation (°C)

PM (kW)		70	70	70	72.5	72.5	72.5	75	75	75
TH (s)		0.4	0.45	0.5	0.4	0.45	0.5	0.4	0.45	0.5
GS (mm)	WP (mm)	Edge Temperature (°C)								
2.4	6.3	1146.41	1203.83	1271.65	1211.86	1288.32	1358.62	1294.99	1373.53	1452.56
2.4	6.5	1162.56	1193.67	1250.98	1201.92	1267.58	1355.85	1277.41	1346.76	1411.22
2.4	6.7	1146.21	1169.32	1260.99	1208.40	1284.44	1325.88	1281.10	1341.49	1428.63
2.5	6.3	1115.48	1183.61	1222.56	1181.22	1240.59	1298.45	1238.30	1314.41	1408.97
2.5	6.5	1104.81	1137.56	1200.39	1144.54	1217.47	1274.61	1222.68	1285.78	1398.39
2.5	6.7	1088.32	1121.54	1189.17	1133.55	1203.45	1260.54	1212.70	1284.79	1354.79
2.6	6.3	1109.42	1099.50	1178.32	1107.12	1186.28	1245.26	1190.45	1258.63	1331.16
2.6	6.5	1094.25	1115.09	1165.46	1129.17	1172.73	1250.44	1196.95	1273.14	1313.49
2.6	6.7	1083.84	1109.23	1152.32	1117.43	1190.37	1227.27	1183.06	1239.37	1297.15

1.2.4.2 Contributions on final temperature distribution

After performing statistical analysis on simulation results, the contribution of each factor on the final temperature could be interpreted. **Table 1.6** shows the contribution factor percentage for each parameter on edge and middle temperature. It can be shown that T_E and T_M are highly influenced by the power and the heating time. Both contribute in more than 70% on final temperature values. Power has more effect on the edge (45.62%) than the

middle temperature (32.92%) while heating time has more contribution on middle temperature (40.05%) than edge temperature (31.84%). The gap has an important effect and it is involved in more than 17% for both middle and edge temperatures. The part width has no significant effect and could be neglected.

Table 1.6 : Contribution factor percentage for each parameter on edge and middle temperature

Parameters	Edge	Middle
PM	45.26 %	32.92 %
TH	31.84 %	40.05 %
WP	1.11 %	2.44 %
GS	18.25 %	17.48 %
PM x TH	0.92 %	2.12 %
PM x GS	Insignificant	0.97 %
Error	2.61 %	4.07 %

1.2.4.3 Simulated versus predicted temperatures

One goal of this study is to find a model that gives the most valid prediction of the edge and surface temperature given the geometrical and machine parameters. The ANOVA statistical study gives equation that describes the predicted relationship between temperatures in function with all other parameters for the edge and the middle point. The fitness of the model should be examined and evaluated. Experimentally, it is a difficult task to measure instantly the temperature distribution across the part section as the process happens very quickly. **Figure 1.11** presents the scatter plot for T_E and T_M . It is clear that for each simulated response value, the predicted value is at the diagonal line, due to the low value of the residual errors. Consequently, for each value of temperatures, the predicted and simulated curves are

nearly identical, which explains the good agreement between the predicted and the measured values. The linear fitting criteria that the prediction equation is able to assume a satisfactory level of accuracy with simulation results.

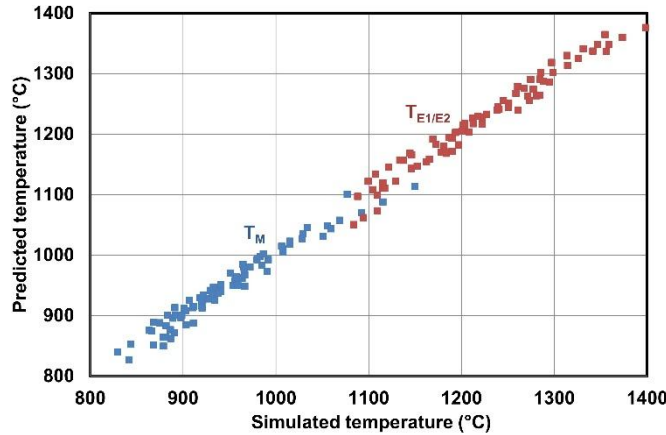


Figure 1.11 : Simulated temperatures versus predicted temperature at middle and edges

After eliminating the non-significant terms, the empirical relationship between the temperatures at the edge and the middle of the heated part by equations 23 and 24. The equations present an approximate model based on linear regression and allows the evaluation of the temperature according the machine parameters and the geometrical factors.

$$T_E = 3415 - 16.66xP_M - 6159xT_H - 57.1W_P - 462.8xG_S + 101.8xP_MxT_H \quad (23)$$

$$T_M = -2709 + 61.3xP_M - 7282xT_H - 62.76xW_P + 2402xG_S + 114.5xP_MxT_H - 37.76xP_MxG_S \quad (24)$$

1.2.4.4 Parameters effects

The average effect of geometrical and machine parameters on the final edge and machine temperature are presented in **Figures 12.a** and **12.b**. Each factor contribute by its own degree on the temperature. The power and heating time have the biggest influence. An increase of 2.5 kW in machine power contribute to an increase of 80 °C in edge temperature and 40 °C on middle temperature. A short increase on the heating time (0.05s) leads to an

important temperature rise for both points, at about 50 °C increase on the edge temperature and 40 °C on middle temperature. Geometrically, the temperature decreases significantly when increasing the gap. A 0.1 mm of gap variation leads to a temperature drop of about 60 °C on the edge and about 40 °C at the middle. The part width (W_P) has no significant influence of the final temperature distribution. A 0.1mm of W_P variation decreases the temperature by 10 °C in the edge and 20 °C at the middle. It is important to note that, unlike other factors, part width has more influence on middle temperature than the edge temperature.

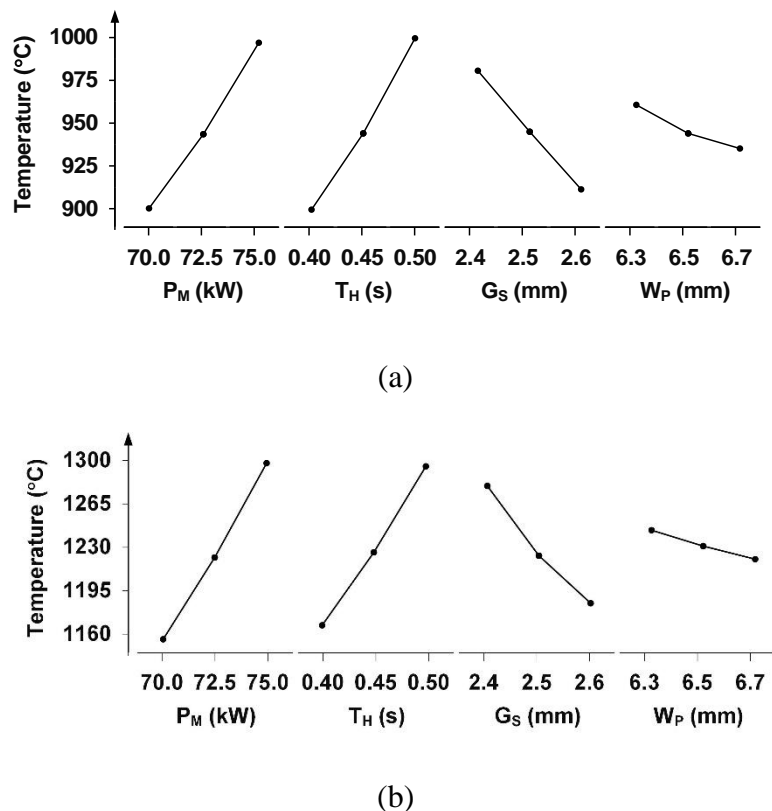
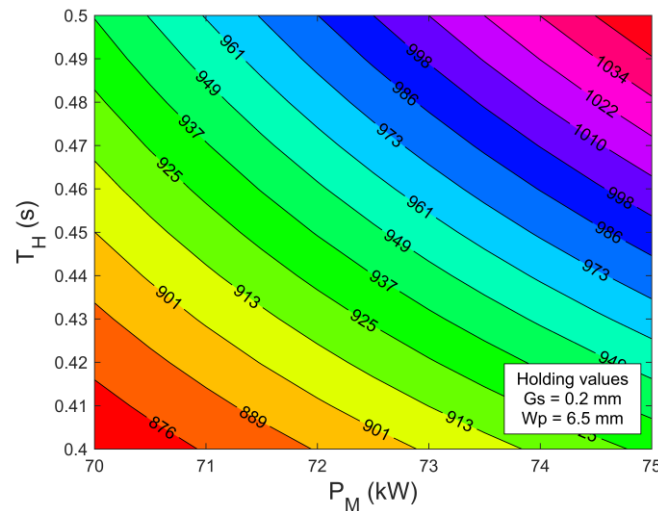


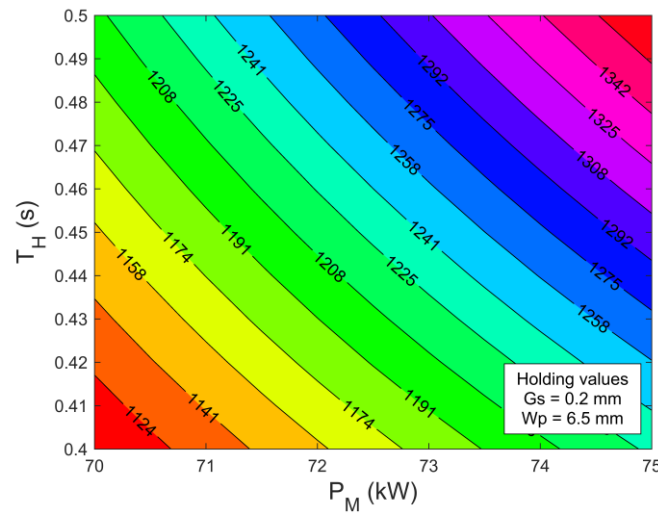
Figure 1.12 : Effect of geometry factors and machine parameters on temperature (a) middle and (b) Edge

The response surface methodology (RSM) given by ANOVA analysis is a fast and powerful way to predict the final temperature in function with the process parameters. Edge and middle temperatures are presented according to the power and heating time values. The gap and the part width are maintained in typical centered values of 2.5 mm and 6.5 mm. It

can be shown that for both points, temperature has a parabolic profile and increases proportionally with the power and heating time. **Figure 1.13** illustrates the RSM obtained in the edge and at the middle of the heated part.



(a)



(b)

Figure 1.13 : Response surface methodology of surface temperature (a) middle (b) edge

1.2.5 Sensitivity study of case depth

The final temperature distribution is converted to the hardness curve using Matlab. In fact, the temperatures according the depth at the middle and at the edge are converted to the hardness curve as explained using **Figure 1.7**. After interpolating the critical depth values d_H , d_L and d_I corresponding respectively to critical temperatures Ac_3 , Ac_1 and Tr , statistical analysis was done to deduce the contribution of geometrical and machine parameters on these simulated critical depth. According to statistical analysis (**Tables 1.7 and 1.8**), the most important factor having effect on the case depth is the heating time with about 50% contribution percentage. The machine power contributes significantly on the final case depth with about 35.4% on the edge and 27% at middle. The influence of the part width is insignificant with about 0.74% on edge and 2.5% at middle. However, the gap has an important effect on the case depth with about 13% contribution percentage on the edge and 17% contribution percentage in the middle. The analysis results also demonstrate that the geometrical factors contribute much more in the middle than at the edge.

Table 1.7 : Contributions in the edge

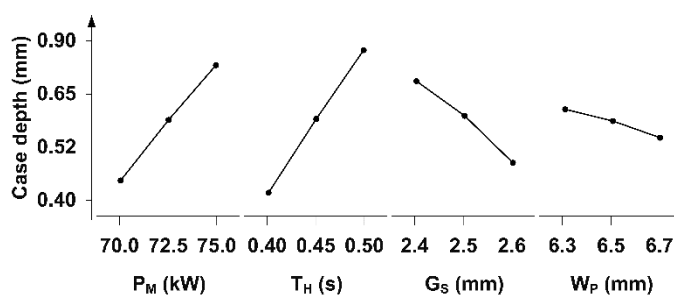
Parameter	d_H	d_L	d_I
P_M	35.39 %	34.54 %	28.22 %
T_H	48.3 %	49.6 %	59.26 %
W_P	0.74 %	0.73 %	0.69 %
G_s	12.91 %	12.48 %	9.47 %
Error	2.66 %	2.66 %	2.36 %

Table 1.8 : Contributions at the middle

Parameter	d_H	d_L	d_I
P_M	26.98 %	30.6 %	24.41 %
T_H	50.01 %	49.46 %	60.45 %
W_P	2.54 %	1.98 %	2.61 %
G_s	16.93 %	15.01 %	9.61 %
Error	3.54 %	2.95 %	2.93 %

1.2.5.1 Parameters effects

Figure 1.14 represents respectively the case depth in the edge and at the middle layer after heating and assuming a perfect quenching process in function of machine power and heating time, maintaining the part width and gap in their centered value. It is clear that case depth has a linear profile and increase in the same rate with time and power. As is known, due to edge effect, the case depth has bigger values on edge than in the middle layer. The case depth value is up to 1.62mm in the edge and 1.04 mm in the middle.



(a)

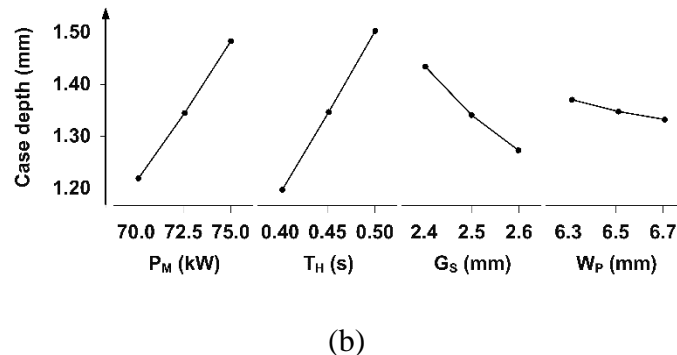
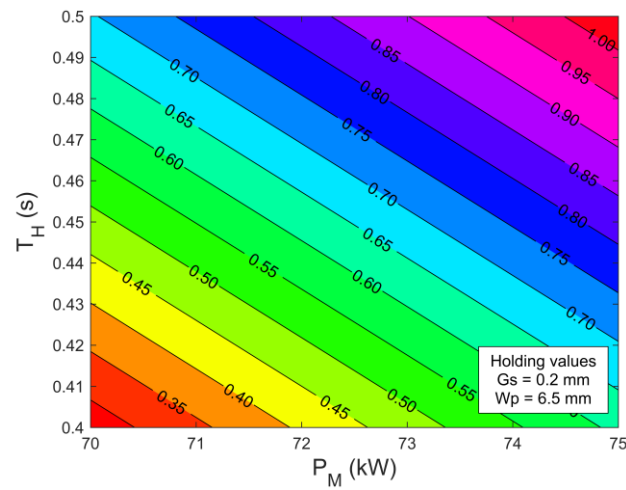
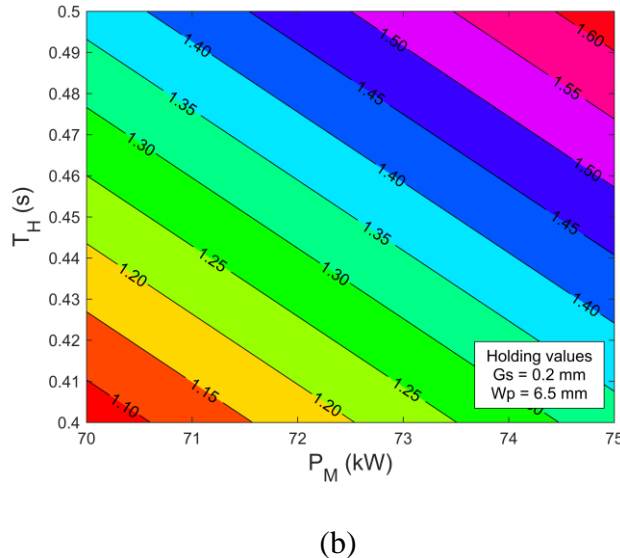


Figure 1.14 : Effect of geometry factors and machine parameters on case depth (a) Middle and (b) Edge

Figure 1.15 describes the average effect of geometrical and machine parameters on the case depth. The response of case depth is analogous to temperature distribution and the effects of variant parameters on it are similar. A small increase in the machine parameters increases the case depth rapidly while increasing the geometrical parameters values have the opposite effects. The case depth is higher under these conditions (75 kW , 0.5 s , $G_s = 2.4 \text{ mm}$ and $W_s = 6.3 \text{ mm}$), and lower under the following configuration (70 kW , 0.4 s , $G_s = 2.6 \text{ mm}$ and $W_s = 6.7 \text{ mm}$).



(a)



(b)

Figure 1.15 : Response surface methodology of case depth in (a) middle and at (b) Edge

1.2.5.2 Simulated versus predicted case depths

ANOVA Analysis gives the following equations describing critical depths d_H , d_L and d_I in function of geometrical and machine parameters. It can be shown from **Figure 1.16** that the predicted and simulated depths values are strongly correlated. The next part will examine the correctness of the predicted model equations with experimental results. **Figure 1.16** presents the scatter plot for depths at edges and in middle locations. It is clear that for each measured response value, the predicted value is close to the diagonal line, due to the low value of the residuals of the predicted values. For each value of depth, the predicted and measured curves are nearly identical, which explains the good agreement between the predicted and the measured values.

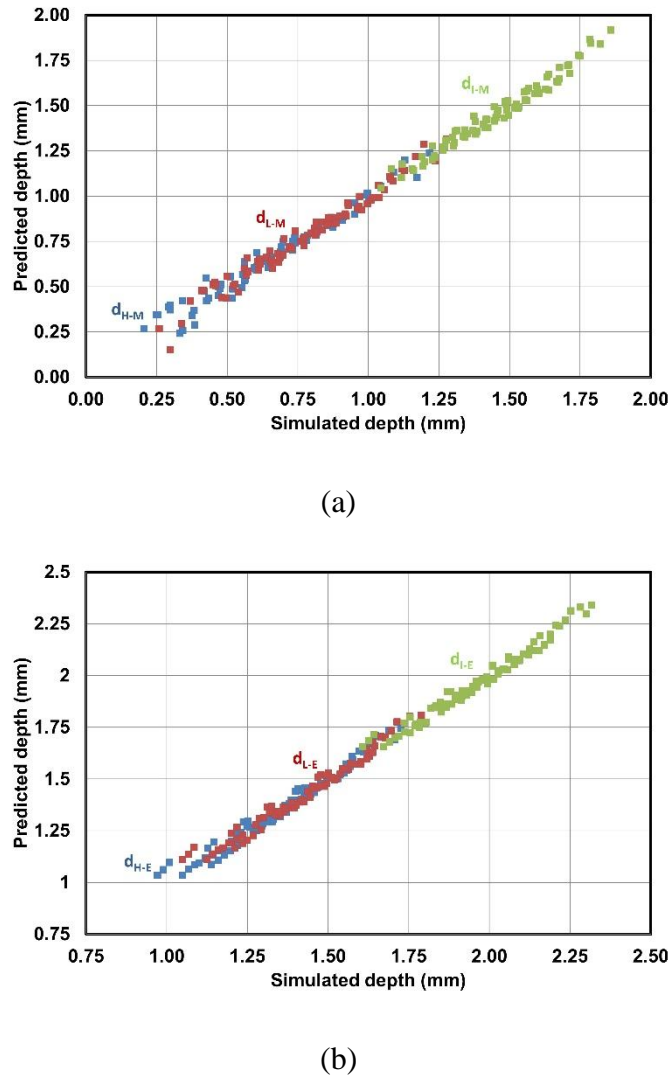


Figure 1.16 : Simulated depths versus predicted depths in (a) middle and (b) edges

1.2.6 Experimental validation

Experimental validation tests were done under the following configurations, illustrated in **Table 1.9**. The obtained results demonstrate that finite element simulation combined to practical tests can be used advantageously for the development of recipes intended to develop mechanical components by induction.

Table 1.9 : Experimental planning

Parameters	P_M	T_H	W_P	G_s	F_R
Test 2	42.9	1	6.5	2.5	200
Test 3	56.1	1	6.5	2.5	200
Unit	kW	s	mm	mm	kHz

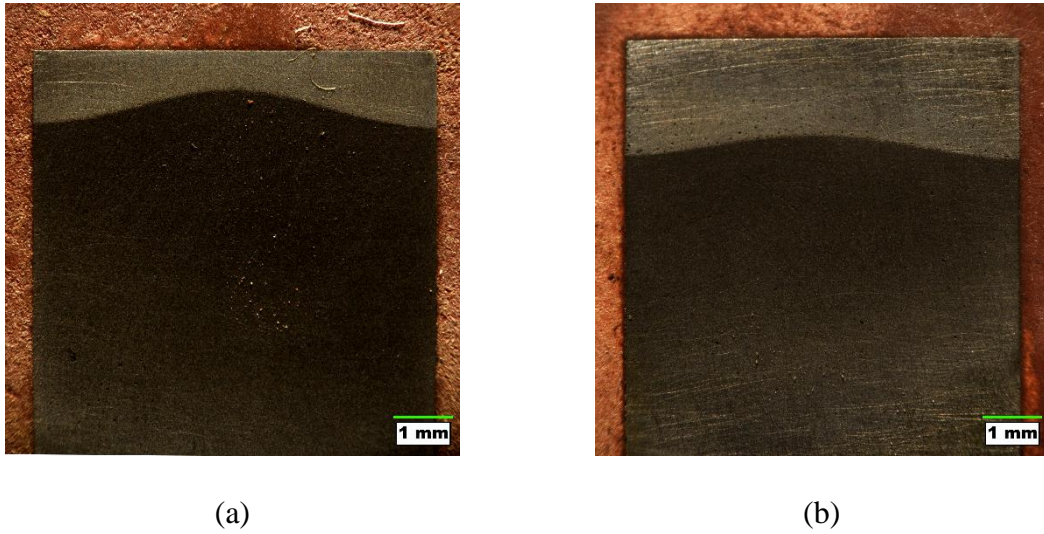


Figure 1.17 : Cross-section of hardness profile obtained by Test 2 (a) and Test 3 (b)

Results show that the prediction model and experimental data fit together and that error between the three curves is relatively low and is about 5% up to 19%. The marge of error is smaller for experimental tests where input power and heating time values are close to those used in the simulation. Still, the mathematical model is reliable for predicting the effect of input parameters on critical depths and to predict the over-tempered zone.

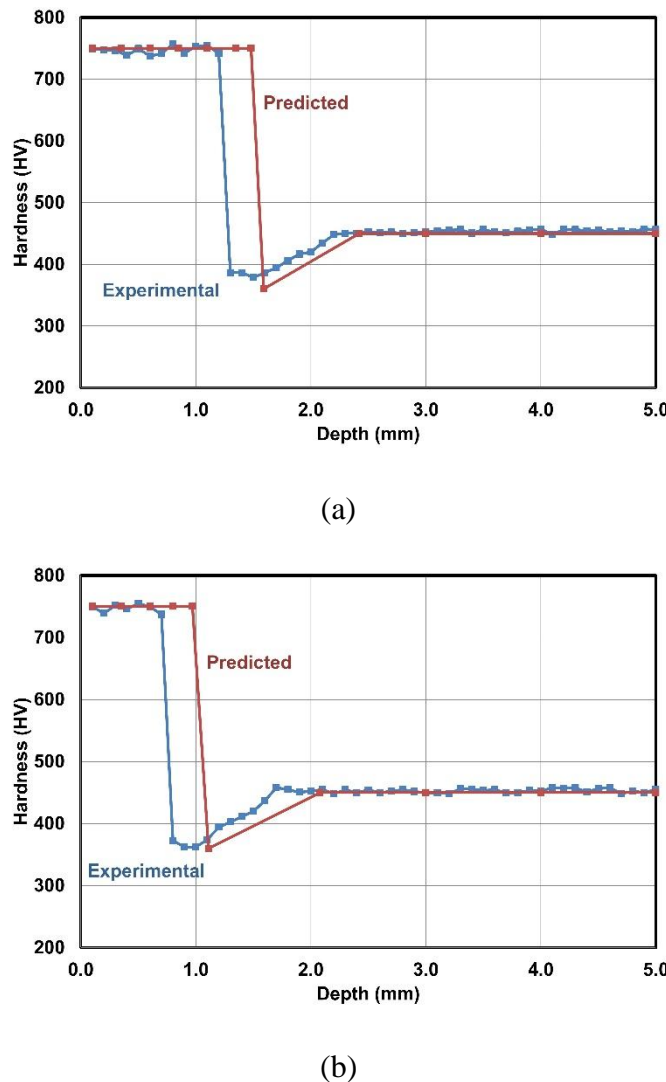


Figure 1.18 : Predicted and measured hardness curves for Test 2, (a) edge and (b) middle

1.2.7 Conclusion

The main feature of this study is the great number of simulation done in order to create a reliable and acceptable model that predicts the effect of geometrical and machine parameters on the hardness depth of an AISI 4340 low-alloy steel disk heated by induction. First, a 2D axis-symmetric model was developed using COMSOL that couple

electromagnetic and thermal heating to create and design the temperature distribution on the disk after induction heating process. A power and mesh convergence study was carried out to identify and select the best and typical machine, geometry configuration for the simulation work. A MATLAB algorithm development has greatly reduced and optimized the simulation time. Statistical analysis using ANOVA on the case depth, which values was extracted from the final temperature distribution, has shown great concordance between the mathematical model and experimental results, with an average error less than 15%. In summary, the obtained mathematical model implies a very good ability to predict the hardness and the overtempering zone when the experimental values are close to simulation parameters input. It is interesting also to expand the developed MATLAB algorithm and mathematical models on other work and studies such as optimization problems and working on complex geometries such as spurs and helical gears.

CHAPITRE 2

OPTIMISATION DE L'EFFET DE BORD D'UN DISQUE EN ACIER 4340 CHAUFFÉE PAR INDUCTION AVEC DES CONCENTRATEURS DE FLUX UTILISANT UN MODÈLE DE SIMULATION PAR ÉLÉMENTS FINIS AXISYMMÉTRIQUE ET AVEC VALIDATION EXPÉRIMENTALE

2.1 RÉSUMÉ EN FRANÇAIS DU DEUXIÈME ARTICLE

Cette recherche est effectuée par une simulation d'éléments finis axisymétrique 2D basée sur le couplage de champs électromagnétiques et de transfert de chaleur appliquée sur un spécimen en acier 4340 avec des concentrateurs de flux chauffés par induction. Le modèle est construit à l'aide du logiciel COMSOL, basé sur une formulation adéquate et tenant compte des propriétés du matériau et des paramètres de processus. Les courants induits et la distribution finale de température obtenue sont analysés par rapport aux dimensions géométriques du modèle. L'originalité de cet article réside dans l'exploitation de données de simulation utilisant la modélisation classique et les techniques d'optimisation permettant d'optimiser le profil de dureté en fonction de facteurs géométriques. La méthode proposée consiste principalement à utiliser des simulations par éléments finis pour modéliser le comportement du processus et déterminer une fonction objective adéquate capable de converger vers le profil de dureté linéaire optimal. Les résultats obtenus démontrent que le profil de dureté finale peut être amélioré et quasi uniforme dans les cas où le gap entre le concentrateur de flux et la pièce principale est réduit, et lorsque le gap entre la pièce principale et l'inducteur est plus important. Cette étude globale permet une bonne exploration de la linéarité de plusieurs profils de température à la fin de chauffe sous différentes combinaisons géométriques et une bonne compréhension du comportement des concentrateurs de flux pour un processus de traitement thermique par induction.

Mots clés - chauffage par induction, disque en acier 4340, modèle 2D, haute fréquence, concentrateurs de flux, optimisation

Ce premier article, intitulé « *Optimization of edge effect of 4340 Steel Specimen Heated by Induction Process with Flux Concentrators – Simulation and Experimental Validation* », fut co-rédigé par moi-même ainsi que par le professeur Noureddine Barka, le professeur Jean Brousseau et le professeur Philippe Bocher. Il fut soumis pour révision et publication dans sa version initiale en **25 Janvier 2019** par les éditeurs de la revue « **Journal of Materials Engineering and Performance** ». En tant que premier auteur, ma contribution à ce travail fut la recherche sur l'état de l'art, le développement de la méthode, la création des modèles de simulation et de prédition, la gestion des données et résultats et la rédaction d'article. Les professeurs Noureddine Barka et Jean Brousseau ont fourni l'idée originale. Ils ont aidé à la recherche sur l'état de l'art, au développement de la méthode ainsi qu'à la révision de l'article. Le professeur Philippe Bocher, quatrième auteur, a contribué à l'exécution des tests expérimentaux.

Submission Confirmation

 Print

Thank you for your submission

Submitted to
Journal of Materials Engineering and Performance

Manuscript ID
JMEP-19-01-17603

Title
Optimization of edge effect of 4340 Steel Specimen Heated by Induction Process with Flux Concentrators -
Simulation and Experimental Validation

Authors
Khalifa, Mohamed
Barka, Noureddine
Brousseau, Jean
Bocher , Philippe

Date Submitted
25-Jan-2019

2.2 OPTIMIZATION OF THE EDGE EFFECT OF 4340 STEEL SPECIMEN HEATED BY INDUCTION PROCESS WITH FLUX CONCENTRATORS USING FINITE ELEMENT AXIS-SYMMETRIC SIMULATION AND EXPERIMENTAL VALIDATION

2.2.1 Abstract

This research is performed by 2D axis-symmetric finite element simulation based on the coupling of electromagnetic fields and heat transfer applied on 4340 Steel Specimen with flux concentrators heated by Induction Process. The model is built using COMSOL software based on an adequate formulation and taking into account the material properties and process parameters. The obtained induced currents and temperature distributions are analyzed versus the geometrical dimensions of the model. The originality of this paper lies in the exploitation of simulation data using classical modeling and the optimization techniques to optimize the hardness profile according to geometrical factors. The proposed method is based on finite element simulations and adequate objective function able to converge to the optimal linear hardness profile. The results demonstrate that the final hardness profile can be quasi-uniform with a narrow flux concentrator gap and when the gap between de master part and the inductor is larger. This overall study allows a good exploration of several hardness profile linearity under various geometrical dimensions and permits a good comprehension of induction heating with flux concentrator behavior.

2.2.2 Introduction

The automotive and aerospace manufacturing industry is always in the face of the challenge of the growing demand for more efficient and higher performance components. In order to improve the mechanical behavior of engineering parts such as gears and crankshaft, basic understanding of failure modes is important. During their service, components are subject to cyclic and heavy loads, and crack initiation is linked essentially with the magnitude and direction of stresses applied to the component. Studies have shown that residual stresses play an important role in the distortion of machined components, and have an important

impact the fatigue life and the endurance of the engineering component [60, 61]. Residual stress arise as a consequence of manufacturing and treatment process of the part, especially in those processes where the internal microstructure of the component undergoes volume expansions due to heat treatments such as welding and surface hardening with rapid cooling [37, 60]. Tensile residual stresses are not beneficial as they increase the likelihood of fatigue failure by promoting crack initiation and growth. Otherwise, compressive residual stresses in the surface layer are very beneficial to counteract crack development and to improve stress corrosion cracking resistance and fatigue behavior [37, 62]. The different processes and methods used in the component manufacturing steps therefore all play an important role in the final distribution of residual stresses [36]. Furthermore, many scientists are trying to develop finite element models (FEM) capable of predicting the residual stresses induced by different manufacturing processes [7, 9, 63, 64]. These models will subsequently minimize the distortion phenomenon while reducing the number of steps and also modify the machining methods without affecting the properties of the components.

In induction hardening, where the surface of parts such gears and disk are heated to high temperature with rapid cooling, a compressive residual stress could be conceived by the generation of high temperatures, microstructural and mechanical properties gradients between the surface layer and the core of the component [20, 40]. Change of austenite to martensite after quenching is accompanied with a hardness and volume increase that is proportional to the carbon percentage contained in the treated material [65]. This thermal expansion due to temperature gradient and phase change produce beneficial state of compressive residual stress that can be predicted and/or controlled according to several factors involved in the induction heating process, such as the cooling rate [66] and final temperature distribution before quenching [67, 68]. Furthermore, the fatigue strength is proportional to the thickness of the hardened surface layer, and changes depending on the hardness distribution [69]. Indeed, the hardened region is directly related to the microstructure composition which could be interpreted from the final temperature distribution of the heating process. Measuring temperature distribution during induction heating process is a difficult task to do regarding the very quick heating rate of the induction

process. Some researchers have developed experimental method to measure surface temperature profile at the end of induction heating [70]. Therefore, developed FEM models are very useful to predict accurately the real behavior of the temperature distribution[32], not to mention that experimental designing and testing technologies are always associated with high costs process.

It is always advantageous to control temperature distribution at the end of the process. In induction heating of disk and gears with single shot, the non-uniformity of power density distribution is dependent to magnetic field distortion at the surface and near the edge of components, so called the edge effect, which could be predicted and controlled by many factors like system geometry, coil power, frequency and heating time [31]. Barka et al. [53] introduced a simple and effective approach to reduce the edge effect for gears without affecting coil geometry or process parameters, the technique consists of putting the main gear between two identical gears with some axial gap and acting like flux concentrators to the middle part. In this paper, the possibility of optimizing this approach is examined and applied on disk made of 4340 low carbon steel, and using FEM model coupled with optimization algorithms with experimental validation to generate the optimal geometrical parameters that gives the best hardness profile at the end of the process.

2.2.3 Methodology

The chosen model is a finite element model of the coil and the treated parts, and well adapted to complex geometries which guarantees an increased precision of simulated phenomena. The proposed algorithm is based on the coupling between numerical simulations and finite element analysis, with the aim of developing a system capable of automatically generating an optimal configuration. Thus, an iterative procedure is used for dimensioning the different gaps between the process components, it consists of an analysis phase of the geometrical combination intended to be optimized, and a minimization phase of the objective function based on the obtained results.

The initial parameters, derived from the experimental data, make it possible to reduce the simulation time and also makes it possible to identify the most influential parameters, thus reducing the number of parameters to be optimized before the optimization process, and the computation times are then reduced significantly. However, the desired speed of the optimization study requires a precise analysis of the chosen geometry structure, thus leading to a significant reduction of the exploration of the solution domain. Finally, the proposed algorithm offers a complete solution, resulting in an optimal geometry structure from objective temperature and constraints of the optimization parameters.

2.2.4 Parametric study

2.2.4.1 Material characterization

The workpiece is a disk made of steel 4340, as used for example in the manufacture of crankshaft crank pins or cranks. The 4340 steel is a material widely used in the automotive and aerospace industry because of its very high hardenability [71]. The 4340 steel is characterized by its robustness, strong toughness, good ductility and immunity against embrittlement. The thermal and electrical properties of this steel are strongly related to the variation of the temperature [71].

Table 2.1 : Chemical composition of 4340 Steel [71]

Element	Ni	Cr	Mn	C	Mo	Si	S	P
Content (%)	1,65 - 2,00	0,700 - 0,900	0,600 - 0,800	0,380 - 0,430	0,200 - 0,300	0,150 - 0,300	0,0400	0,0350

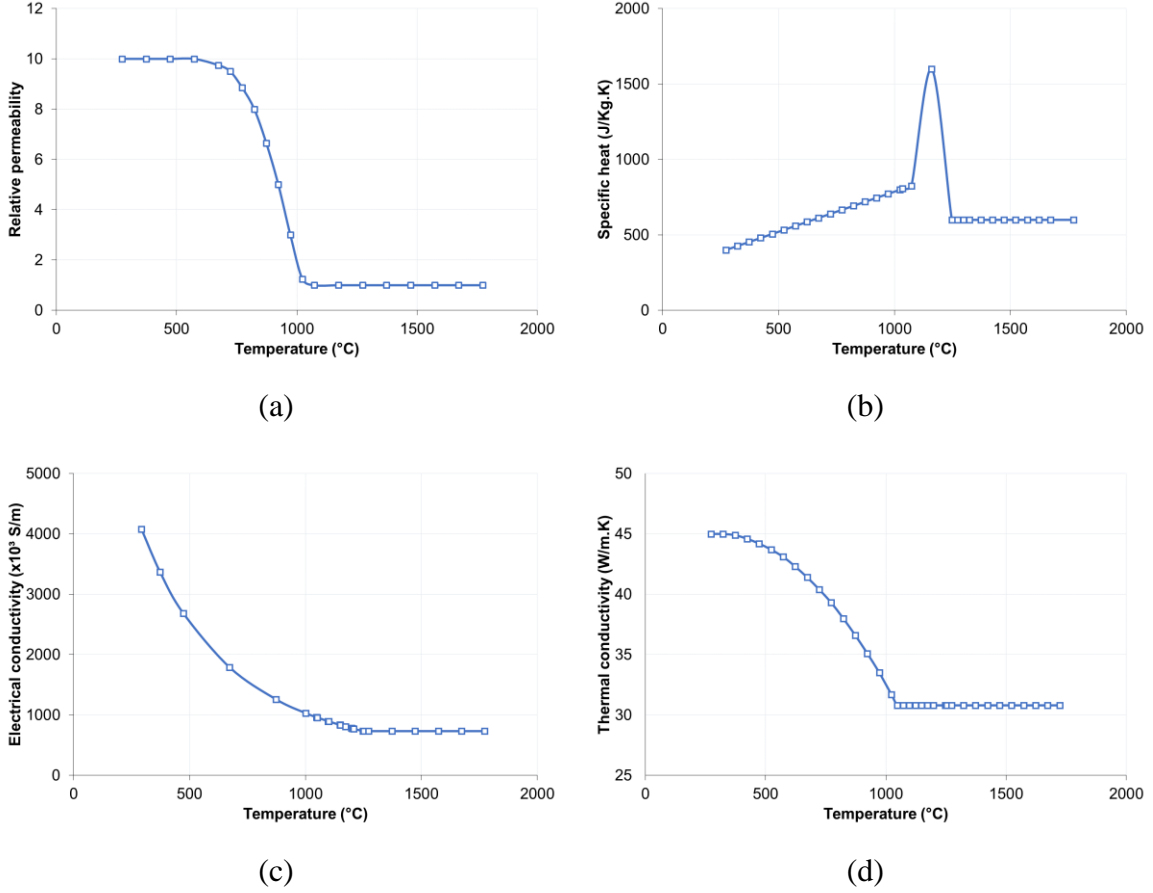


Figure 2.1 : Evolution of electrical, magnetic and thermal properties vs temperature of the 4340 steel [72]

2.2.5 Geometry

The 4340 steel disk having the properties mentioned above will be placed horizontally against a copper coil with a squared useful section with a horizontal gap G_a . In the coil circulates an alternative current characterized by its density J_E and its frequency Fr . The disk will be placed vertically between two 4340 steel disk of identical shapes and geometries and spaced by a vertical gap G_c . These two disk serves as a flux concentrators which has a key role to concentrate the electromagnetic flux in order to reduce the edge effect affecting the piece placed in the middle [53].

Since the geometrical properties of the disk and the inductor coil are invariant by orthogonal symmetry with respect to their symmetry axes, the 3D simulation model can be reduced to a 2D axis-symmetric model, which makes it possible to reduce considerably the calculation and simulation time. The **Figure 2.2** illustrates the different geometrical parameters involved in the design of the system.

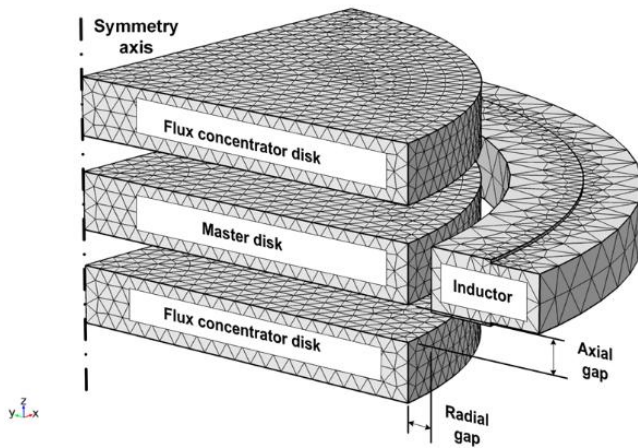


Figure 2.2 : Schematic presentation of the model geometry

The machine factors that are involved in the induction heat treatment process are mainly the external current density J_E , the external current frequency F_r , and the heating time T_H .

The study will be done at high frequency, i.e. $F_r = 200$ kHz, and a fast heating time, i.e. $T_H = 0.5$ s. The external current density is to be changed to ensure that the surface temperature of the master disk at the end of heating is greater than the austenitization temperature of the steel 4340, i.e. about 850°C.

2.2.6 Optimization study

The steps of the finite element optimization method could be summarized in the following flowchart in **Figure 2.3**:

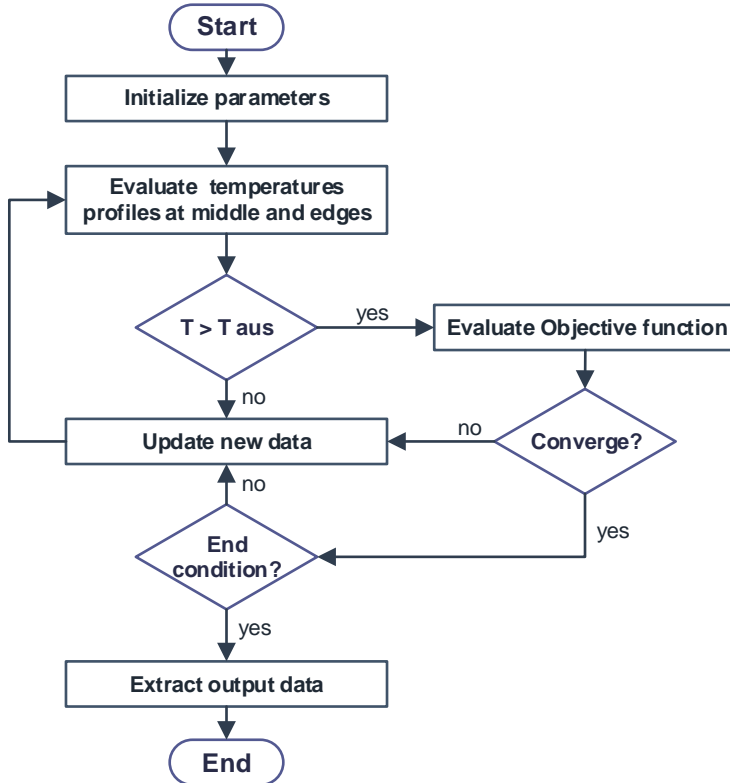


Figure 2.3 : Flowchart of the optimization procedure

The objective function is an analytic function. The optimization algorithm uses the vector of the parameter θ = (radial gap, axial gap) to minimize the difference between the middle and the edge profiles temperature of the part. If this difference is less or equal to the stopping conditions ε then the optimization is complete and a couple of optimal gaps are taken. To summarize, the algorithm's objective is to find the vector θ that minimizes the objective function $F(\theta)$. The objective function is an analytic function defined as:

$$F(\theta) = \sum_{i=1}^n (T_{E_i}(\theta) - T_{M_i}(\theta))^2 \rightarrow \min \quad (1)$$

T_M , and T_E : are respectively the temperatures at each middle and edge node i after the heating process as illustrated in **Figure 2.4**. θ is the vector of the two parameters, which are the axial gap and the radial gap.

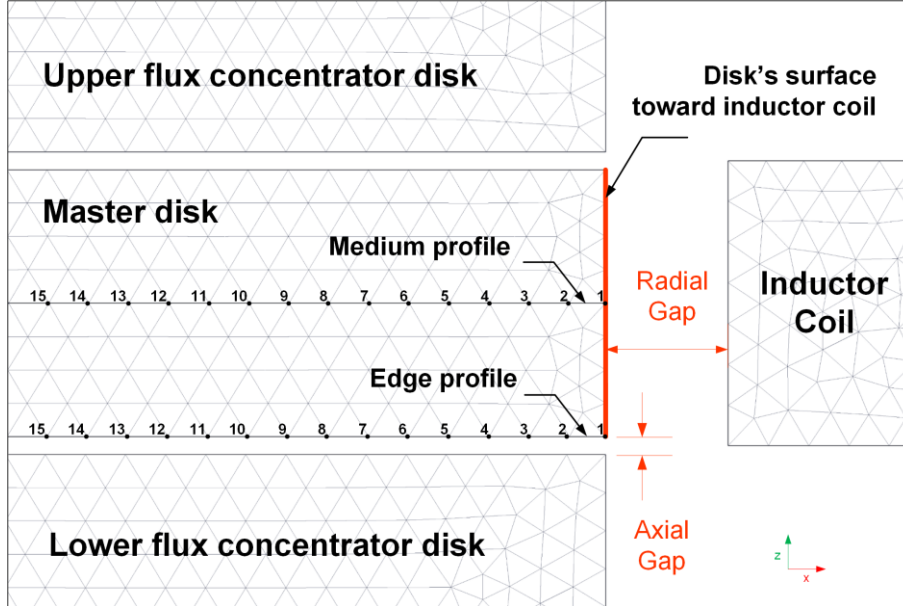


Figure 2.4 : 2D model showing nodes to evaluate at the medium and the edge

The ranges of the radial gap G_R and the axial gap G_A are very restricted and inspired by the technical and experimental feasibility. Radial gap could vary in the range of 1 to 5 mm, while axial gap could vary in the range of 0.2 up to 3 mm. The deviation of the axial and radial gaps for each iteration is controlled by the simulation program and varies with a pitch of 0.2 mm for the axial gaps and 0.25 mm for the radial gap, these values are chosen regarding experimental feasibility.

As the study space is confined and well controlled (medium scale problem), the minima of the objective function will be of the same order, so the uselessness of applying a global optimization algorithms in this case due to expensive in time calculation. The chosen algorithm is that of Quasi Newton [73], which is very useful for non-linear optimization and black box type problems. The choice of the Quasi Newton algorithm for optimization is based on two arguments. The first is because the algorithm requires only information about the gradient in each calculation step and this can be evaluated by discretizing the gradient with the finite difference method at each iteration [74]. The second argument focuses on the ease of calculating the inverse of the Hessian matrix by approximation at each iteration, thus giving speed to the computation and to the optimization process [74].

After obtaining the optimal parameters vector, it suffices to go to the validation step to check the performance of the sized part, with respect to the physical constraints. The result's accuracy is dependent on the temperature profile's quality at the surface of the part. The perfect profile is a constant temperature that is higher than the austenitization temperature of the 4340 steel. At the same time, the temperature is gradually decreasing with the workpiece depth. The first property must be introduced in the optimization algorithm as an additional constraint to add to the maximum and minimum bounds on the parameters that must be defined based on physical considerations. Although the chosen structure in this example is a simple, the computational load is important, either in relation to the computation time at the level of the finite element modeling steps, or at the level of the optimization process, then to obtain a greater precision it is essential to choose the right parameters of meshes and the criteria of stops for the optimization algorithm. At this point, the choice of initial conditions θ_0 (03 mm, 03 mm) is already done.

2.2.6.1 Numerical Simulation

As described above, the study involved the calculation of the inverse Hessian matrix in each iteration, and respecting the constraints defined to guarantee a sufficient heating level at the surface. Simulations started under the following combination described in **Table 2.2**.

Table 2.2. Initial parameters used in optimization process.

Parameter	Radial Gap	Axial Gap	Power	Heating Time
Level	3	3	95	0.5
Unit	mm	mm	kW	s

As illustrated in **Figure 2.5**, a total of 05 global iterations were performed to reach a local minimum with over 76 numerical calculations that were carried out to evaluate the hessian matrix and to respect problem constraints. Results lead to an optimized radial gap of 3.1 mm and an optimized axial gap of 0.44 mm. The temperature profile after the heating process under the optimized configuration was analyzed in the middle and the edges of the disk.

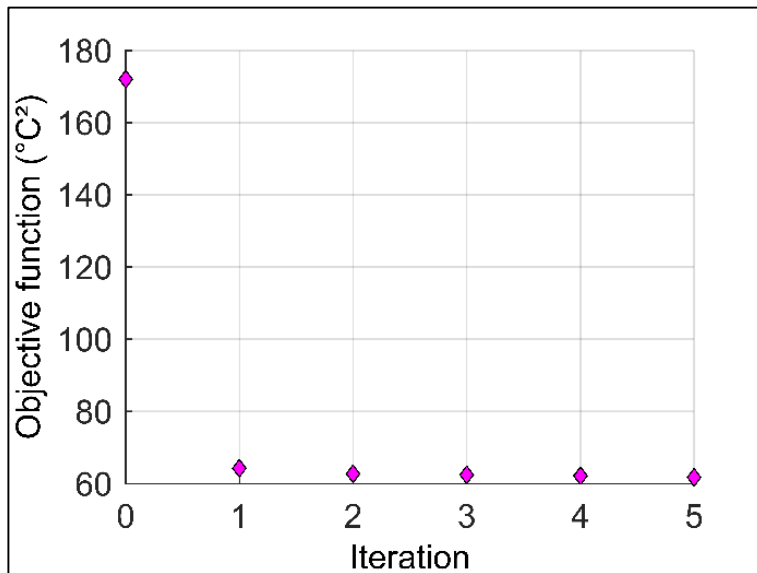


Figure 2.5 : Evaluation of objective function in each global iteration during optimization process

Figure 2.6 illustrates temperature distribution surfaces for the optimized final configuration and for the initial configuration where gaps with flux concentrators and coil are non-optimized.

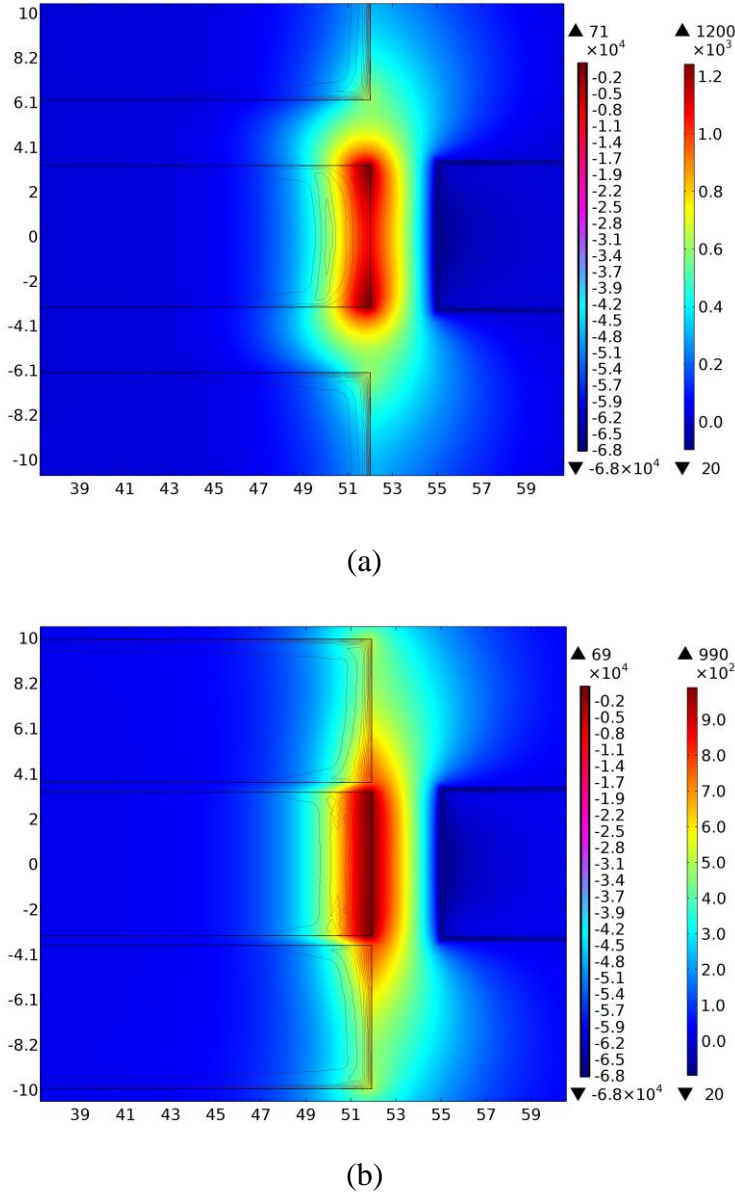


Figure 2.6 : Temperature distribution surface after the heating process (a) with initial parameters (b) with optimal parameters

In **Figures 2.7 and 2.8** the temperature along radial line are shown to explain the heating penetration depth at the end of the process across the disk. The influence of adjusting the slave flux concentrators and the coil position is observed clearly as the temperature penetrate evenly the core of the disk. High temperatures are maintained in the surface and the region heated above AC₃=780°C [71] is limited to a depth of about 0.8-0.9mm from the

surface. Martensitic transformation will appear if a fast quenching is achieved to the disk directly after the heating process.

Uniform temperature distribution ensures uniform distribution of hard martensite on the surface of the workpiece. Furthermore, the temperature at the surface can be controlled and higher hardened depths are achievable by increasing the power and the heating time of the process[32]. The effect of flux concentrators and coil position have a light effect on the quantity of energy absorbed by the treated part comparing to the power and the heating time. But concentrators and coil position have much important effect of how this absorbed energy is distributed at the core of the disk.

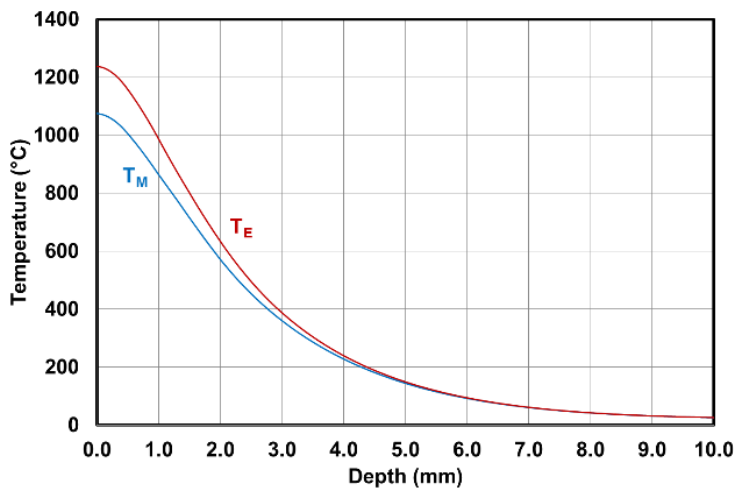


Figure 2.7 : Temperature profile in the middle and the edges with initial gap parameters

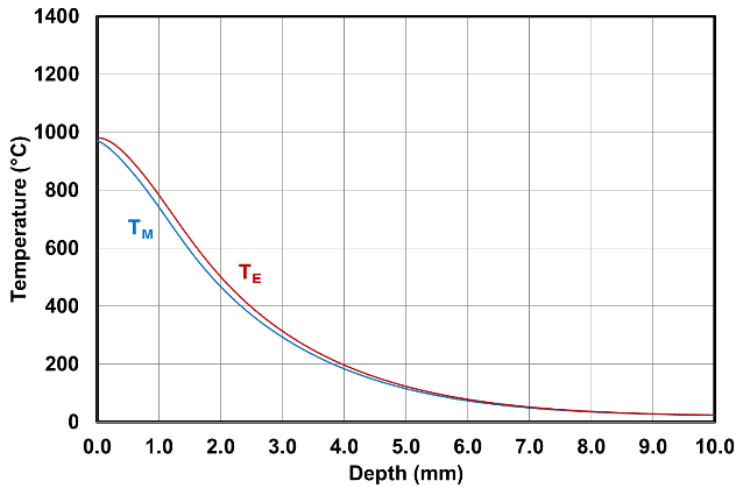


Figure 2.8 : Temperature profile in the middle and the edges with optimized gap parameters

2.2.7 Experimental validation

The experimental validation tests were conducted on the induction machine located at the induction heat treatment laboratory at the École de technologie supérieure (Montréal, CANADA). This machine is equipped with two medium and high frequency power generators. We use the second generator that consists of a thyristor radiofrequency generator (RF), operating at 200 kHz and providing a maximum power of 450 kW.

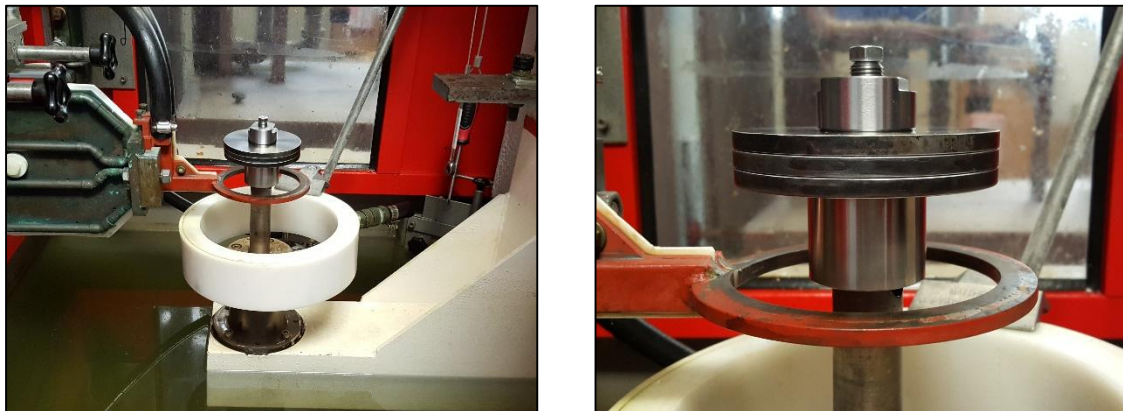


Figure 2.9 : Induction machine and operation system

2.2.7.1 Experimental setup

The three disk used for the experimental validation are 4340 steel disks of identical shapes and geometries having an outer diameter of 104.3 mm and a thickness of 6.5 mm. They are placed vertically and spaced by a gap of 0.4mm as shown in **Figure 2.9**. The master disk and the flow concentrators are mounted together on a prefabricated steel support mounted on the vertical rod of the machine which holds the transverse and rotational movement of the assembly. The spacing between the disk is guaranteed using two 1010 steel shims, used specifically for precision alignment, leveling, and spacing on shafts and machinery. Each shim has a thickness of 0.2 ± 0.05 mm with an outer diameter of 31.75mm.

The coil is made of copper and its outer diameter is 140 mm and internal diameter is 110 mm. and a useful section of 49 mm^2 ($7 \text{ mm} \times 7 \text{ mm}$) with a 2 mm thickness. The cooling of the inductor during heating is ensured with a 38 l / min flow of distilled water. The piece is brought back after the final heating in the shower section where the piece is cooled with jets of a solution with 92% of water and 8% of polymers used in tempering. The shower system is made of PVC and has an outside diameter of 150 mm and internal diameter of 125 mm. The experimental setup is typically the same used in simulation model, and it is shown schematically in **Figure 2.10**.

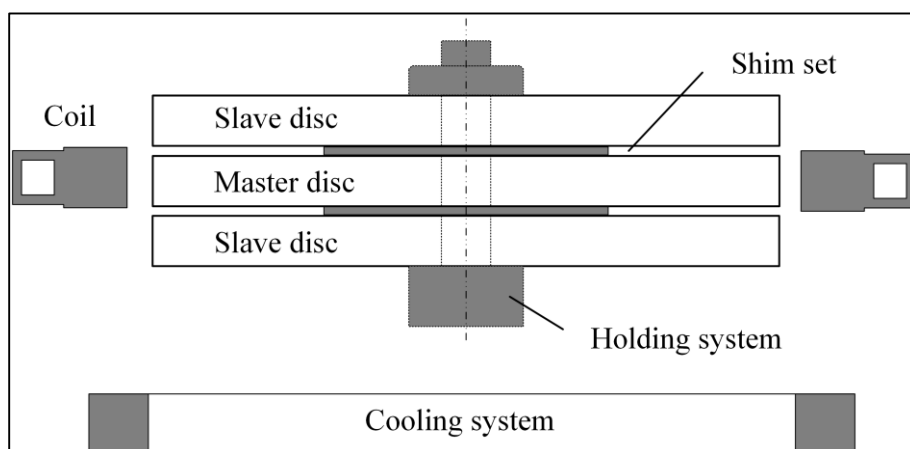


Figure 2.10 : Experimental setup scheme

2.2.7.2 Metallographic Analysis

Figure 2.11 shows the hardness profiles obtained on the edges of the treated master disk. The brighter and upper regions represent hard martensite transformed after the heating and quenching process while the gray regions are in the form of an un-tempered and non-transformed martensite.

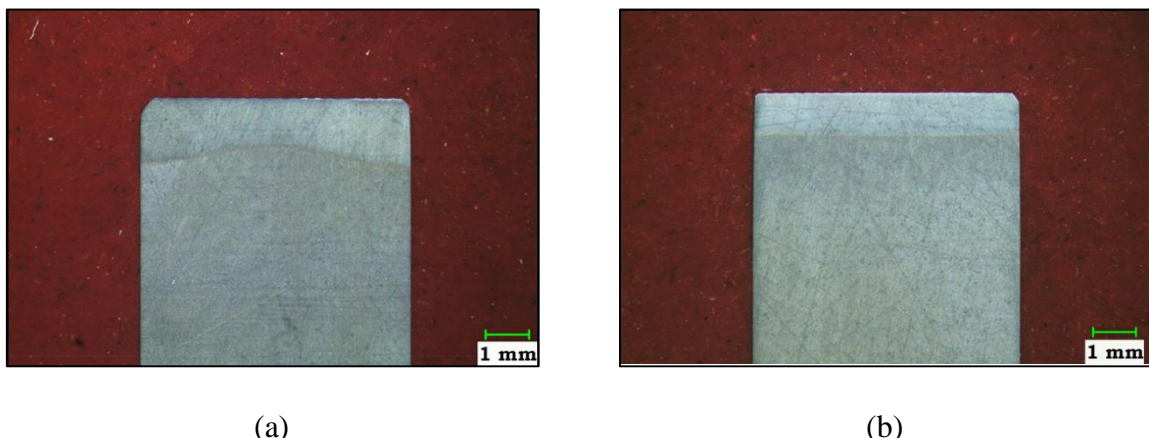


Figure 2.11 : Hardened profiles revealed after Nital etching: (a) with no flux concentrator
(b) with flux concentrators using optimized parameters.

It is clear that the electromagnetic edge effect that causes a non-uniform hardness profile as seen in **Figure 2.11** has been controlled which leads to a more linear and uniform profile. To quantify this linearity, hardness measurements were made at the three characteristic regions, the middle and both left and right edges. **Figure 2.12** shows the hardness measurements in the pre-defined regions. Results show that the three curves of hardness have the same appearance. The hardness is maximum at the surface (about 61HRC) and extends to a depth of 0.9mm which is the hardened or the case depth. The hardness drops drastically from a depth of 1 mm (about 37HRC) and then increases gradually to reach its initial value while approaching the disk core.

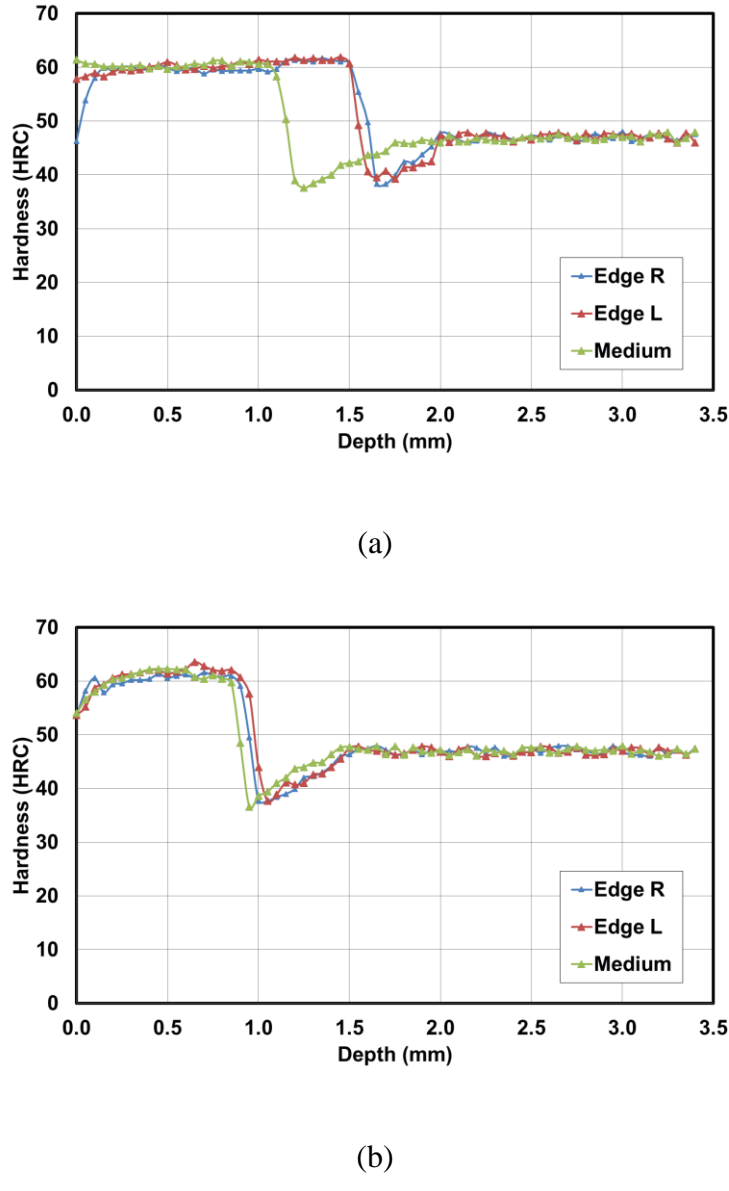


Figure 2.12 : Hardness profile (a) without flux concentrators (b) with flux concentrators and optimized parameters.

2.2.8 Discussion

It is well known that the case depth could be extracted directly by simulation from the temperature profile after the heating process [32, 48]. Case depth is related to martensite

formation after rapid cooling of austenite. Austenite is only formed in regions where temperature exceeds 800°C in the case of AISI 4340 [71].

The **Table 2.3** and the bar graph illustrated in **Figure 2.13** represents the measures, the average and the standard deviation values of the case depth for the left, right edges and middle of the disk for each induction heating process.

Table 2.3. Case depth measured for each induction heating method.

Case depth (mm)	Classic without flux concentrators	With flux concentrators and no gap optimization	With flux concentrator and gap optimization	With finite element simulation
Left Edge	1.5	0.95	0.9	0.95
Middle	1.15	1.1	0.8	0.8
Right edge	1.5	1.15	0.95	0.95
average	1.383	1.067	0.883	0.900
Standard deviation	0.202	0.104	0.076	0.087

The difference between left edge and right edge case depth is due to a non-controllable slight dissymmetry of the disk surface toward the coil center during experimental tests. However, the case depth values extracted by simulations present similar results comparatively to case depth values obtained by experiment. Results show a difference on the average of 2% and a difference on the standard deviation of 12% between simulation and experiments. The initial standard deviation of the case depth obtained by a classic induction heating process is about 0.202. Therefore, the presence of flux concentrators has improved the case depth profile by 48.5% with a standard deviation of about 0.104 without gap optimization, and improved by 62% with a standard deviation of about 0.076 using gap optimization.

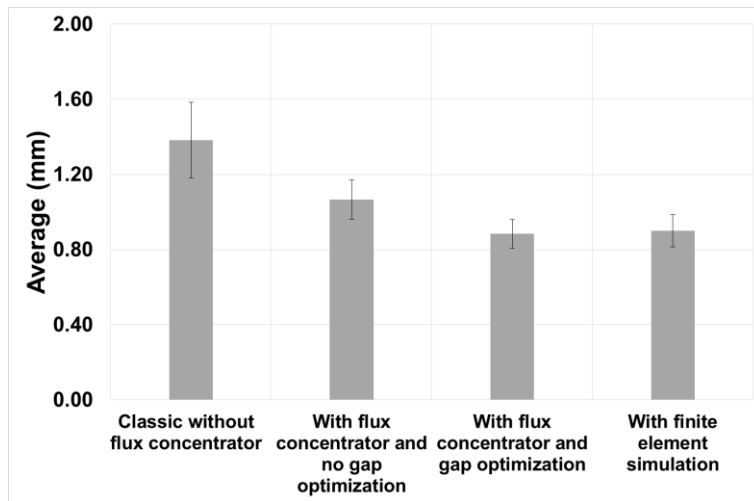


Figure 2.13 : Bar graph of average and standard deviation of case depth for each induction heating method

It is evident that the implemented optimization algorithm has succeeded in optimizing the temperature profile and to obtain the best case depth profile at the disk surface while respecting the previously imposed constraints. The final temperature at the edge of the part is linear and sufficiently higher than the austenitization temperature.

Despite the fact that the power and heating time during the heating process were kept constant, and the value of the radial gap has been changed of about 0.1mm, the average final temperature has decreased by 200°C compared to the initial average, which automatically leads to a decrease in the case depth average of about 0.5mm compared to classic induction heating average. This decrease is because the energy supplied by the inductor and consumed by the flux concentrators becomes greater due to the reduction of the axial gap, thus decreasing the energy consumed by the middle part.

To balance the case depth decrease, other process parameters can be adjusted, such as increasing the external current density and the process heating time, or adjusting the part or the coil shape. On the other hand, such compensation may lead to a slight increase in the process operating costs, so it can be said that the optimization is reliable only in relation to the objective initially underlined.

2.2.9 Conclusion

This paper has presented an original and comprehensive approach permitting the reduce of the edge effect on the hardness profile of an AISI 4340 disk with flux concentrators and obtain the best hardness profile using finite element simulation. First, a 2D model has been built using COMSOL by coupling the electromagnetic and thermal fields. Second, an optimization study has been performed to eliminate the edge effect using additional disks acting as flux concentrators. Finally, the simulation model has been validated by a comparative analysis with experiment results. The optimal coil position and gap between the part and flux concentrators permitting the elimination of the edge effect is then founded. It was shown that it is possible to reach the best hardness profile by using the flux concentrator and adjusting the geometrical parameters of the process. Overall, the obtained results show that the simulation is useful also to understand the edge effect and how this phenomenon can be reduced. Consequently, they certainly help induction-heating engineers to choose the good parameters for the induction machine and achieve the desired hardness profile. The developed method could be used also to optimize the surface treatment of parts with different shapes like spurs and helical gears.

CHAPITRE 3

RÉDUCTION DE L'EFFET DE BORD À L'AIDE DE LA MÉTHODOLOGIE DE SURFACE DE RÉPONSE ET DE LA MODÉLISATION D'UN RÉSEAU NEURAL ARTIFICIEL D'UN ENGRÈNAGE DROIT TRAITE PAR INDUCTION AVEC DES CONCENTRATEURS DE FLUX

3.1 RÉSUMÉ EN FRANÇAIS DU DEUXIÈME ARTICLE

Le but de l'étude est de déterminer l'effet des paramètres de contrôle impliqué dans le processus de chauffage par induction sur la distribution finale de la température et la profondeur durcie d'un engrenage droit placé entre deux autres engrenages de formes identiques et opérants comme des concentrateurs de flux, en utilisant deux approches différentes. Les concentrateurs de flux ont pour fonction de corriger la répartition de la chaleur dans la pièce à la fin du processus de chauffage et de créer une meilleure distribution de profondeur durcie entre le milieu et le bord de l'engrenage. Les propriétés mécaniques de l'engrenage pourraient être améliorées en minimisant l'effet de bord au niveau de la dent. Ainsi, l'optimisation du gradient de température entre les plans du milieu et du bord en variant les paramètres de contrôles du procédé de traitement par induction a été étudiée. Deux approches structurées et complètes pour concevoir un modèle efficace basé sur l'analyse de variance (ANOVA) et les réseaux de neurones artificiels (ANN) ont été développées pour la prédiction du profil de température et l'effet de bord. Les résultats obtenus démontrent que le modèle statistique était capable de prédire avec précision le comportement de la température et de la profondeur durcie. Dans la phase finale, plusieurs tests expérimentaux ont été menés sur la machine à induction pour valider les résultats de la simulation et le modèle de prédiction.

Mots clés — Chauffage par Induction, Concentrateur de Flux, Réseau de Neurones artificiels, Méthodologie de Surface de Réponse

Ce troisième article, intitulé « *Reduction Of Edge Effect Using Response Surface Methodology And Artificial Neural Network Modeling Of A Spur Gear Treated By Induction With Flux Concentrators* », fut co-rédigé par moi-même ainsi que par le professeur Noureddine Barka, le professeur Jean Brousseau et le professeur Philippe Bocher. Il fut soumis pour révision et publication dans sa version initiale en **25 Janvier 2019** par les éditeurs de la revue « **The International Journal of Advanced Manufacturing Technology** ». En tant que premier auteur, ma contribution à ce travail fut la recherche sur l'état de l'art, le développement de la méthode, la création des modèles de simulation et de prédiction, la gestion des données et résultats et la rédaction d'article. Les professeurs Noureddine Barka et Jean Brousseau ont fourni l'idée originale. Ils ont aidé à la recherche sur l'état de l'art, au développement de la méthode ainsi qu'à la révision de l'article. Le professeur Philippe Bocher, quatrième auteur, a contribué à l'exécution des tests expérimentaux.

Envoyé à: 25/01/2019 23:22:33

JAMT-D-19-00371 - Submission Confirmation

De: Advanced Manufacturing Technology <em@editorialmanager.com>
 À: Mohamed Khalifa <med.khalifa@live.fr>

Dear Mr. Khalifa:

Thank you for submitting your manuscript, "Reduction of edge effect using response surface methodology and artificial neural network modeling of a spur gear treated by induction with flux concentrators", to The International Journal of Advanced Manufacturing Technology.

The submission id is: JAMT-D-19-00371
 Please refer to this number in any future correspondence.

As we are now processing manuscripts via our online submission system, please note that you will no longer need to submit an electronic copy by email or hardcopy by post of your manuscript to our Editorial Office.

During the review process, you can keep track of the status of your manuscript.

Your username is: Medkalifa

If you forgot your password, you can click the 'Send Login Details' link on the EM Login page at
<https://www.editorialmanager.com/jamt/>.

With kind regards,

The Editorial Office
 The International Journal of Advanced Manufacturing Technology

3.2 REDUCTION OF EDGE EFFECT USING RESPONSE SURFACE METHODOLOGY AND ARTIFICIAL NEURAL NETWORK MODELING OF A SPUR GEAR TREATED BY INDUCTION WITH FLUX CONCENTRATORS

3.2.1 Abstract

The aim of the study is to determine the effect of each parameter involved in the induction heating process on the final temperature distribution and case depth dispersion of a spur gear placed between two other gears having identical shapes and acting as a flux concentrator using two different approaches. The purpose of flux concentrators is to correct the heat distribution in the part at the end of the heating process, and to produce a better case depth gap between the middle and the edge of the gear. Mechanical properties of the gear could be improved by minimizing of the edge effect at the tooth, thus the optimization of temperature gradient between the middle and the edge plan by varying geometrical and machine parameters was studied. Two structured and comprehensive approaches to design an efficient model based on Analysis of Variance (ANOVA) and Artificial Neural Networks (ANN) for the estimation of quality and the prediction of temperature profiles and edge effect was developed. The obtained results demonstrate that the statistical model was able to predict accurately the behavior of temperature and case depth distribution. In the final phase, several experimental tests were conducted on the induction machine to validate the simulation results and the prediction model.

Key words — Induction Heating, Flux Concentrator, Artificial Neural Network, Response Surface Methodology

3.2.2 Introduction

The induction hardening [32] has proven its success in the metallurgical industry because of its remarkable productivity, its energy efficiency and its ability to handle and process metallic parts with complex geometric shapes such as for gears and splines [23, 37]. This process has become popular in many industrial applications such as brazing [75],

molding [15, 16] and for the surface hardening applied mainly to mechanical parts for automotive and aerospace industry [19, 26, 31]. Industrial advantages of induction heating include the ability to heat particular areas of treated part, provide high mechanical properties and lower manufacturing costs [20]. One of the major drawbacks in the induction heat treatment is the edge effect due to concentration of magnetic fields at the part edges. For a mechanical part treated conventionally by induction like external spur gears, with single shot and high frequency for example, the induced currents tend to penetrate more the tip of the gear than its root, and the edge than the middle, which results from a strong temperature gradient between these areas [23]. This phenomenon is undesirable because the strong temperature gradient created by induced currents between the edge and the middle at the end of heating followed by quenching creates a non-uniform martensite layer on the gear surface [32, 61, 76]. The distribution and penetration of the induced currents and final temperature is linked to several factors, such as the machine power, the frequency, the heating time, the gap between the master part and with the inductor coil [31, 32, 77]. Gear heat treatment requires the importance of keeping the distortion as low as possible during the heating process. Different approaches were investigated to deploy new solutions and techniques in order to optimize final distortion at the end of induction heating process [31, 77]. Gear heat treatment developers are always looking to improve their products quality without increasing the process costs. They generally seek to modify the parameters related to the induction machine components such as the frequency, the machine power or the type of the inductor. New techniques are used like flux concentrators to improve the quality of heat treated parts. [78]. These concentrators concentrate the electromagnetic waves on very specific regions of the piece, which makes it possible to control the penetration of the induced currents and the distortion of the temperature. This technique improves the efficiency and quality of induction heat treatment but are very costly. Another type of flux concentrator is introduced by Barka et al. [53] offer new simpler and cheaper variants and this approach consists in taking the master gear to be heated in a sandwich between two other gears having the same geometry and acting as flux concentrators. The technique consists of putting away the principal gear in parallel with two slave gears of the same size and geometries that act as flow concentrators

to the master gear. This technique has the advantage of increasing productivity, faster treating cycles and less distortion by decreasing the temperature gradient between the tip and the root of treated part at the surface, this temperature gradient is thus optimized by choosing an optimal configuration, which finally leads to an acceptable result [53]. However, the effects of the parameters and factors employed in this technique are not analyzed statistically, and no prediction models for estimating the temperature profile according to the involved parameters has been developed yet.

During this study a large number of simulations were carried out, each simulation involves a unique combination of both geometric and machine parameters that characterize the induction heat treatment with flux concentrators such as power machine, heating time and components relative positions. Simulation results are statistically analyzed, and prediction models were developed using ANOVA and artificial neural networks (ANN) to predict the temperature distribution at the end of heating based on data extracted from the simulations.

3.2.3 Theoretical Background

3.2.3.1 Induction heating process

The formulation of induction heating process is described by an electromagnetic field retrieved from Maxwell's equations in time-varying form with neglecting displacement fields and introducing the magnetic vector potential related to the magnetic flux. Which could be written as [23]:

$$\frac{1}{\mu} \nabla^2 \mathbf{A} + j\omega\sigma\mathbf{A} = -\mathbf{J}_e \quad (1)$$

With \mathbf{A} and \mathbf{J}_e describes respectively the magnetic vector potential and the source current density in the coil. ω is the angular frequency of the current with $\omega = 2\pi f$, and f is the

current frequency. μ and σ are temperature dependent parameters that represent respectively magnetic permeability and electrical conductivity of the workpiece material.

The induced eddy current density J_i could be written from Eq. (1) as

$$J_i = -j\omega\sigma A \quad (2)$$

The resolution of Eq. (2) made it possible to determine the eddy current density as a function of magnetic vector potential A , which in turn could be deduced by resolving Eq. (2). The amount of heat generated inside the metal part due to joule heating is evaluated using the following equation.

$$\dot{Q}_{ind} = \int_V \frac{|J_i|^2}{\sigma} dV \quad (3)$$

The heat generated by induction is introduced into the heat equation in order to calculate the temperature distribution in the workpiece. In induction heating, the heat transfer is described by Fourier's equation and it is given by:

$$\rho C \frac{\partial T}{\partial t} = \nabla \cdot (k \nabla T) + \dot{Q}_{ind} \quad (4)$$

Where T is the temperature. ρ , C and k are non-linear temperature dependent properties and represents respectively the mass density, the specific heat and the thermal conductivity of workpiece material. A part of energy is lost by convection and radiation due temperature differences between workpiece and surrounding air. Convection and radiation heat flux losses \dot{Q}_c and \dot{Q}_r between the workpiece and open air are defined respectively as

$$\dot{Q}_c = h_c(T_s - T_a) \quad (5)$$

$$\dot{Q}_r = \varepsilon \sigma_s (T_s^4 - T_a^4) \quad (6)$$

Where h_c is the convection coefficient, ε is the emissivity and σ_s is the Stefan-Boltzmann constant.

3.2.3.2 Predictive modeling using RSM

RSM is an optimization approach method that treats simulation models as a black box [79], it shows the interaction between the inputs and objective function where internal variables and mathematical modeling are very complex or neglected. It determines the output response influenced by a series of continuous or discretized values of independent inputs variables, generally acquired by an experiment design (DOE).

RSM usually fits second-order polynomial models if fitting first-order polynomial model is poor or insufficient and it is not adequate to represent the local response function. Second-order polynomial models could be written as [80]:

$$y = \beta_0 + \sum_{i=1}^n \beta_i z_i + \sum_{i=1}^n \beta_{ii} z_i^2 + \sum_{1 < i < j < n} \beta_{ij} z_i z_j \quad (7)$$

Where y is the predicted response, z_i and z_j are the design variables and $\beta_0, \beta_i, \beta_{ii}$ and β_{ij} are regression parameters. Eq.7 can be written in a matrix notation as

$$Y = Z * B + \epsilon \quad (8)$$

Where Y is the observation vector determined according to the inputs combination into the experimental design, B is regression parameters vector, Z is the matrix of the values of the design inputs and ϵ is the error vector. Regression parameters vector B can be estimated using the ordinary least squares (LS) method.

$$B_{LS} = (Z^T Z)^{-1} Z^T Y \quad (9)$$

3.2.3.3 Predictive modeling using ANN

ANN are non-linear processing systems/model biologically inspired from the brain's neural structural. ANN consists of a large number of connected small computational units called neurons. Each neuron receives many simultaneous inputs x_i and multiply each inputs by a connection weights w_i , all n products are summed with a bias and fed through a transfer function f to generate a single output Y [81].

$$S = \sum_{i=1}^n x_i w_i + b \quad (10)$$

The transfer function could be a liner or non-linear algorithmic process applied on the summation total. The most used transfer function are *purelin*, *logsig* and *tansig*. The *logsig* transfer function could be written as:

$$\text{logsig}(S) = \frac{1}{1 + e^{-S}} \quad (11)$$

The architecture of an ANN is defined by the arrangement of neurons in relation to each other's; these neurons are structurally grouped into layers. Most applications used for solving the non-linear regression problem requires networks that contain at least three normal types of layers acting as input, hidden, and output layers. The layer of input and hidden neurons receive the scaled data from input files or previous layers while the output layer sends scaled results information to be employed as a solution of diverse problems like those related to prediction, function approximation, pattern classification and system identification [82].

This kind of network, also known as multi-layer feed-forward neural network or Multiple Layer Perceptron, once structured and defined, the networks are trained, using a learning function. The purpose of a learning function is to adjust the connection weights and bias according to some neural based algorithm in order to reduce the error between the network output and the desired real results. The network accuracy is evaluated using a

performance function, such as Mean squared normalized error MSE or the Mean absolute error MAE [81].

Many learning functions are in common use, the back propagation algorithm is widely used to teach feed-forward neural networks and is the most popular and effective in solving non-linear problems. The back-propagation algorithm is an iterative method used to find a local minimum of the error function where weights are updated using a variety of gradient descent algorithms. The gradient is determined by propagating the computation backwards from output layers to first hidden layer. Typical feed forward back-propagation applications include image processing, optimization, process control, forecasting and prediction [81].

3.2.4 Simulation Model

The complex geometric shape of a spur gear tooth mark the difficulty of having a uniform surface temperature between the edge and the middle after heating. In order to have the most efficient possible heat treatment, the piece surfaces must be heated taking into account the temperature limits. The temperature in any point on the surface of the part after heating must be at least equal to the temperature necessary to transform the metallography structure of the involved material into an austenite structure, and also be careful not to overheat part temperature above the melting temperature of the AISI 4340 Steel. Thus, it will be necessary to know the typical configuration that takes into account these thermal constraints.

3.2.4.1 Process Parameters Selection

The parameters involved in an induction process are multiple, and each parameter has its own degree of influence on the final temperature distribution and amplitude [31]. The approach used in this section is to adjust the heating time and the geometrical parameters (gap between the parts and gap with the coil), and to modify the imposed current density J_e to reach desired minimum temperature distribution.

The imposed current density J_E is variable because it is directly related to the machine power P_M , the latter is usually among the most important factors on the final temperature of an induction [53], while geometric parameter and heating time values were fixed taking into account their experimental feasibility.

The Model was created taking into account the rotational and the planar symmetrical shape of the gear and coil, the simulation efforts were made using COMSOL Multiphysics software.

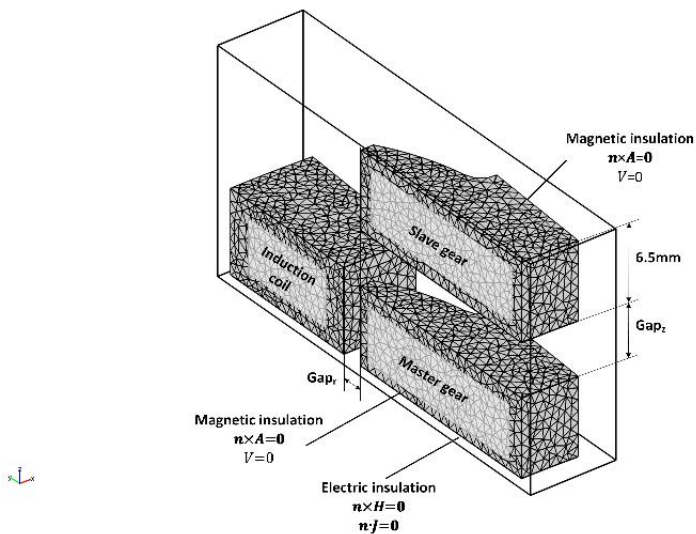


Figure 3.1 : Model with flux concentrators

The process has been simulated with adjusting the heating time at 0.5s. For induction heating process, this time is considered sufficiently so the heat can propagate deeply in the tip according to the intensity of the induced currents created on the surface of the gear. The axial gaps between the master gear and both flux concentrators acting as slave gears have been fixed at 2 mm, and the radial gap with the inductor is fixed to 2 mm, the choice of these two values is a function of practical and experimental geometry constraints. The frequency of study is a high frequency, fixed at 200 kHz. A pre convergence study has been realized under COMSOL software to determine the appropriate mesh value for the simulations. The mesh size value used in the study varies between 0.1mm and 1 mm with a step of 0.05mm. Obtained results show that a mesh size value of 0.5mm offer best quality and stability; further

reduce of mesh size will contribute to a magnificent computation time effort. Imposed current density vary by a step of $1 \times 10^{10} \text{ A/m}^2$ from $5 \times 10^{10} \text{ A/m}^2$ to $15 \times 10^{10} \text{ A/m}^2$ as maximum value. The surface temperature is measured at four locations of the middle part which represents the temperature profile at the tip of the middle area (T_{TM}), the temperature at the tip of the edge area (T_{TE}), the temperature at the root of the middle area (T_{RM}) and the temperature at the root of the edge area (T_{RE}). The selected parameters are resumed in **Table 3.1**.

Table 3.1 : Parameter configuration

Parameter	Heating time	Radial gap	Axial gap	Frequency	Mesh size
Value	0.5	2	2	200	0.5
Unit	s	mm	mm	kHz	mm

Results show that the final temperature evolves linearly with the imposed current density J_e but undergoes variations around $900 \text{ }^\circ\text{C}$ and $1400 \text{ }^\circ\text{C}$ due to the change of physical and chemical behavior of the 4340 steel by the effect of temperature around the critical points as illustrated in **Figure 3.2**.

Considering the limits of the temperature which must be lower than the melting temperature and higher than the austenitization temperature of the 4340 steel at any point in the surface of the part, the imposed current density was taken around $12 \times 10^{10} \text{ A/m}^2$.

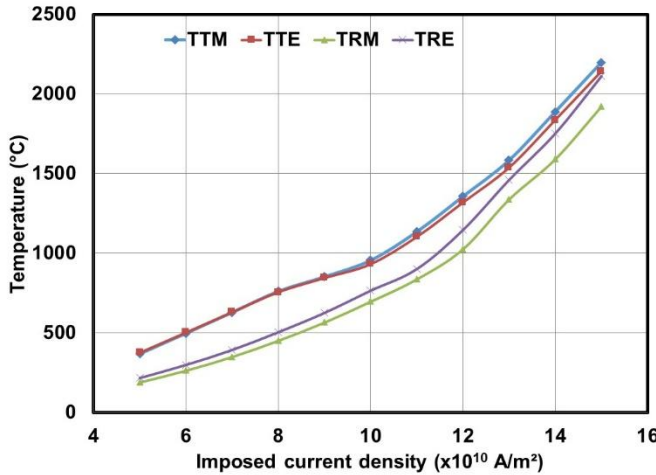


Figure 3.2 : Temperature vs imposed current density.

Table 3.2 : Simulation parameters

Parameters	imposed current density J_E	Heating Time	Radial gap	Axial gap	Frequency
Level	12×10^{10}	0.5	2	2	200
Unit	A/m^2	s	mm	mm	kHz

3.2.4.2 Experimental design

A factorial matrix that contains all possible combinations of all input factors is considered the best approach for performing such simulations. The orthogonal networks (RO) developed by Taguchi represent a smart and robust factorial and fractional design. Used in most simulation studies similar to this article, this strategy can achieve a high level of quality while strictly reducing the number of tests necessary to collect all statistically significant data.

Two machine parameters and two geometrical factors are considered in this study, machine parameters are external current density and heating time, the geometrical factors are

identified by the relative position of the master gear to the other process components, specifically represented by the radial gap between the master gear and inductor R_G , and the axial gap between master gear and slave gear A_G . Each parameter level and range are inspired by the ability to cover the experimental feasibility domain. External current density varies from $11.75 \times 10^{10} \text{ A/m}^2$ to $12.05 \times 10^{10} \text{ A/m}^2$ with a step of $0.15 \times 10^{10} \text{ A/m}^2$, while heating time varies from 0.5 s to 0.6 s with a step of 0.05 s. Master gear to coil gap varies from 2.0 mm to 2.4 mm with a step of 0.2 mm while the axial gap varies from 0.4 mm to 1.2 mm with a step of 0.4 mm. Based on the number of parameters considered and their levels (3 levels for the 4 parameters), an orthogonal network of 81 combinations is used.

Levels of machine parameters and geometric factors such as power and gaps are taken to ensure complete austenitization of the steel layer during heat treatment, and are presented in **Table 3.3**. The 81 numeric simulations are performed using a coupling between COMSOL Software combined to a MATLAB code in order to approximate the hardness curve. The useful results extracted for each simulation are the four temperature profile T_{TE} , T_{TM} , T_{RE} and T_{RM} and the difference between extracted temperature couple at the edge and the medium.

Table 3.3 : Scratching parameters and their level

Parameters	Unit	Code	Level 1	Level 2	Level 3
External current density	(x1010A/m ²)	A	11.75	11.90	12.05
Heating time	s	B	0.50	0.55	0.60
Radial gap	mm	C	2.0	2.2	2.4
Axial gap	mm	D	0.4	0.8	1.2

3.2.5 Results and discussion

The study was conducted for the high frequency (HF) and the temperature distribution was controlled by varying the imposed current density. For all variations, the tooth and root temperature values were measured in the edge and medium of the gear.

3.2.5.1 Temperature Analysis

Analysis of temperature distribution and induced current density in accordance to the configuration in **Table 3.2** are represented in **Figure 3.3.a.** and **Figure 3.3.b.** Results show that the use of high-frequency cause that current density is more concentrated between the pitch point and tip of the tooth gear causing an increase of the heat at the tip of the tooth. The entire volume of the tip is heated above the critical point AC_3 and nearly same amount of heat is diffused in the edge and in the middle with no significant temperature difference between both regions. The temperature difference between those recorded at the tip of the tooth at the edge and in the middle is about $30\text{ }^{\circ}\text{C}$ and is about $60\text{ }^{\circ}\text{C}$ in the root, while temperature difference between the tip and the root is about $200\text{ }^{\circ}\text{C}$ for both sections. As the core of the tip remains unaffected, the gear heating has a non-uniform pattern and affected heated depth is about 20% of affected depth at the tip of the tooth. Gear failure is most likely to initiate from the root radius toward a zero-stress point at the tooth center line under the root circle, thus, the root of gearing must be sufficiently hardened [20, 83], the kind of pattern resulted using flux concentrators and by above parameters combination is desirable because it minimizes distortion and meets that hardness criterion.

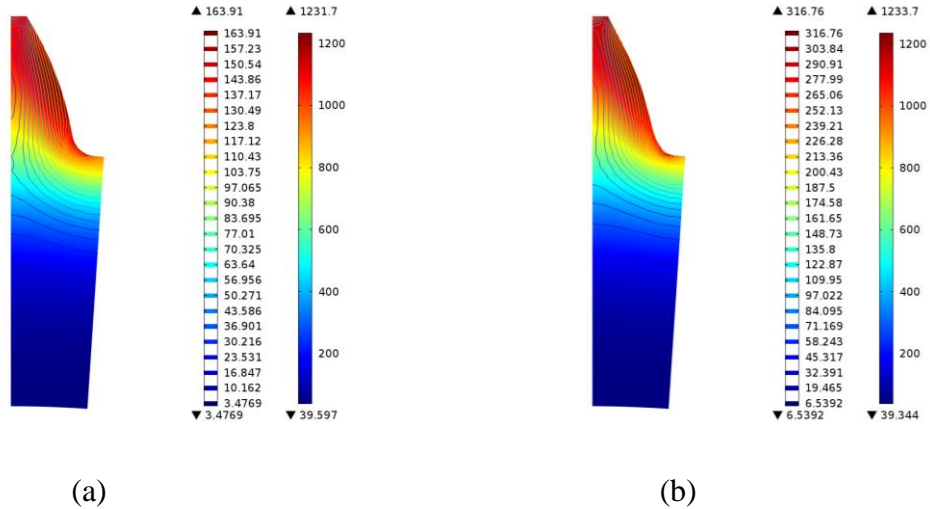


Figure 3.3 : Temperature ($^{\circ}\text{C}$) and current density (A/mm^2) distribution at the end of heating (a) Edge and (b) middle

3.2.5.2 ANOVA Analysis on Temperature difference

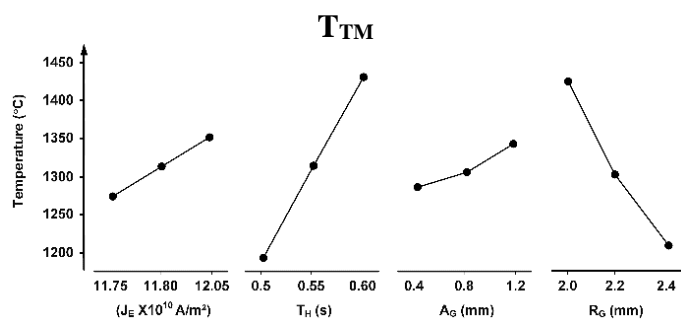
ANOVA is a statistical technique that reveals all the necessary information about process parameters and can help determine the impact and contribution of each of this parameter on final temperatures values [84, 85]. The ANOVA analysis was performed with a step-by-step mode, which automatically eliminates non-significant terms.

Analysis results show that the residual is small and represents less than 10 % of the variation in these final temperatures. The radial gap is the parameter having the most important effect; its contribution varies between 30 and 42%. The heating time has a significant effect on the final temperatures, with a contribution of 24% to 48%. These two parameters have more effect on the middle profile than the edge profile. The gap between the gear and the inductor keeps almost the same effect on all regions of the gear. This gap does not have much effect on the final temperature except in the gear root edge, and its contribution to the other regions is very small. Moreover, this small contribution does not reflect its effect on the temperature difference between the medium and the tip of the tooth.

Table 3.4 : Percent contributions of process parameters

	A	B	C	D	Residual
T_{TM}	5,30	48,58	41,49	2,97	1,67
T_{TE}	4,50	49,72	38,07	5,58	2,12
T_{RM}	7,45	31,3	39,87	17,11	4,27
T_{RE}	5,89	24,33	30,94	34,61	4,23

ANOVA tables have been also used to evaluate the significance and contribution of design parameters on every process characteristic temperature point, indicating how temperature evolve for any change of design parameter. Main effect plot for every gear characteristic point is illustrated in **Figure 3.4**. The statistical results from the ANOVA temperature contribution analysis are presented in **Table 3.4**. The heating time and the radial gap are the factors which brings the greatest contribution to the variability in all the temperatures. The contribution percentage attributable to the error is small which means that no important factor has been omitted from the experimental plan.



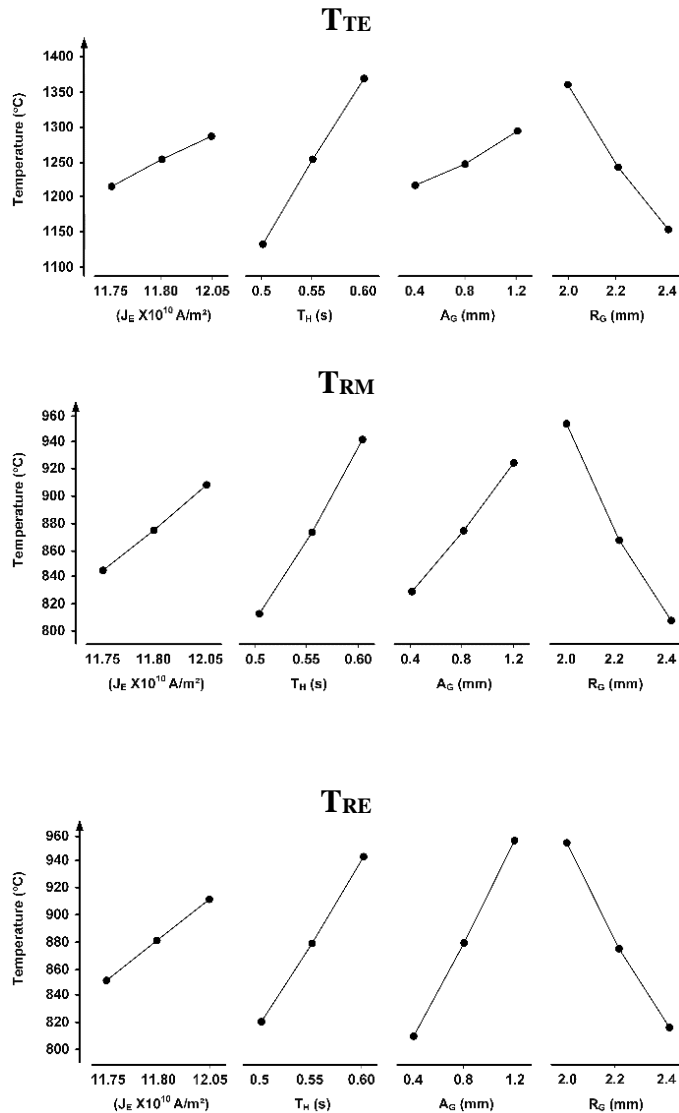


Figure 3.4 : Main effect plot of temperature versus simulation parameters

Figure 3.5 show the scatter plot for predicted vs simulated temperatures. For each simulated temperature value, the predicted value is on the diagonal line, due to the low value of the residual errors. Therefore, for each temperature value, the predicted and simulated curves are almost identical, which explains the good agreement between the predicted and simulated values. The linear fit criterion shows that the prediction equation can provide a satisfactory level of precision with the results of the simulation.

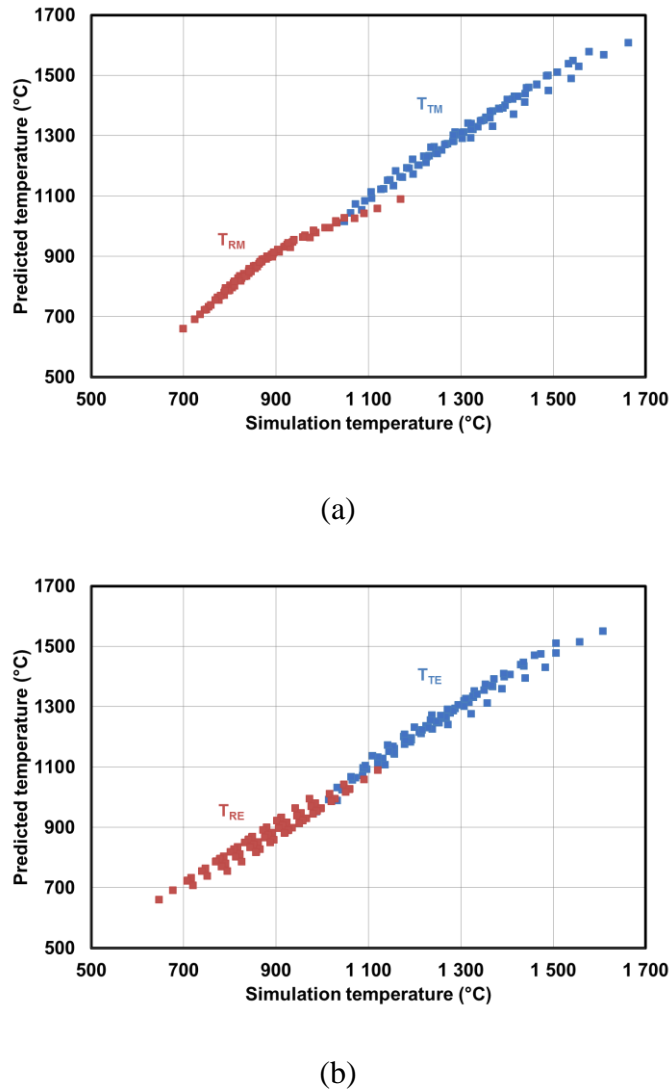


Figure 3.5 : simulated vs ANOVA predicted temperature (a) Medium (b) edge plan

3.2.5.3 Contributions on temperature difference

The purpose of adding flux concentrators in the induction heat treatment process is to reduce the temperature difference between the middle and the r edge areas of the gear's tooth[53]. It will be more interesting for this study to evaluate the contribution of machine parameters and geometric factors on this temperature difference. ANOVA analysis was performed in

parallel with a step-by-step mode to determine the impact of the parameters on the temperature difference already determined from the previous simulations.

Table 3.5 : Analysis of variance results on temperature difference at the tip

Source	DF^a	C%	SS^b	MSadj^c	F-Value	P-Value	R2	R2adj
Model	6	92.67	8561.10	855.298	93.79	0.01	92.67	92.08
Error	74	7.33	677.16	9.151				
Total	80	100	9238.26					

Table 3.6 : Analysis of variance results on temperature difference at the root

Source	DF	C%	SS	MSadj	F-Value	P-Value	R2	R2adj
Model	12	97	12596.5	3532.747	615.92	0.13	97.00	96.47
Error	68	3	390	5.736				
Total	80	100	12986.6					

^a Degree of Freedom. ^b Sum of squares. ^c Mean square.

The analysis of ANOVA, resumed in **Table 3.5** and **Table 3.6** clearly indicates that gap between master gear and slave gear has the most significant effect on temperature profile between not only the middle and the edge, but also between the tip of the tooth and the root of the same surface. Increasing this gap clearly causes a significant variance on the temperature difference, and thus the edge effect could be minimized and optimized.

The main effect plot is shown in **Figure 3.6**. The lines are almost horizontal for current density and heating time factors, indicating that the temperature difference is unaffected by the change of these machine parameters. Although, the lines have negative slopes for geometrical factors and shows a non-linear behavior for the axial gap factor. The lowest point

in both plot is selected as the most desirable condition that minimizes the edge effect between the middle and the edge of the gear, which could be decided by the level of the axial gap within the range of 0.4mm to 0.8mm.

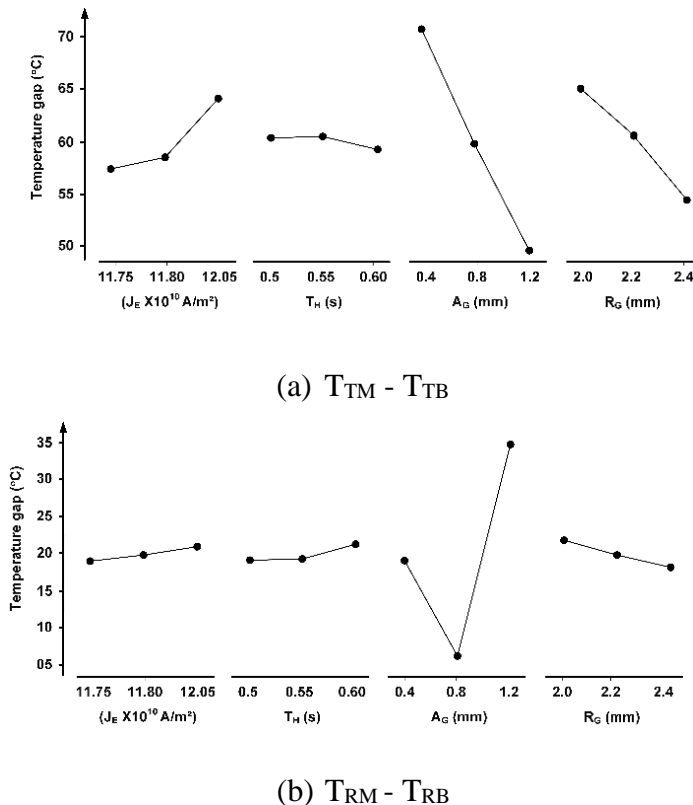


Figure 3.6 : Main effect plot of temperature difference versus simulation parameters

The simulation temperature difference data for the tip and root area are plotted versus predicted temperature difference data fitted by ANOVA analysis, and are shown in **Figure 3.7**. The goodness of fitting could also be measured by the coefficient of determination R^2 [86], where the values closer to 1 indicates better fit. Results are shown in **Table 3.7** for both prediction models.

Table 3.7 : Coefficient of determination for the prediction model

Gear area	R^2	R^2 (adj)
Tip	0.9267	0.9208
Root	0.9700	0.9647

Results show that data are very close to the diagonal line, and a very good fitting between the simulation and prediction data, and a good agreement between the simulated and predicted data for the tip area with 92% and better correlation for the root area with 97%. The high measure of R^2 is expected because all data are acquired from simulation results, where the process parameters are extremely controlled and limited. However, R^2 tend to be lower for the prediction of real experiments where the environment parameters are less controllable. The temperature difference prediction at the root is slightly better because of the higher number of interacted factors used in the analysis of the root than for tip. Hence, the achieved results demonstrate that the ANOVA model gave an excellent prediction with good performance of the temperature difference between the edge and the middle of the gear.

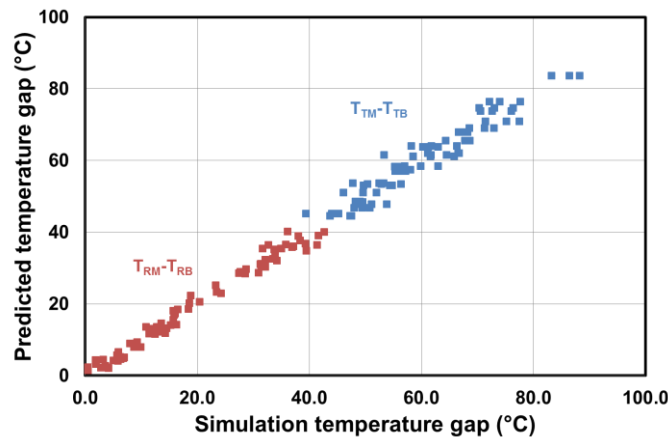


Figure 3.7 : Simulated temperature difference vs predicted by ANOVA

3.2.5.4 RSM of temperature difference using ANOVA

Based on the ANOVA prediction model, the response surface has been drawn to show the influence of the most significant parameters (External current density versus axial gap with fixed heating time and the radial gap) on the temperature difference between edge and the middle of the gear. The results are presented in **Figure 3.8**. Graphs indicate that an increase of external current density and reduction of axial gap leads to an enhancement in the final temperature difference which raises the edge effect. It is clearly observed that the axial gap has an important non-linear effect on final temperature difference profile. On the tip area, best temperature profile could be achieved for lower external current density and higher axial gap values. On the root area, external current density has a non-significant effect and it's not responsible for any gap of the results, which confirm the main effect plot results discussed earlier. Lower temperature difference on the root could be obtained in the range of 0.5mm to 0.7mm of the axial gap. In this range, better temperature profile at the end of heating could be obtained at the end of heating, and thus reducing the edge effect considerably at the gear tooth. However, the empirical model given by ANOVA contains linear interacted terms and cannot predict the non-linear behavior accurately for a large range of one of these factors. The cross terms have a very important effect on the temperature difference which makes the phenomenon more and more complex. The next section exposes the ANN modeling to predict the case depth gap which could be interpreted directly from temperature distribution at the end of heating and quenching process between the edge and the middle of the gear.

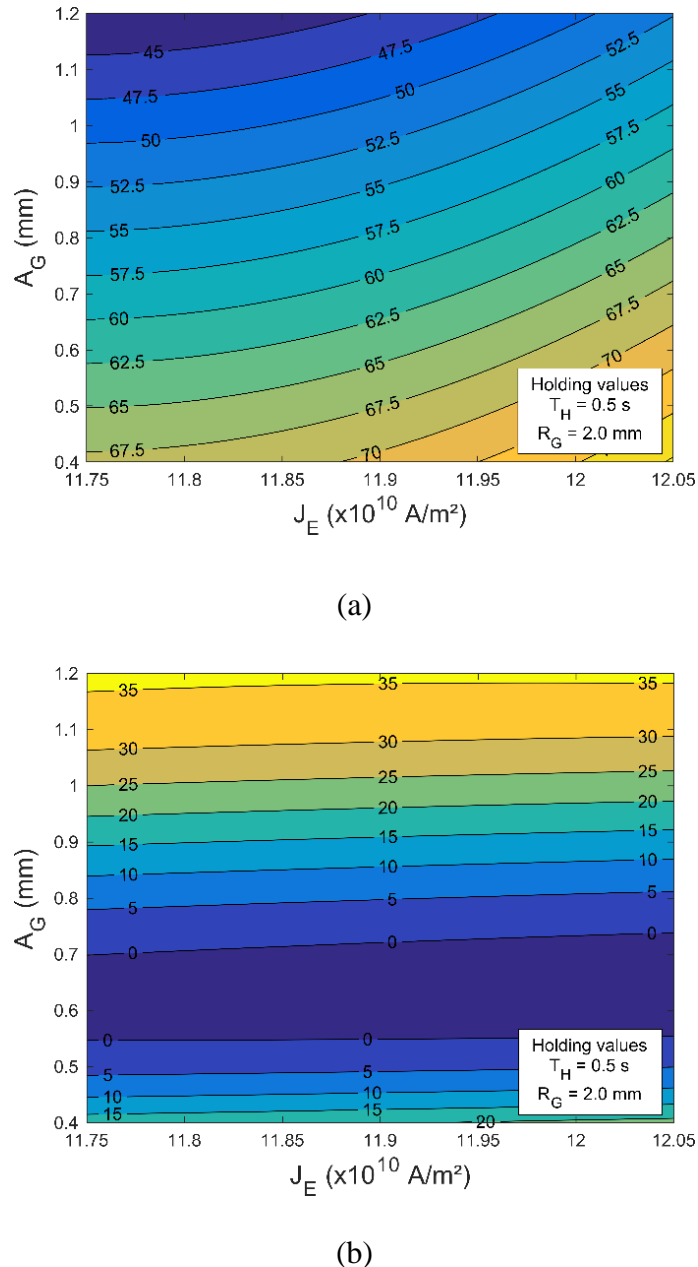


Figure 3.8 : RSM of temperature difference based on ANOVA analysis (a) tip (b) root

3.2.5.5 ANN modeling of Case Depth Gap

Compared to other techniques, Artificial Neural Network (ANN) modeling provides more efficient modeling capacity, particularly when the relationship between input parameters and the output parameters is non-linear. Among all existing networks, the MLP (Multi-Layered Perceptron) is the most used structure diverse application such as process modeling and characterization [87, 88], prediction [89] etc. As with the case of temperature difference, neural networks can be used in cases where no sufficient knowledge about the nature of the dependency between the various parameters exist. This is very useful to reduce the efforts of simulations and experiments. For this study, an MLP neuron network is used to predict the case depths and the case depth gap between the edge and the middle at the end of heating according to the input process parameters. Although various neural network techniques can be used in this approach, MLP networks seem to be the most appropriate because of their simplicity and flexibility. As illustrated in **Figure 3.9**, the network structure used in this study comprises 14 hidden layer neurons and an output layer having 06 neurons equivalent to the desired output numbers. The input neurons represent the induction heating parameters.

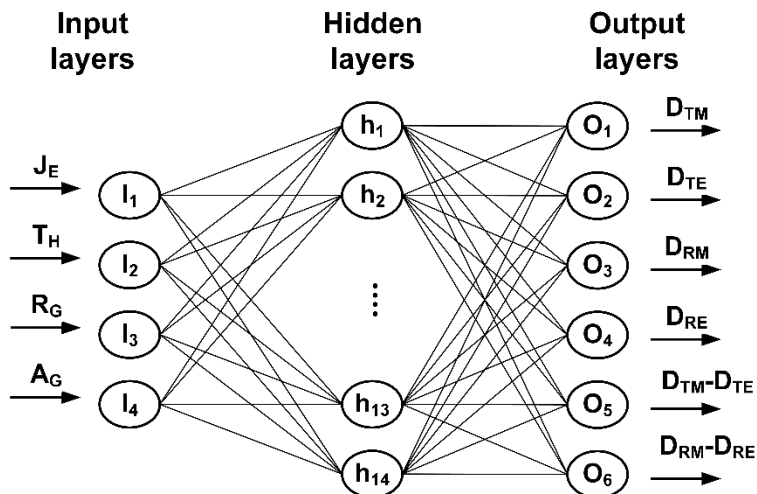


Figure 3.9 : Architecture of the ANN model used for prediction of the final case depths

D_{TM} , D_{TE} , D_{RM} and D_{RE} represents respectively the case depth at the tip middle, the case depth at the tip edge, the case depth at the root middle and the case depth at the root edge. The data set, containing the extracted temperature values from the 81 simulations, was divided into 3 parts, 70% of the data are used for the training process, 15% for the validation and 15% for the verification. The criterion used to measure network performance was the mean squared error (MSE). During the learning step, the input data is normalized to be in a range between -1 and 1. The weights and bias of the network are initialized at small values randomly to avoid rapid saturation of the activation functions.

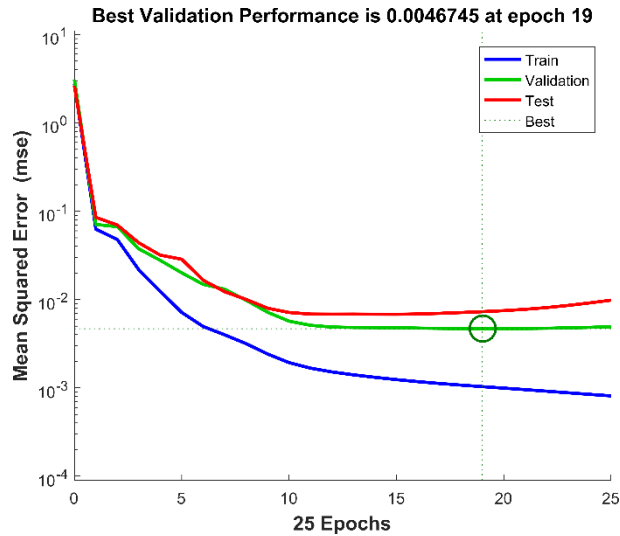


Figure 3.10 : Training, validation and test mean squared errors
(performance is 8.48×10^{-4}).

3.2.5.6 Case Depth Prediction

Once the network learning step is performed, the 27 combinations of verification data are applied as input parameters. The ANN outputs model are compared with those obtained by simulation.

The **Figure 3.11** illustrates the point clouds for D_{TM} , D_{TE} , D_{RM} and D_{RE} case depths predicted by the neural network as a function of the case depth obtained by the simulation.

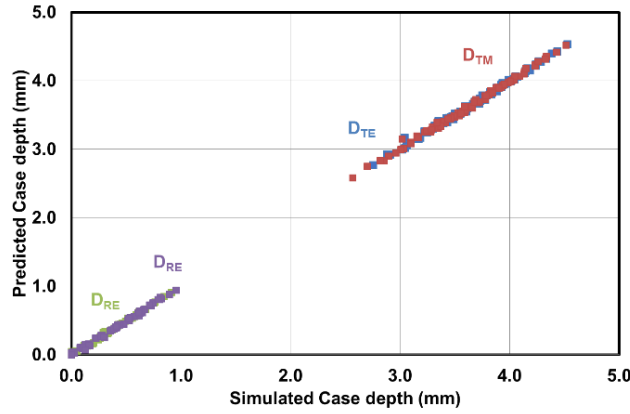


Figure 3.11 : Simulation vs ANN predicted case depth

The data is mainly located around the bisector, which underlines the good accuracy of the model. The **Figure 3.11** show that the network is well trained and very efficient.

3.2.5.7 Case Depth Difference Prediction

From the same neural network, the two case depth gap characterizing the hardness gradient between the middle and the edge of the gear are extracted. **Figure 3.12** shows the point clouds for the $D_{TM}-D_{TE}$ and $D_{RM}-D_{RE}$, the case depth gap predicted by the neural network as a function of the case depth gap obtained by the simulation.

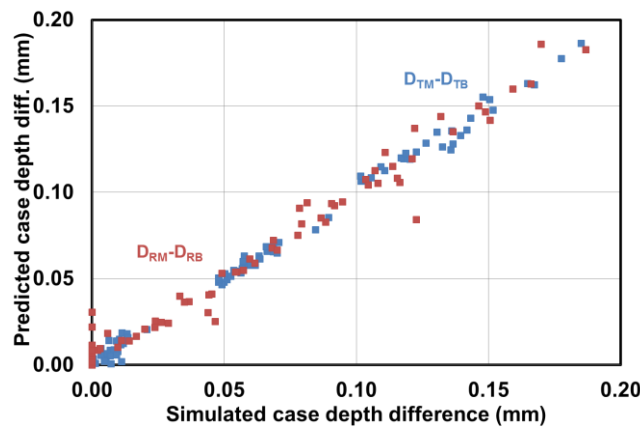
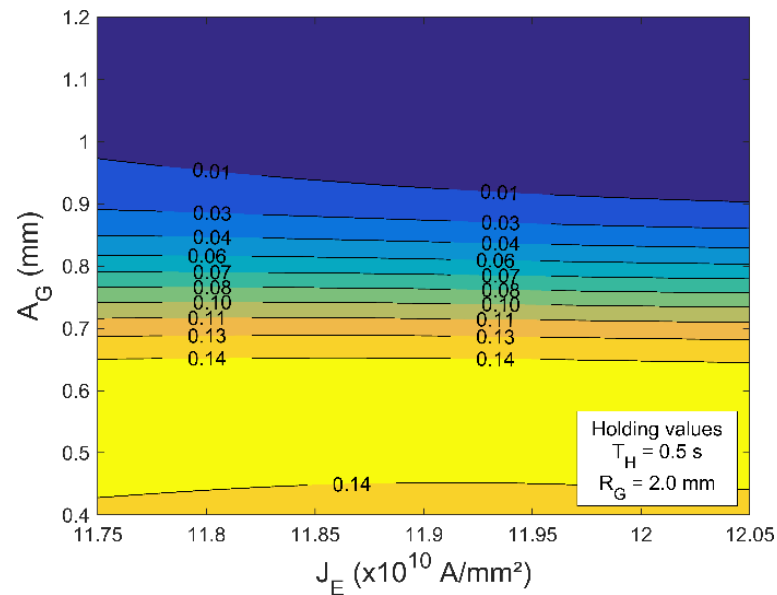


Figure 3.12 : simulated vs predicted case depth gap on the tip and the root using ANN

The error between the predicted and the simulated case depth gap is relatively small compared to that obtained with the ANOVA analysis. The model created by the neural network is thus more robust and reliable on this approach.

The output surfaces have been drawn using the simulated MLP neural network on **Figure 3.13**. Results confirm the non-linear behavior of different input parameters on the edge effect. As can be seen in **Figure 3.13**, for important machine power values with an axial gap around 0.9mm, no significant temperature difference between the edge and the middle occur, and for that the heating process could be optimized. Therefore, ANN indicated its ability to overcome the limitation of the prediction model of RSM.



(a) $D_{TM} - D_{TE}$

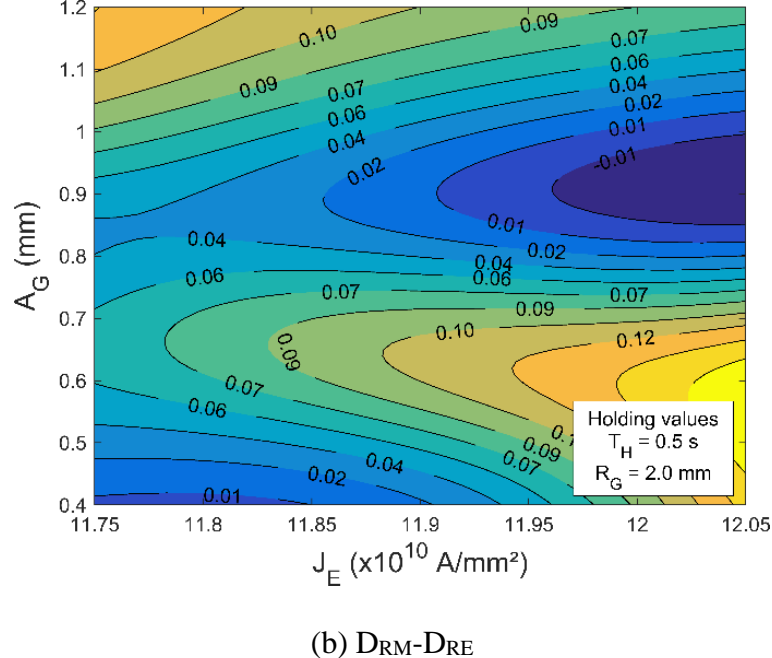


Figure 3.13 : case depth gap on tip and root based as predicted by ANN analysis

The large amount of data that can be generated by the simulation makes it possible to form a neural network capable of predicting the final temperatures accurately with flow concentrators. ANOVA is able to provide good predictions on the final temperatures themselves but unable to predict the differences between these temperatures. While the neural network is able, in both cases, to give good results in terms of relative error.

3.2.5.8 Experimental Validation of the ANN Model

This part concerns the experimental validation with a set of chosen combinations of input parameters. Four validation tests are performed to validate the hardened depth at the tooth tip and the tooth root in both edge and medium area.

An induction machine with a maximum power of 450 kW was used to validate the finite element and the ANN model. The inductor machine is equipped with two medium and high frequency power generators. A thyristor radiofrequency generator (RF) operating at 200 kHz (HF) was used. The gears used are made of 4340 steel and having identical shape and

geometry. Outer diameter of gears is 104.3 mm and the thickness is 6.5 mm. The master gear was placed on a prefabricated mounting kit between the two slave gears acting as flux concentrators. A 1010 steel shim was used to ensure spacing between the gears, each shim has a thickness of $0.2 \text{ mm} \pm 0.05 \text{ mm}$ with an outer diameter of 31.75 mm. The coil is made of copper having an outer diameter of 140 mm and internal diameter of 110 mm, with a useful section of 7x7 mm. Quenching is ensured with a jet of a solution containing 92% water and 8% of polymers. Parameters used in experimental validation are resumed in **Table 3.8**.

Table 3.8 : Parameters used in validation of the neural network

Parameters	Unit	Test 1	Test 2	Test 3	Test 4
Machine power	kW	156.5	143	156.5	156.5
Heating time	s	0.5	0.55	0.5	0.55
Radial gap	mm	2.3	2.3	2.3	2.3
Axial gap	mm	0.2	0.6	0.6	1

After adjusting the imposed current density J_e to obtain a suitable temperature distribution at the gear surface, a ratio between this imposed current density J_e and the power provided by the induction machine into the inductor must be determined for each current density level. The utility of this relation is to help the induction heat treaters to apply practical recipes for parts under various conditions from a normalized machine power values. This ratio between P_M and J_e was established based on the work of Barka et al. [32].

The average power supplied to the room during the heating process can also be evaluated by the simulation. This power provided by induction machines (P_M) can be represented as a linear function with the density of the initial imposed current density (J_e), as represented in **Figure 3.14**.

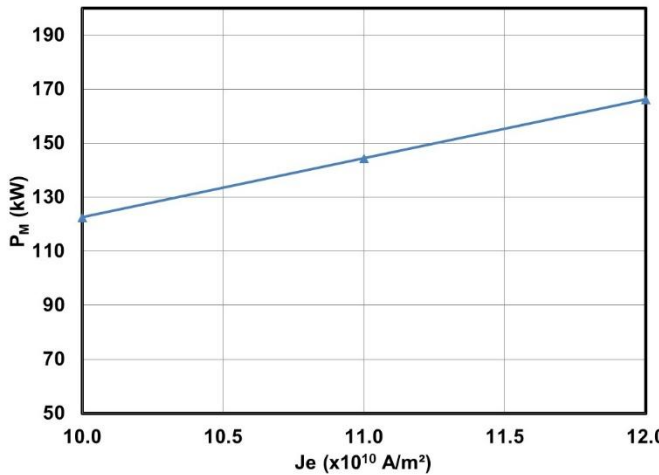


Figure 3.14 : Machine power vs imposed current density

Observation of the hardness profile is used to evaluate the case depth layer and if the general shape is in agreement with the simulation. In **Figure 3.15**, the hardened layer on the edge and at the middle are pictured. Hardness measurement are also presented in **Figure 3.16**. The hardened depth is significantly higher on teeth tip than on teeth root, confirming simulation results. Hardness measurement results are summarized in **Table 3.9** and **Table 3.10**. Hardened depth on the tooth tip was found between 2.4mm and 3.5mm, while between 0.2mm and 0.6mm on the root. In both areas, the measured case depth differences between the tooth edge and middle is very insignificant, and vary between 0 mm and 0.2mm.

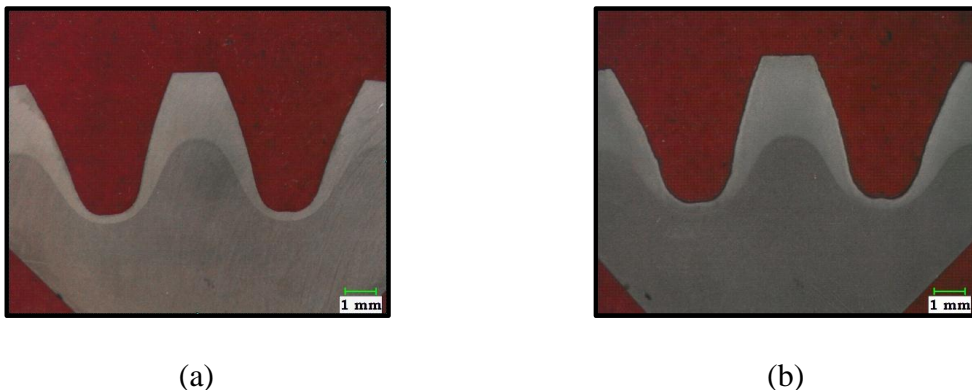


Figure 3.15 : Shape of the case-hardened profile on the tip and the root of Test 03
 (a) edge (b) medium

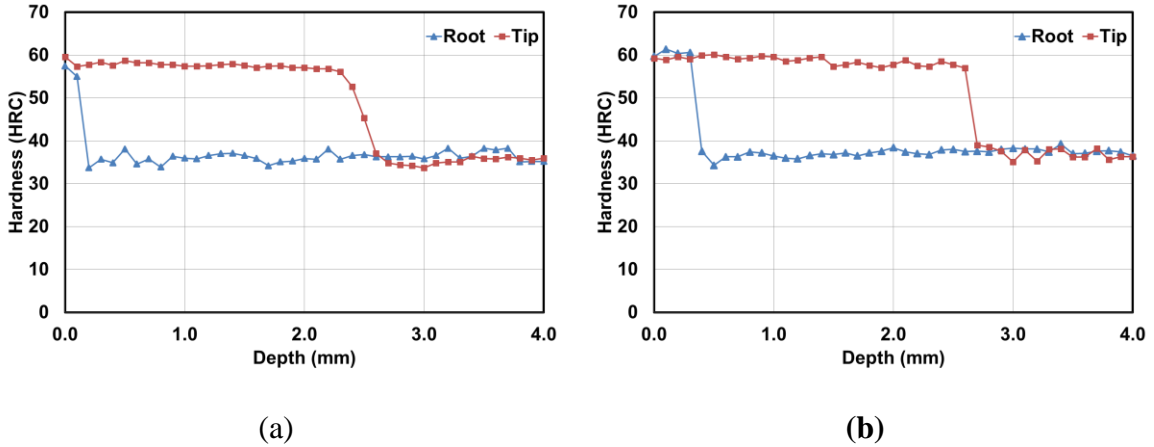


Figure 3.16 : Hardness measurement on the tip and the root of Test 03
 (a) edge (b) medium

The hardened layers on the edge show mostly the exact shape in the middle in all experimental tests, which confirm accurately the ability of the flux concentrator approach to reduce the edge effect on the gear tooth and affirm simulation results. Thus, better results are achievable when the axial gap in the range of 0.6 mm and 1 mm.

In fact, for the narrow axial gap around 0.2 mm, the induced currents penetrate deeper ward the middle of the tooth than toward the side of the tooth, which produces a higher temperature and higher case depth gradient between the two areas as a result. Otherwise, for wide axial gap dimensions, the effect of flux concentrator's slaves gear diminishes, the middle gear absorbs much more power and the heating process becomes similar to a classic induction heating process. Therefore, the phenomena is made possible by the better understanding of axial gap effect on the edge effect behavior.

Table 3.9 : Comparison of measured and ANN predicted case depth on the gear tip

Test N°	Edge Tip	Medium Tip	Difference (mm)		Error %
	Measure (mm)	Measure (mm)	Measured	Predicted	
1	3.10	3.25	0.15	0.2	33%
2	3.30	3.50	0.2	0.13	35%
3	2.45	2.60	0.15	0.15	0%
4	3.90	3.85	0.05	0.03	40%

Table 3.10 : Comparison of measured and ANN predicted case depth on the gear root

Test N°	Edge Root	Medium Root	Difference (mm)		Error %
	Measure (mm)	Measure (mm)	Measured	Predicted	
1	0.35	0.45	0.10	0.12	20%
2	0.40	0.45	0.05	0.05	0%
3	0.20	0.35	0.15	0.14	7%
4	0.60	0.60	0.00	0.00	0%

In experimental investigation, the change of power machine and heating time affects significantly the shape and the penetration of hardened depth through gear core. But with a slight effect on the variation of the case depth between difference between the middle and the edge, affirming the ANOVA results showed earlier.

The prediction of case depth differences by ANN was compared to the measured case depth differences in **Figure 3.16**. The results show an average error of 7% on the tooth root and about 27% on the tooth tip. The tooth root prediction is excellent while the tooth tip prediction is less accurate. These errors might therefore come from the limitation of the simulation model. However, the ANN model is effective in modeling of the case depth difference since the inaccuracy with the measured data is less than 0.05mm in most tests.

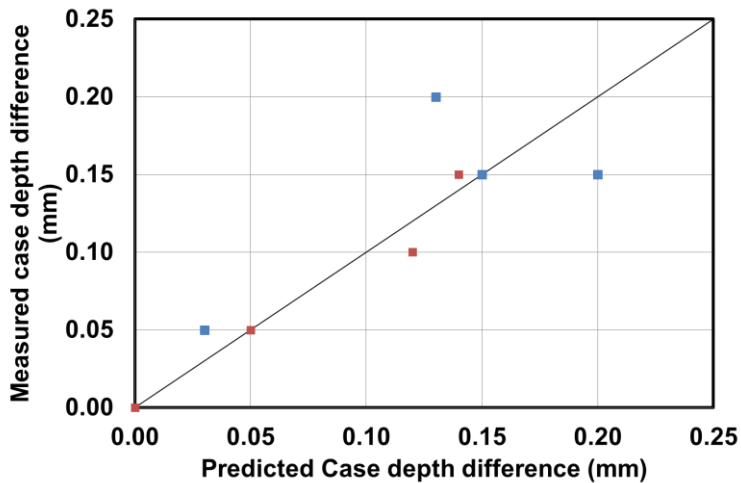


Figure 3.17 : Measured vs predicted case depth difference on the tip and the root

3.2.6 Conclusion

In this project, a structured and comprehensive approaches was developed to design models based on finite element analysis, ANOVA and the artificial neural networks methods to create a tool for predicting temperature profile and case depth at the end of heating period of a gear located between two gears acting as flux concentrators and heat-treated by induction. Both modeling techniques yielded good prediction results except that the neural network was much more efficient with respect to case depth gap between the root and the gear tip, and also to describe the edge effect behavior versus input parameters. The modeling procedure can be considered efficient and has succeeded in producing conclusive results, despite the complexity of the process analyzed. Prediction model based on ANN model is more accurate because the ANN can handle non-linear problems. Experimental investigation demonstrates that the neural network model presents an accurate and effective technique to predict and reduce the edge effect under different machines and geometrical parameters and conditions. Experimental results are also very promising for future researches on residual stress distribution and load-carrying capacity of the case-hardened spur gears heat treated by induction and using flux concentrators.

CONCLUSION GÉNÉRALE

La production des pièces mécaniques de haute performance traitées thermiquement par induction passe nécessairement par la bonne compréhension des différents phénomènes physiques d'origine électromagnétique, thermique et mécanique pouvant affecter la structure de la surface extérieure lors de processus de durcissement. Réalisé dans le cadre des activités de recherche en maîtrise en ingénierie dans les laboratoires de l'UQAR, ce mémoire de maîtrise présenté sous forme d'articles porte une attention particulière à la bonne compréhension du comportement thermomécanique des pièces en acier 4340 lors du procédé de traitement thermique par induction faisant usage de concentrateurs de flux. Pour ce faire, une approche structurée en trois phases a été adoptée comme suit :

- i. Réalisation d'un plan de simulation basé sur la méthode Taguchi suivi d'une validation expérimentale afin d'identifier et évaluer les effets des paramètres de contrôle sur l'effet de bord d'un disque 4340 traité par induction.
- ii. Optimisation de la distribution de la température à la fin de chauffe afin de minimiser l'effet de bord d'un disque en acier 4340 traité par induction avec des concentrateurs de flux et en utilisant des méthodes d'optimisation numériques.
- iii. Développement d'un modèle de prédiction avec ANOVA et en réseau de neurones artificiel pour la prédiction du profil de dureté d'un engrenage droit traité par induction avec des concentrateurs de flux.

La première phase du projet a permis de développer un modèle prédictif fiable et acceptable qui prédit l'effet des paramètres machines et paramètres géométriques sur la profondeur durcie d'un disque chauffé par induction. L'étape de caractérisation thermomécanique fut réalisée en trois parties. La première partie fut dédiée aux travaux de modélisation en 2D par un logiciel de calcul par éléments finis avec couplage des phénomènes électromagnétiques et de transfert de chaleur, afin de quantifier adéquatement la distribution de température dans le cas d'un disque en acier 4340. Les résultats furent

ensuite extraits pour tracer les profils de dureté à partir des profils de températures obtenues et furent validés expérimentalement. En deuxième partie, une campagne de simulation a été conduite en se basant sur un design orthogonal proposé par la méthode de Taguchi en considérant deux facteurs géométriques, le gap radial entre le disque et l'inducteur, et la largeur du disque ainsi que deux facteurs machines, la puissance fournie à l'inducteur, le gap axial entre le disque à traité et les concentrateurs et le temps de chauffe. Cette partie s'est achevée par la création et le développement d'un modèle de prédiction caractérisant l'effet de bord en fonction des paramètres d'entrées. La troisième partie fut réalisée pour la validation expérimentale du modèle de prédiction précédemment développé. Des analyses statistiques ont démontré une bonne concordance entre le modèle de prédiction et les résultats expérimentaux, avec une erreur maximale de l'ordre de 19% entre la profondeur prédictive et la profondeur mesurée.

La deuxième phase du projet a été consacrée au développement de techniques d'optimisation destinées à réduire l'effet de bord d'un disque en acier 4340 durci par induction. Deux approches fondamentales d'optimisation ont été utilisées pour donner le meilleur résultat possible. La première approche est inspirée des travaux de recherches précédents, dans lesquels on emploie des concentrateurs de flux type maître esclave pour uniformiser la distribution du champ électromagnétique à travers la pièce principale et pour restreindre l'effet de bord causé par un fort gradient de température entre le milieu et le bord à la fin de chauffe. La deuxième approche employée a fait appel à des algorithmes d'optimisation compilés simultanément avec un modèle de simulation numérique 2D faisant intervenir les concentrateurs de flux dans la géométrie du modèle de chauffage par induction précédemment étudié. L'optimisation fut appliquée exclusivement sur les paramètres géométriques du procédé, représenté par le gap radial entre le disque principal et l'inducteur, et le gap axial entre le disque principal et les concentrateurs de flux. Les résultats de simulation, validée expérimentalement, ont montré que les approches proposées sont très efficaces à réduire considérablement l'effet de bord à la fin de traitement. De plus, une concordance remarquable fut obtenue suite à cette étude entre le modèle de simulation et le test de validation expérimental avec une erreur d'ordre de 2%.

La troisième phase a porté sur des engrenages, pièces de géométries plus complexes. La modélisation par éléments finis a fait intervenir les mêmes paramètres de contrôle employés précédemment et appliqués sur une géométrie axisymétrique maillée en 3D et ramenée à une section angulaire comportant une seule dent afin de réduire le temps de calcul. Des analyses statistiques ont été conduites pour développer des modèles de prédition de profil durci à la tête et à la racine de l'engrenage par la méthode de surface de réponse (RSM) avec ANOVA et par des réseaux de neurones artificiels. La procédure de modélisation peut être considérée comme efficace et a réussi à produire des résultats concluants avec l'expérimentation malgré la complexité du procédé étudié. Le modèle de prédition basé sur les réseaux de neurones démontre une bonne fiabilité et une bonne capacité à gérer plus efficacement des problèmes non linéaires. Les tests expérimentaux démontrent que l'inexactitude entre les profondeurs durcies mesurées pratiquement et les profondeurs durcies prédites est inférieure à 0,05 mm dans la plupart des tests, avec une erreur relative variant entre 0% à 40% entre la simulation et l'expérimentation. Le modèle de réseau de neurones constitue donc une technique précise et robuste pour prédire et réduire l'effet de bord sous différentes combinaisons de paramètres de contrôle machines et sous différentes conditions géométriques.

Les résultats généraux effectués dans le cadre de ce projet de maîtrise conduisent aux résultats suivants :

- La puissance fournie à l'inducteur et le temps de chauffe contribuent ensemble à plus de 84% de la variation de la profondeur durcie au bord et au milieu d'un disque traité classiquement par induction.
- Les paramètres géométriques ont un effet négligeable sur la variation de la profondeur durcie si la pièce est traitée par induction sans concentrateurs de flux.
- La contribution de puissance fournie à l'inducteur et le temps de chauffe devient négligeable sur la variation d'effet de bord (ou encore la différence

entre la profondeur durcie entre le milieu et le bord de la pièce) avec l'emploi des concentrateurs de flux.

- Le gap entre la pièce principale et les concentrateurs est le facteur le plus important sur la variation d'effet de bord.
- La profondeur durcie est toujours plus importante à la tête par rapport à la racine de la dent de l'engrenage même avec l'utilisation des concentrateurs de flux. Toutefois, il est souhaitable d'utiliser ces concentrateurs pour réduire considérablement l'effet de bord entre le milieu et le bord de l'engrenage traité.
- Des valeurs élevées de gap (gap supérieur à 1 mm) entre la pièce à traiter et les concentrateurs de flux sont non souhaitables pour atteindre une distribution uniforme de profil durci à la fin de traitement. Des valeurs dans l'intervalle 0.4 mm à 0.8 mm donnent les meilleures distributions possibles pour toutes les géométries étudiées.
- La modélisation par éléments finis démontre son efficacité et fiabilité pour la simulation des phénomènes complexes faisant intervenir les phénomènes couplés de l'électromagnétisme et de transfert de chaleur.
- Les meilleurs résultats de prédiction des modèles de simulation simplifiés sont obtenus avec l'emploi des réseaux de neurones. Toutefois la prédiction par réseau de neurones de la distribution du profil durci en utilisant des données d'entraînement extraites de la simulation numérique est satisfaisante, mais peut être plus perfectionnée avec une campagne des tests expérimentaux.

Finalement, les travaux effectués dans ce projet de recherche ont conduit à une meilleure compréhension du procédé de traitement thermique par induction avec l'emploi des concentrateurs de flux lorsqu'appliqué sur des disques et des engrenages droits en acier 4340. Une piste intéressante pour des travaux futurs serait de mesurer l'impact des concentrateurs de flux et les valeurs géométriques optimales déterminées dans ce projet, sur

l'endurance et la résistance à la fatigue des disques et des engrenages droits. D'autres travaux futurs pourraient se réaliser en adoptant des techniques consistantes de modélisation par réseaux de neurones artificiels pour la prédiction des comportements mécaniques des pièces traitées par induction avec des concentrateurs de flux à partir des campagnes d'essais purement expérimentales.

RÉFÉRENCES BIBLIOGRAPHIQUES

- [1] E. Neely and T. Bertone, "Practical metallurgy and materials of industry. 2003," ed: Prentice Hall. Ohio.
- [2] J. S. Selvan, K. Subramanian, and A. Nath, "Effect of laser surface hardening on En18 (AISI 5135) steel," *Journal of Materials Processing Technology*, vol. 91, no. 1-3, pp. 29-36, 1999.
- [3] R. S. Lakhkar, Y. C. Shin, and M. J. M. Krane, "Predictive modeling of multi-track laser hardening of AISI 4140 steel," *Materials science and engineering: a*, vol. 480, no. 1-2, pp. 209-217, 2008.
- [4] H. R. Shercliff and M. Ashby, "The prediction of case depth in laser transformation hardening," *Metallurgical Transactions A*, vol. 22, no. 10, pp. 2459-2466, 1991.
- [5] M. Lee, G. Kim, K. Kim, and W. Kim, "Control of surface hardnesses, hardening depths, and residual stresses of low carbon 12Cr steel by flame hardening," *Surface and coatings technology*, vol. 184, no. 2-3, pp. 239-246, 2004.
- [6] M. Lee, G. Kim, K. Kim, and W. Kim, "Effects of the surface temperature and cooling rate on the residual stresses in a flame hardening of 12Cr steel," *Journal of materials processing technology*, vol. 176, no. 1-3, pp. 140-145, 2006.
- [7] D. Couvard, T. Palin-luc, P. Bristiel, V. Ji, and C. Dumas, "Residual stresses in surface induction hardening of steels: Comparison between experiment and simulation," *Materials Science and Engineering: A*, vol. 487, no. 1-2, pp. 328-339, 2008.
- [8] Y. Han, E.-L. Yu, and T.-X. Zhao, "Three-dimensional analysis of medium-frequency induction heating of steel pipes subject to motion factor," *International Journal of Heat and Mass Transfer*, vol. 101, pp. 452-460, 2016.
- [9] D. Ivanov, L. Markegård, J. I. Asperheim, and H. Kristoffersen, "Simulation of Stress and Strain for Induction-Hardening Applications," *Journal of Materials Engineering and Performance*, vol. 22, no. 11, pp. 3258-3268, 2013/11/01 2013.
- [10] T. Munikamal and S. Sundarraj, "Modeling the Case Hardening of Automotive Components," *Metallurgical and Materials Transactions B*, vol. 44, no. 2, pp. 436-446, 2012.
- [11] M. Tarakci, K. Korkmaz, Y. Gencer, and M. Usta, "Plasma electrolytic surface carburizing and hardening of pure iron," *Surface and Coatings Technology*, vol. 199, no. 2-3, pp. 205-212, 2005.
- [12] M. Béjar and R. Henríquez, "Surface hardening of steel by plasma-electrolysis boronizing," *Materials & Design*, vol. 30, no. 5, pp. 1726-1728, 2009.
- [13] W. Xu, W. Ding, Y. Zhu, X. Huang, and Y. Fu, "Understanding the temperature distribution and influencing factors during high-frequency induction brazing of CBN super-abrasive grains," *The International Journal of Advanced Manufacturing Technology*, vol. 88, no. 1-4, pp. 1075-1087, 2016.
- [14] B. Reul, "Method and device for brazing connections by induction heating," ed: Google Patents, 2012.
- [15] P. Guerrier, G. Tosello, K. K. Nielsen, and J. H. Hattel, "Three-dimensional numerical modeling of an induction heated injection molding tool with flow visualization," *The International Journal of Advanced Manufacturing Technology*, vol. 85, no. 1-4, pp. 643-660, 2015.
- [16] P. Guerrier, K. Kirstein Nielsen, S. Menotti, and J. Henri Hattel, "An axisymmetrical non-linear finite element model for induction heating in injection molding tools," *Finite Elements in Analysis and Design*, vol. 110, pp. 1-10, 2016.
- [17] G. M. Mucha, D. E. Novorsky, and G. D. Pfaffmann, "Method for hardening gears by induction heating," ed: Google Patents, 1987.
- [18] Y. Kawase, T. Miyatake, and K. Hirata, "Thermal analysis of steel blade quenching by induction heating," *IEEE transactions on magnetics*, vol. 36, no. 4, pp. 1788-1791, 2000.
- [19] H. Hammi, A. El Ouafi, N. Barka, and A. Chebak, "Scanning Based Induction Heating for AISI 4340 Steel Spline Shafts-3D Simulation and Experimental Validation," *Advances in Materials Physics and Chemistry*, vol. 07, no. 06, pp. 263-276, 2017.
- [20] R. E. Haimbaugh, *Practical Induction Heat Treating*, Second Edition ed. ASM International, 2015.

- [21] P. M. Unterweiser, *Heat treater's guide: standard practices and procedures for steel*. Asm Intl, 1982.
- [22] K. C. Ltd, "Heating with 2 different frequency waves," ed: Koshuha Co. Ltd, 2016.
- [23] R. V. L. D, C. R, and B. M, *Handbook of Induction Heating*. New York, 2003.
- [24] M. Forzan, E. Toffano, and S. Lupi, "Compensation of induction heating load edge- effect by space control," *COMPEL - The international journal for computation and mathematics in electrical and electronic engineering*, vol. 30, no. 5, pp. 1558-1569, 2011/09/13 2011.
- [25] A. Candeo, C. Ducassy, P. Bocher, and F. Dughiero, "Multiphysics modeling of induction hardening of ring gears for the aerospace industry," *IEEE Transactions on Magnetics*, vol. 47, no. 5, pp. 918-921, 2011.
- [26] X. Fu, B. Wang, X. Zhu, X. Tang, and H. Ji, "Numerical and experimental investigations on large-diameter gear rolling with local induction heating process," *The International Journal of Advanced Manufacturing Technology*, vol. 91, no. 1-4, pp. 1-11, 2016.
- [27] K. Gao, Z. Wang, X.-p. Qin, and S.-x. Zhu, "Numerical analysis of 3D spot continual induction hardening on curved surface of AISI 1045 steel," *Journal of Central South University*, vol. 23, no. 5, pp. 1152-1162, 2016.
- [28] C. Chaboudez, S. Clain, R. Glardon, D. Mari, J. Rappaz, and M. Swierkosz, "Numerical modeling in induction heating for axisymmetric geometries," *IEEE transactions on magnetics*, vol. 33, no. 1, pp. 739-745, 1997.
- [29] M. Erdogan and S. Tekeli, "The effect of martensite particle size on tensile fracture of surface-carburised AISI 8620 steel with dual phase core microstructure," *Materials & design*, vol. 23, no. 7, pp. 597-604, 2002.
- [30] R. Caruso, B. J. Gómez, O. de Sanctis, J. Feugeas, A. Díaz-Parralejo, and F. Sánchez-Bajo, "Ion nitriding of zirconia coated on stainless steel: structure and mechanical properties," *Thin Solid Films*, vol. 468, no. 1, pp. 142-148, 2004/12/01/ 2004.
- [31] N. Barka, "Study of the machine parameters effects on the case depths of 4340 spur gear heated by induction—2D model," *The International Journal of Advanced Manufacturing Technology*, 2017.
- [32] N. Barka, P. Bocher, and J. Brousseau, "Sensitivity study of hardness profile of 4340 specimen heated by induction process using axisymmetric modeling," *The International Journal of Advanced Manufacturing Technology*, vol. 69, no. 9-12, pp. 2747-2756, 2013.
- [33] P. G. Kochure, "Mathematical modeling for selection of process parameters in induction hardening of EN8 D steel," *IOSR Journal of Mechanical and Civil Engineering*, vol. 1, no. 2, pp. 28-32, 2012.
- [34] K.-Y. Bae, Y.-S. Yang, and C.-M. Hyun, "Analysis for the angular deformation of steel plates in a high-frequency induction forming process with a triangle heating technique," *Proceedings of the Institution of Mechanical Engineers, Part B: Journal of Engineering Manufacture*, vol. 227, no. 3, pp. 423-429, 2013.
- [35] M.-S. Huang and Y.-L. Huang, "Effect of multi-layered induction coils on efficiency and uniformity of surface heating," *International Journal of Heat and Mass Transfer*, vol. 53, no. 11-12, pp. 2414-2423, 2010.
- [36] H.-B. Besserer *et al.*, "Induction Heat Treatment of Sheet-Bulk Metal-Formed Parts Assisted by Water-Air Spray Cooling," *steel research international*, vol. 87, no. 9, pp. 1220-1227, 2016.
- [37] R. C. Dmytro, Krause; Florian, Nürnberger; Friedrich-Wilhelm, Bach; Lorenz, Gerdes; Bernd, Breidenstein, "Investigation of the surface residual stresses in spray cooled induction hardened gearwheels," *International Journal of Materials Research*, vol. Vol. 103, No. 1, pp. 73-79., 2012.
- [38] K. H. and V. P., "Influence of process parameters for induction hardening on residual stresses," *Materials and Design*, 2001.
- [39] P. G. Kochure and K. N. Nandurkar, "Application of Taguchi Methodology in Selection of Process Parameters For Induction Hardening Of EN8 D Steel," *International Journal of Modern Engineering Research (IJMER)*, vol. Vol.2, no. 5, pp. 3736-3742 2012.
- [40] D. Hömberg *et al.*, "Simulation of multi-frequency-induction-hardening including phase transitions and mechanical effects," *Finite Elements in Analysis and Design*, vol. 121, pp. 86-100, 2016.

- [41] J. Montalvo-Urquiza, Q. Liu, and A. Schmidt, "Simulation of quenching involved in induction hardening including mechanical effects," *Computational Materials Science*, vol. 79, pp. 639-649, 2013.
- [42] L. Jakubovičová, G. Andrej, K. Peter, and S. Milan, "Optimization of the Induction Heating Process in Order to Achieve Uniform Surface Temperature," *Procedia Engineering*, vol. 136, pp. 125-131, 2016.
- [43] J. Barglik, A. Smalcerz, R. Przylucki, and I. Doležel, "3D modeling of induction hardening of gear wheels," *Journal of Computational and Applied Mathematics*, vol. 270, pp. 231-240, 2014.
- [44] F. Cajner, B. Smoljan, and D. Landek, "Computer simulation of induction hardening," *Journal of Materials Processing Technology*, vol. 157-158, pp. 55-60, 2004.
- [45] K. Sadeghipour, J. A. Dopkin, and K. Li, "A computer aided finite element/experimental analysis of induction heating process of steel," *Computers in Industry*, vol. 28, no. 3, pp. 195-205, 1996/06/01/1996.
- [46] N. Barka, P. Bocher, J. Brousseau, and P. Arkinson, "Effect of Dimensional Variation on Induction Process Parameters Using 2D Simulation," *Advanced Materials Research*, vol. 409, pp. 395-400, 2011.
- [47] N. Barka, A. Chebak, and A. El Ouafi, "Simulation of Helical Gear Heated by Induction Process Using 3D Model," *Advanced Materials Research*, vol. 658, pp. 266-270, 2013.
- [48] N. Barka, A. El Ouafi, P. Bocher, and J. Brousseau, "Explorative Study and Prediction of Overtempering Region of Disc Heated by Induction Process Using 2D Axisymmetric Model and Experimental Tests," *Advanced Materials Research*, vol. 658, pp. 259-265, 2013.
- [49] C. Myers, J. Osborn, C. Tiell, R. Goldstein, and R. T. Ruffini, "Induction Heat Treating-Optimizing Performance of Crankshaft Hardening Inductors-Using Fluxtrol A in crankshaft induction coils resulted in a 100% improvement in coil lifetime while improving," *Industrial Heating*, vol. 73, no. 12, pp. 43-50, 2006.
- [50] M. Khalifa, N. Barka, J. Brousseau, and P. Bocher, "Sensitivity study of hardness profile of 4340 steel disc hardened by induction according to machine parameters and geometrical factors," *The International Journal of Advanced Manufacturing Technology*, vol. 101, no. 1, pp. 209-221, 2019/03/01 2019.
- [51] V. Rudnev, "An objective assessment of magnetic flux concentrators," *Heat treating progress*, pp. 19-23, 2004.
- [52] T. Zhu, P. Feng, X. Li, F. Li, and Y. Rong, "The Study of the Effect of Magnetic Flux Concentrator to the Induction Heating System Using Coupled Electromagnetic-Thermal Simulation Model," in *2013 International Conference on Mechanical and Automation Engineering*, 2013, pp. 123-127.
- [53] N. Barka, A. Chebak, A. El Ouafi, M. Jahazi, and A. Menou, "A New Approach in Optimizing the Induction Heating Process Using Flux Concentrators: Application to 4340 Steel Spur Gear," *Journal of Materials Engineering and Performance*, vol. 23, no. 9, pp. 3092-3099, 2014.
- [54] V. Rudnev, D. Loveless, and R. Cook, *Handbook of Induction Heating*, Second edition. ed. (Manufacturing engineering and materials processing, no. 61). Boca Raton: CRC Press, Taylor & Francis Group, 2017, pp. xxi, 749 pages.
- [55] X. Guo *et al.*, "Numerical simulations and experiments on fabricating bend pipes by push bending with local induction-heating process," *The International Journal of Advanced Manufacturing Technology*, vol. 84, no. 9-12, pp. 2689-2695, 2015.
- [56] S. Achraf, L. Benjamin, V. Nicolas, and B. Philippe, "Temperature history Modelling and Validation of fast induction hardening process," presented at the HES-16 Heating by Electromagnetic Sources, Padua (Italy), 2016.
- [57] H. Wen and Y. Han, "Study on mobile induction heating process of internal gear rings for wind power generation," *Applied Thermal Engineering*, vol. 112, pp. 507-515, 2017.
- [58] K.-Y. Bae, Y.-S. Yang, C.-M. Hyun, and S.-H. Cho, "Derivation of simplified formulas to predict deformations of plate in steel forming process with induction heating," *International Journal of Machine Tools and Manufacture*, vol. 48, no. 15, pp. 1646-1652, 2008.
- [59] J. Jin, *The Finite Element Method in Electromagnetics*. New York: John Wiley & Sons Inc., 2002.

- [60] P. J. Withers, "Residual stress and its role in failure," *Reports on Progress in Physics*, vol. 70, no. 12, p. 2211, 2007.
- [61] V. Savaria, F. Bridier, and P. Bocher, "Predicting the effects of material properties gradient and residual stresses on the bending fatigue strength of induction hardened aeronautical gears," *International Journal of Fatigue*, vol. 85, pp. 70-84, 2016.
- [62] M. N. James, D. G. Hattingh, D. Asquith, M. Newby, and P. Doubell, "Applications of Residual Stress in Combating Fatigue and Fracture," *Procedia Structural Integrity*, vol. 2, pp. 11-25, 2016/01/01/ 2016.
- [63] M. Meo and R. Vignjevic, "Finite element analysis of residual stress induced by shot peening process," *Advances in Engineering Software*, vol. 34, no. 9, pp. 569-575, 2003/09/01/ 2003.
- [64] D. Deng, "FEM prediction of welding residual stress and distortion in carbon steel considering phase transformation effects," *Materials & Design*, vol. 30, no. 2, pp. 359-366, 2009/02/01/ 2009.
- [65] P. R. Woodard, S. Chandrasekar, and H. T. Y. Yang, "Analysis of temperature and microstructure in the quenching of steel cylinders," *Metallurgical and Materials Transactions B*, vol. 30, no. 4, p. 815, 1999/08/01 1999.
- [66] Z. Li, B. L. Ferguson, V. Nemkov, R. Goldstein, J. Jackowski, and G. Fett, "Effect of Quenching Rate on Distortion and Residual Stresses During Induction Hardening of a Full-Float Truck Axle Shaft," *Journal of Materials Engineering and Performance*, vol. 23, no. 12, pp. 4170-4180, 2014/12/01 2014.
- [67] P. V. H. Kristoffersen "Influence of process parameters for induction hardening on residual stresses," *Materials and Design*, 2001.
- [68] V. Nemkov, R. Goldstein, J. Jackowski, L. Ferguson, and Z. Li, "Stress and Distortion Evolution During Induction Case Hardening of Tube," *Journal of Materials Engineering and Performance*, vol. 22, no. 7, pp. 1826-1832, 2013/07/01 2013.
- [69] J. Komotori, M. Shimizu, Y. Misaka, and K. Kawasaki, "Fatigue strength and fracture mechanism of steel modified by super-rapid induction heating and quenching," *International Journal of Fatigue*, vol. 23, pp. 225-230, 2001/01/01/ 2001.
- [70] B. Larregain, N. Vanderesse, F. Bridier, P. Bocher, and P. Arkinson, "Method for Accurate Surface Temperature Measurements During Fast Induction Heating," *Journal of Materials Engineering and Performance*, vol. 22, no. 7, pp. 1907-1913, 2013/07/01 2013.
- [71] H. Chandler, *Heat Treater's Guide: Practices and Procedures for Irons and Steels*. ASM International, 1994.
- [72] A. Senhaji, "Simulation numérique de la chauffe par induction électromagnétique d'un disque en AISI 4340," École de technologie supérieure, 2017.
- [73] C. C. A. Floudas and P. M. Pardalos, *Encyclopedia of Optimization*. Springer-Verlag, 2006.
- [74] Z. Wei, G. Li, and L. Qi, "New quasi-Newton methods for unconstrained optimization problems," *Applied Mathematics and Computation*, vol. 175, pp. 1156-1188, 2006 2006.
- [75] C. Jiang, H. Chen, Q. Wang, and Y. Li, "Effect of brazing temperature and holding time on joint properties of induction brazed WC-Co/carbon steel using Ag-based alloy," *Journal of Materials Processing Technology*, vol. 229, pp. 562-569, 2016.
- [76] D. H. M. S.B. Rao, "Experimental Characterization of Bending Fatigue Strength in Gear' leilethi," *Gear Technology*, no. February 2003, 2003.
- [77] D. Tong, J. Gu, and G. E. Totten, "Numerical investigation of asynchronous dual-frequency induction hardening of spur gear," *International Journal of Mechanical Sciences*, vol. 142-143, pp. 1-9, 2018.
- [78] S. J. Midea and P. Lynch, "Tooth-by-tooth induction hardening of gears (and how to avoid some common problems)," in *Proc. Thermal Process. Gear Solutions*, 2014, pp. 46-51.
- [79] J. P. C. Kleijnen, Response Surface Methodology, Tilburg: CentER Discussion Paper, 2014, p. 26. [Online]. Available.
- [80] G. E. P. Box and N. R. Draper, *Response Surfaces, Mixtures, and Ridge Analyses*, Second Edition ed. (Series in Probability and Statistics). New Jersey: John Wiley & Sons, 2007.

- [81] M. T. Hagan, H. B. Demuth, and M. H. Beale, *Neural network design*, 1st ed. Boston, Mass.: PWS Publishing Company (a division of International Thomson Publishing inc.), 1996.
- [82] J. Schmidhuber, "Deep learning in neural networks: an overview," (in eng), Neural Netw, Research Support, Non-U.S. Gov't Review vol. 61, pp. 85-117, Jan 2015.
- [83] L. E. Alban, Systematic analysis of gear failures. Metals Park, Ohio: American Society for Metals, 1993, pp. viii, 232 p.
- [84] N. R. Draper and H. Smith, *Applied regression analysis*. John Wiley & Sons, 2014.
- [85] B. Coto, V. G. Navas, O. Gonzalo, A. Aranzabe, and C. Sanz, "Influences of turning parameters in surface residual stresses in AISI 4340 steel," *The International Journal of Advanced Manufacturing Technology*, vol. 53, no. 9, pp. 911-919, 2011/04/01 2011.
- [86] J. J. Faraway, "Practical regression and ANOVA using R," ed: University of Bath Bath, 2002.
- [87] N. B. Ilyes Maamri, Abderrazak El Ouafi, "ANN Laser Hardening Quality Modeling Using Geometrical and Punctual Characterizing Approaches," *Coatings*, vol. 8, no. 6, 2018.
- [88] F. J. Pontes, J. R. Ferreira, M. B. Silva, A. P. Paiva, and P. P. Balestrassi, "Artificial neural networks for machining processes surface roughness modeling," *The International Journal of Advanced Manufacturing Technology*, vol. 49, no. 9, pp. 879-902, 2010/08/01 2010.
- [89] P. Palanisamy, I. Rajendran, and S. Shanmugasundaram, "Prediction of tool wear using regression and ANN models in end-milling operation," *The International Journal of Advanced Manufacturing Technology*, vol. 37, no. 1, pp. 29-41, 2008/04/01 2008.